

# Modelling of Rosetta Langmuir Probe Measurements

---

Alexander Sjögren





UPPSALA  
UNIVERSITET

**Teknisk- naturvetenskaplig fakultet  
UTH-enheten**

Besöksadress:  
Ångströmlaboratoriet  
Lägerhyddsvägen 1  
Hus 4, Plan 0

Postadress:  
Box 536  
751 21 Uppsala

Telefon:  
018 – 471 30 03

Telefax:  
018 – 471 30 00

Hemsida:  
<http://www.teknat.uu.se/student>

## Abstract

# Modelling of Rosetta Langmuir Probe Measurements

---

*Alexander Sjögren*

The Rosetta spacecraft, which is on its way to the comet 67P/Churyumov-Gerasimenko, has two Langmuir probes onboard to measure plasma properties on its journey and in the region around the comet. The measurements depend on the potential around Rosetta, which is mostly disturbed by the spacecraft potential, the wake created behind the spacecraft, and photoelectrons emitted from the surface of the spacecraft.

In order to make a correct analysis of the measurements made with the two probes, it is needed to understand what parts of the potential measured is due to the various effects presented above, and what part is the actual potential in space. To better understand this, simulations have been made with the software SPIS (Spacecraft Plasma Interaction System) for the cases of Rosetta in vacuum, in the flowing solar wind without photoelectrons emitted from the spacecraft, and in the solar wind with photoelectrons. The plasma parameters and solar distance as well as spacecraft potential have been varied to understand the scaling of the effects. Two simple models of Rosetta have been used and compared, except for the case when photoelectrons are introduced where only one model could be used.

The simulations show that of the various cases studied, the photoelectrons have the biggest effect on the potential measured. It is shown that the potential measured is lowered by about 10% when the probes are in the photoelectron cloud in front of the spacecraft with respect to the Sun. The wake created behind the spacecraft will lower the potential measured on the order of a couple percents. It is also shown that the potential variations due to the asymmetric shape of Rosetta is small compared to the effects of the photoelectrons and the wake.

Handledare: Anders Eriksson  
Ämnesgranskare: Mats André  
Examinator: Tomas Nyberg  
ISSN: 1401-5757, UPTec F09 063



DEGREE PROJECT

# MODELLING OF ROSETTA LANGMUIR PROBE MEASUREMENTS

ALEXANDER SJÖGREN

Swedish Institute of Space Physics

Uppsala, Sweden

OCTOBER 8, 2009



*To my wife Anne, my fifty starving children, and my three legged dog.*



## ABSTRACT

The Rosetta spacecraft, which is on its way to the comet 67P/Churyumov-Gerasimenko, has two Langmuir probes onboard to measure plasma properties on its journey and in the region around the comet. The measurements depend on the potential around Rosetta, which is mostly disturbed by the spacecraft potential, the wake created behind the spacecraft, and photoelectrons emitted from the surface of the spacecraft.

In order to make a correct analysis of the measurements made with the two probes, it is needed to understand what parts of the potential measured is due to the various effects presented above, and what part is the actual potential in space. To better understand this, simulations have been made with the software SPIS (Spacecraft Plasma Interaction System) for the cases of Rosetta in vacuum, in the flowing solar wind without photoelectrons emitted from the spacecraft, and in the solar wind with photoelectrons. The plasma parameters and solar distance as well as spacecraft potential have been varied to understand the scaling of the effects. Two simple models of Rosetta have been used and compared, except for the case when photoelectrons are introduced where only one model could be used.

The simulations show that of the various cases studied, the photoelectrons have the biggest effect on the potential measured. It is shown that the potential measured is lowered by about 10% when the probes are in the photoelectron cloud in front of the spacecraft with respect to the Sun. The wake created behind the spacecraft will lower the potential measured on the order of a couple percents. It is also shown that the potential variations due to the asymmetric shape of Rosetta is small compared to the effects of the photoelectrons and the wake.



## SAMMANFATTNING

Ombord på rymdfarkosten Rosetta, som är på väg mot kometen 67P/Churyumov-Gerasimenko, finns två Langmuir-prober som mäter plasmaparametrar både under resan och runt kometen. Mätningarna beror på potentialen runt Rosetta, som i sin tur bland annat påverkas av Rosettas potential, den vak som bildas bakom Rosetta samt även av fotoelektronerna som emitteras från Rosettas yta.

För att göra en korrekt analys av de data som samlas in med de två proberna krävs en modell som anger vilka delar av den uppmätta potentialen som kan relateras till de ovan nämnda effekterna, och vilka delar som är den faktiska potentialen i omgivningen. Ett första led i att skapa en modell har varit att med hjälp av mjukvaran SPIS (Spacecraft Plasma Interaction System) simulera Rosetta i tre olika miljöer; vakum, den flödande solvinden utan fotoelektroner emitterade från Rosettas yta, samt i solvinden med fotoelektroner. För att få en förståelse för hur de olika effekterna skalar har plasmaparametrar samt Rosettas potential varierats för olika simuleringar. Två enkla modeller av Rosetta har använts, förutom i det fall när fotoelektroner är inkluderade då endast en av modellerna är möjlig att använda.

Simuleringarna visar att av de studerade fallen har fotoelektronerna störst effekt på den uppmätta potentialen. När proberna befinner sig i fotoelektronmolnet, framför Rosetta sett relativt solen, sjunker potentialen med cirka 10%. I vaken som bildas bakom Rosetta sänks den uppmätta potentialen med ett par procent jämfört med omgivande regioner. Även den asymmetriska utformningen av Rosetta påverkar mätningarna, men simuleringarna visar att effekterna av Rosettas asymmetri är små jämfört med fotoelektronerna och vaken bakom Rosetta.



## ACKNOWLEDGMENTS

There are many people that helped me to get this job done, but of course there is one who has been more important than anybody else. This is my supervisor, always with a smile on his face and a solution in his backpack, Dr. Anders Eriksson at IRFU. He was the one who introduced me to the subject, introduced me to SPIS and threw me into the world of simulations that I have spent some months inside. I am really grateful that I got the opportunity to work with Anders and I have learned more than I could ever imagine when starting the thesis work.

It has also been of great importance to have someone else working with SPIS at the same time as myself, in my case Thomas Nilsson has been doing simulations of the Cassini spacecraft. In the process of learning SPIS, it was a big step to meet Simon Clucas and Dave Rogers at ESA, who spent two full days teaching us how to use it. Without that help, I would still be stuck in the vacuum. I also received a lot of support from Bertil Segerström at IRFU to get the computers running, quite crucial for this project. I am also thankful for being able to work in the friendly environment of IRFU and all the people I have met everyday at the office. It is also important to be able to leave the world of SPIS sometimes, for this I am thankful that Madeleine Holmberg was around at every lunchbreak and every other moment that the world's problems needed to be discussed and solved.



# CONTENTS

Contents	xv
1 Introduction	1
1.1 Background	1
1.2 The Rosetta Mission	1
1.3 Plasma	4
1.4 Solar Wind	4
1.5 The Langmuir Probes Onboard Rosetta	5
1.6 SPIS - Spacecraft Plasma Interaction System	6
2 Simulations and Results	9
2.1 Geometry	10
2.2 Vacuum	13
2.3 Plasma without Photoelectrons	22
2.4 Plasma and Photoelectrons - Reference Simulation	34
2.5 Plasma and Photoelectrons - Various Distance from the Sun	40
2.6 Plasma and Photoelectrons - Various Spacecraft Potential	48
2.7 Plasma and Photoelectrons - Various Photoelectron Temperature	53
3 Conclusions	61
4 Future Work	63
References	65
A Listing of all Simulations	67
B How to Make a Simulation of the Rosetta Spacecraft	73
B.1 The World inside SPIS	73
B.2 Creating a Model	74
B.3 Customizing SPIS	78
B.4 Configuring Simulation Settings and Starting the Simulation	79
B.5 Exporting and Saving the Data	81
B.6 Looking at the VTK files - Working with ParaView	81
B.7 Final Words about the Rosetta Simulations	82
C Coordinates for the Rosetta Model	85

CONTENTS

---

D The electronSpeedUp Parameter	89
E Simulation with Booms in Shadow	93

# 1

## INTRODUCTION

### 1.1 Background

Imagine the time a couple of thousand years ago. There were no cars, street lights or computer screens to disturb the darkness during the nights. People were familiar with the night sky, they knew how it changed with time, both the daily and seasonal variations. All of a sudden, a huge bright object shows up travelling over the sky, even leaving a speed stripe behind. No wonder people were scared! Imagination sets in and the object was described as something predicting the death of kings or attacks from heavenly beings. Even as late as in 1910 newspaper reported that the Halley's comet would poison millions of people due to the cyanogen left in the tail that the Earth was crossing, which also was a step forward as scientists now could measure what is inside the tail.

Nowadays, the appearance of a comet is a beautiful scenery on the night sky for most people. A lot of people know that a comet is a small heavenly object, travelling in elliptical orbits around the Sun and showing the tail as it is approaching its perihelion, the point in its orbit where it is closest to the Sun. When it comes to the research on comets, there is still lots to learn. The latest comet missions are the NASA missions Deep Impact and Stardust. Deep Impact was observing the comet Tempel 1 and at the same time sent down a special impactor spacecraft on crash course with the nucleus of the comet. In this way, the cloud coming out from the comet after the impact could be observed (NASA, 2006). Stardust approached the comet Wild 2 and flew within 250 km from its nucleus, analyzing the outgassing particles and observing the comet (NASA, 2009a).

ESA, in cooperation with other space agencies, has now taken the next step in expanding the understanding of comets. The project is named the Rosetta mission and will be further presented in the next section.

### 1.2 The Rosetta Mission

Rosetta (shown in Figure 1.1) is the first mission ever which is designed to orbit and also send a lander down to a comet. It is an ambitious project with an ambitious name; the name Rosetta comes from the Rosetta stone which was the key to unlock mysteries of the ancient Egypt. In a similar way, the spacecraft Rosetta is intended to help us understand more about the mysteries how our solar system was formed, some 4600 million years ago.

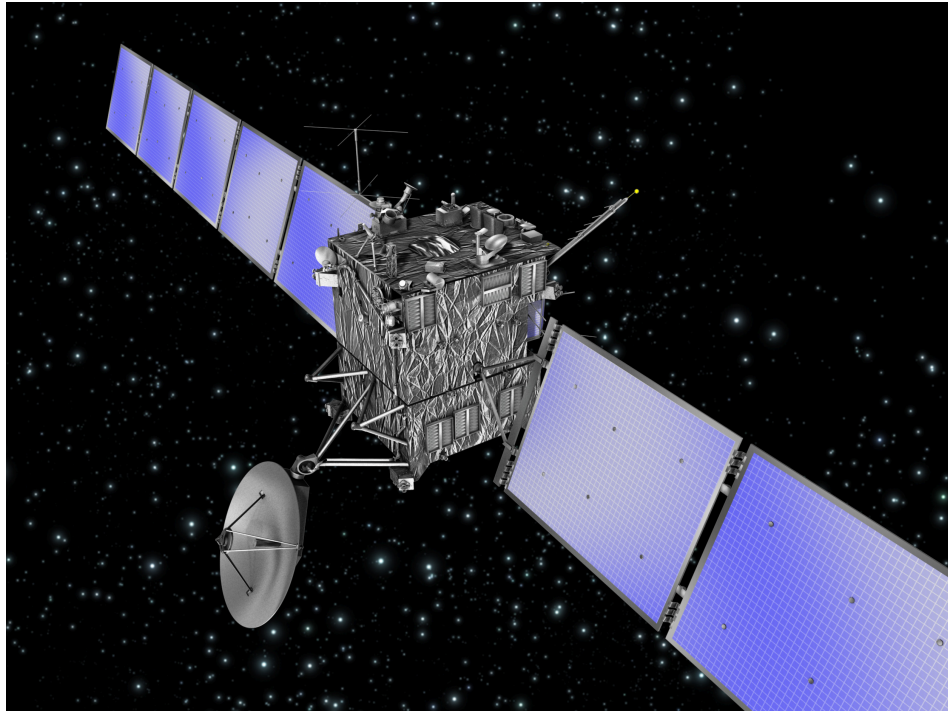


**Figure 1.1:** Artist view of the Rosetta spacecraft. Copyright: ESA.

The mission is an ESA (European Space Agency) project, together with various national European space agencies, and also NASA. It was approved in 1993 and was first scheduled to be launched in January 2003 on an Ariane-V rocket. The comet to be visited by Rosetta and its lander, Philae, was 46P/Wirtanen. Due to a failure of the Ariane-V rocket in December 2002, ESA was forced to postpone the launch and select another target comet, as the launch window for 46P/Wirtanen was closed. The new comet selected was 67P/Churyumov-Gerasimenko and Rosetta was launched on March, 2, 2004 (Glassmeier et al., 2007).

Rosetta is scheduled to arrive at the 67P/Churyumov-Gerasimenko in 2014. At that time, the spacecraft will have done four gravity assists (Earth-Mars-Earth-Earth) and rendez-vous with the comet at a distance of about 4 AU from the Sun. The comet is at that point speeding up towards its perihelion. Rosetta will orbit the comet, and the lander Philae will descend to the surface of the comet. It will take the comet approximately one year from rendez-vous until it reaches the perihelion at 1.2 AU (NASA, 2009b). A couple of months later the Rosetta mission is supposed to end.

A main reason to visit a comet is that comets are believed to contain the least processed material of all the bodies in the solar system, in other words the material most similar to that which the solar system was formed from. Therefore, visiting a comet will give us clues about how the comet was formed, which ultimately leads to clues about how the solar system was formed. When a comet travels towards its perihelion, the closest point to the Sun in its orbit, it will become more and more active (which means more out-gassing of materials from the comet surface) due to the increased solar radiation. Rosetta

will travel together with 67P/Churyumov-Gerasimenko from rendez-vous at about 4 AU, through the onset of activity (at around 3 AU) to the point of maximum activity at perihelion (Glassmeier et al., 2007).

Rosetta is best described as a cuboid shaped body of 2.8x2.1x2.0 meters, and two large solar panels, stretching about 15 meter each from the spacecraft body, giving 64 square meters of solar panel area. Rosetta together with the lander is shown in Figure 1.2. Rosetta will be the first spacecraft to use solar cells as the main power source as far out in the Solar System as the Jupiter orbit (Bond, 2001).

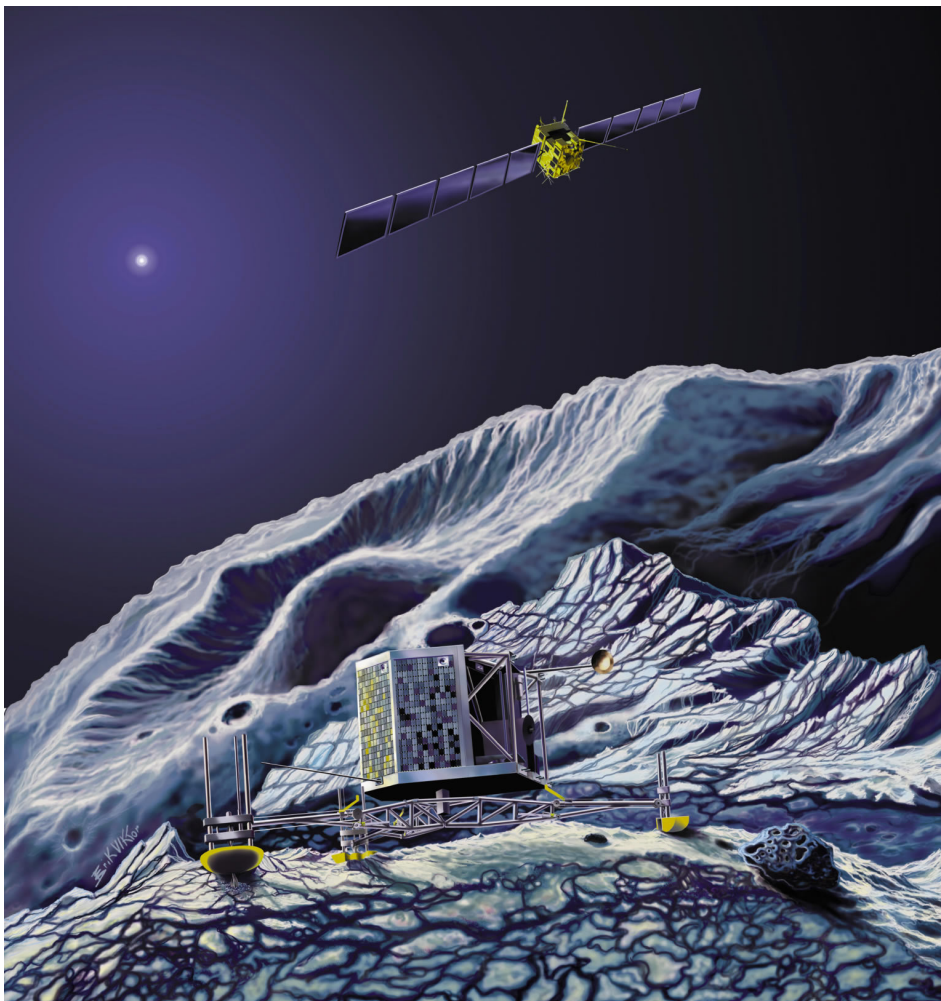


**Figure 1.2:** Artist view of the Rosetta orbiter and lander after being sent down to the comet. Copyright: ESA.

Rosetta is carrying a lot of instruments; 16 on the orbiter itself, and another 10 on the lander. The contribution from IRF<sup>1</sup> in Uppsala are two Langmuir Probes (LAP, see

<sup>1</sup>Institutet för Rymdfysik / Swedish Institute of Space Physics, <http://www.irfu.se>

Chapter 1.5). All of the instrumentation is attached to the spacecraft body, or to the lander. The solar panels will mainly be directed facing the Sun at right angle in order to absorb a maximum of sunlight. The instruments on the spacecraft body should however be able to be directed in almost any direction desired. Therefore the spacecraft body and the solar panels can be rotated independently around the axis following the length of the solar panels (see for example Figure 2.4 in Chapter 2).

### 1.3 Plasma

Plasma is often called the fourth state of matter, and it is estimated that 99% of the baryonic matter in the universe is in the plasma state (Engwall, 2006). So what is the definition of a plasma? One commonly used definition is stated by Chen (1984): *A plasma is a quasineutral gas of charged and neutral particles which exhibits collective behaviour.* The term collective behaviour means that the motion of one particle is influenced by the total fields from all particles, not only by the single particles close by. When it comes to the quasineutrality, a somewhat longer description is needed.

A plasma has the ability to shield out local electric potentials in the plasma. If, for example, two spherical, oppositely charged bodies are placed inside the plasma to create a potential difference, and hence an electric field between them, electrons will gather around the positively charged sphere and ions will gather around the negatively charged sphere (assuming the particles can not recombine with the spheres). This creates a thin sheath around each sphere, cancelling out the potential of the spheres as seen by the plasma particles outside the sheath. The phenomenon is known as *Debye shielding* and the shielding distance, or thickness of the sheath, is called *Debye length*. The Debye length is given by Chen (1984) as

$$\lambda_d = \sqrt{\frac{\epsilon_0 k_B T_e}{n_e e^2}}, \quad (1.1)$$

where  $\epsilon_0$  is the vacuum permittivity,  $k_B$  is the Boltzmann's constant,  $T_e$  is the electron temperature,  $n_e$  is the electron density and  $e$  is the elementary charge.

The definition of quasineutrality can now be understood. On scales larger than the Debye length, the number densities of electrons and ions will be approximately the same,  $n_i \approx n_e \approx n$ , where the number  $n$  is known as the plasma density. The plasma will therefore be neutral. This neutrality could however break down on scales smaller than the Debye length, hence the word quasineutrality. For a thorough description of plasma and plasma properties, please see for example Chen (1984). For Rosetta, the environment encountered during all the time until 2014 (except the planetary flybys) is the solar wind plasma, presented in the next section.

### 1.4 Solar Wind

The Sun is one of the key factors for us to be able to live on the Earth, and most people enjoy the light coming from the Sun. Together with the emission of light, the Sun also emits a stream of particles (electrons and ions), known as *the solar wind*. The solar wind

has an average speed of about 400-450 km/s, plasma density of about  $5 \text{ cm}^{-3}$ , and temperature on the scale of 5-15 eV (about 100 000 K) (McFadden et al., 2006). This constant flow of plasma charges a spacecraft, and also produces a *wake* behind the spacecraft.

Due to the big mass ratio between ions and electrons, the thermal velocity of the electrons is much higher than for the ions, when at almost the same temperature. The thermal velocity for the electrons is also larger than the flow speed of the plasma, while the opposite is true for the ions. As the plasma flows towards a spacecraft, the flowing particles will be blocked by the spacecraft, creating a volume behind it where the ions will not enter due to the fact that the flow speed is larger than the thermal ('randomized') speed. This void is known as a wake. The thermal motion of the electrons allows them to fill this volume, and so the wake gets negatively charged. When making measurements of the solar wind it is important to understand how the instruments are affected by this wake. In addition, photoelectrons emitted by the spacecraft or solar panels may further disturb the plasma environment. The Langmuir probe instrument is particularly affected by these effects. In the upcoming section, a short introduction of Langmuir probes is presented, which will show how these probes are working to measure the plasma properties.

### 1.5 The Langmuir Probes Onboard Rosetta

Onboard Rosetta, there are two Langmuir probes, which together with associated electronics make up the LAP instrument of the Rosetta Plasma Consortium (RPC). The primary task of the probes is to measure fluid plasma parameters, such as plasma density, electron temperature, and plasma flow speed. By doing this as Rosetta is orbiting the comet on its journey towards perihelion, the outgassing of the comet and its interaction with the space environment can be studied in more detail (Eriksson et al., 2007).

The two probes are identical, except for the booms by which they are attached to the spacecraft body, which differ in length. The probes themselves are titanium spheres of 25 mm radius, mounted on a stub which is 15 cm long. The stubs are attached to the booms, 2.24 and 1.62 m of length, respectively. The probes together with the booms attaching them to the spacecraft is shown in Figure 1.3.

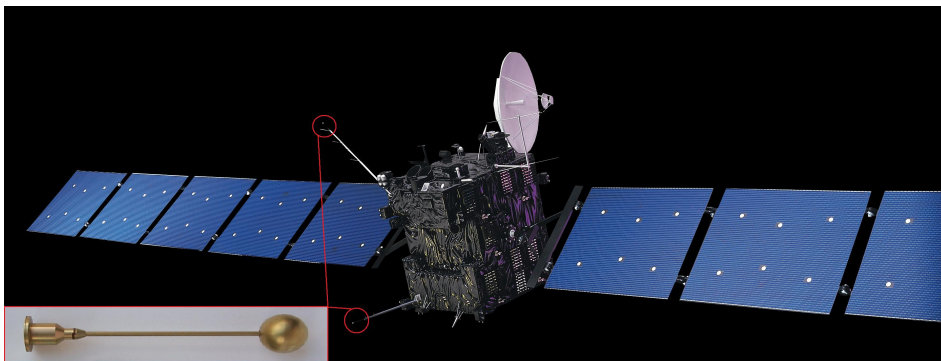


Figure 1.3: Rosetta and the Langmuir Probes. Copyright: ESA.

Each of the probes can be put at a positive or negative potential with respect to the

spacecraft, and depending on the sign of the potential it will either attract electrons or ions from the surrounding plasma. The potential is varied in a sweep and the current collected at the probe is recorded. By comparing the observed current-voltage curve to theoretically known relations, the electron density  $n_e$  and temperature  $T_e$  can be calculated. The probes can also be used in other operational modes, and thereby measure different phenomena. For example, by keeping the probe bias voltage constant, it is possible to measure the changes in probe current due to fluctuations in plasma density and temperature (Eriksson et al., 2007).

For the long journey towards the comet, and also when first arriving at the comet, plasma conditions will be dominated by the solar wind. The solar wind is a tenuous plasma, much less dense than the plasma around the comet when coming closer to the Sun, which is the kind of plasma the probes are ultimately designed for. In the tenuous solar wind plasma, the probe current will be dominated by photoelectrons emitted from the spacecraft body and solar panels. In this case, a technique found to be more useful is to instead apply a controlled bias current,  $I_B$ . The measured quantity is now the potential between the probe and the spacecraft,  $V_{PS}$ , for each probe. The value of  $V_{PS}$  is related to the spacecraft potential with respect to the plasma,  $V_S$  (Cully et al., 2007).  $V_S$  is a basic parameter when studying the spacecraft-plasma interactions and also gives an estimation of the number density in tenuous plasma such as the solar wind.

To derive  $V_S$  from  $V_{PS}$ , we must understand what other factors than  $V_S$  that influence our measurement. The photoelectron cloud from the spacecraft and solar panels gives rise to a decrease in the potential of the plasma with respect to the spacecraft, at the positions of the probes. As the booms carrying the probes will not always be sufficient to take the probes outside this cloud (when in front of the spacecraft where the cloud mainly is), the measured potential will be influenced by the photoelectrons, depending on the distance and orientation with respect to the Sun. There might also be an effect due to the wake forming behind the spacecraft, where the potential between the probes and spacecraft could drop due to the lack of ions. Such phenomena around Rosetta have been studied previously (Roussel and Berthelier, 2004; Berthelier and Roussel, 2004), but not to the detail needed to quantify the impact on LAP measurements. This is why it is needed to examine these effects, which is done in this project by using a spacecraft plasma interaction software, in this case SPIS, presented in the next section.

## 1.6 SPIS - Spacecraft Plasma Interaction System

When a spacecraft is travelling in an environment like the solar wind, it will interact with the surrounding plasma, which can build up a net charge on the spacecraft surface. As a result of the interaction, plasma measurements made with high accuracy sensors onboard the spacecraft can be disturbed. Another issue that might come up is potential differences between the surfaces. Such voltages might lead to sparks which can ultimately destroy subsystems, which has happened several times. One example is the Japanese satellite ADEOS (Nakamura, 2005). While this is not an issue for Rosetta, it explains the commercial interest in spacecraft plasma interactions.

To be able to model such effects as spacecraft charging and plasma influence on measurements, European experts in spacecraft plasma interactions gathered under an ESA initiative in the year 2000. The meeting led to the development of a first prototype of

a spacecraft charging code; *PicUp3-D*. The code was developed with sponsorship from ESA, IRF, CNRS<sup>2</sup>, and CNES<sup>3</sup>. Based on experiences from *PicUp3-D*, SPIS was developed by ONERA<sup>4</sup> and Artnum<sup>5</sup>. SPIS is under an open source license (GPL) and is freely available from the homepage of the project<sup>6</sup> (Roussel et al., 2008).

The SPIS code is based on Java and Jython, and has third party open source tools for modelling, meshing (GMSH<sup>7</sup>) and post processing (Paraview<sup>8</sup> and Cassandra<sup>9</sup>) included in the package. A description on how to run SPIS is presented in Appendix B.

To model the plasma in SPIS, a coupling between a matter and a field model is used. There exists two versions of the matter model; particle in cell (PIC) and global Maxwell-Boltzmann distribution. The main model, which is the one used in this project, is the PIC. In the version of SPIS used for this report (3.7 RC09), there is no support for the magnetic fields. There are however settings for the inclusion of effects of a static external magnetic field, and this is planned to be implemented in upcoming versions, or could even be implemented by the user her- or himself (Roussel et al., 2005).

When the PIC model is used, the plasma particles are represented by charged macroparticles. These macroparticles represent of a set of many real particles within a finite volume. The macroparticles interact with the electric (and magnetic, when implemented) fields, and the positions of the macroparticles are calculated by solving the equations of motions,

$$\begin{cases} \frac{d\mathbf{v}}{dt} = \frac{q}{m}(\mathbf{E} + \mathbf{v} \times \mathbf{B}) \\ \frac{d\mathbf{x}}{dt} = \mathbf{v} \end{cases}, \quad (1.2)$$

where  $\mathbf{v}$  is the particle velocity vector,  $q$  is the particle charge,  $m$  is the particle mass,  $\mathbf{E}$  is the electrical field,  $\mathbf{B}$  is the magnetic field and  $\mathbf{x}$  is the particle position vector. The motion is integrated with a leap-frog scheme (Forest et al., 2006) and the density is determined by linear interpolation from the positions of the macroparticles. The electric field can be derived from the charge densities and currents from the macroparticles; the equation to solve for the electric field is the Poisson equation,

$$\nabla^2 \phi = -\frac{\rho}{\epsilon_0}, \quad (1.3)$$

where  $\phi$  is the potential,  $\rho$  is the charge density and  $\epsilon_0$  is the permittivity of vacuum (Forest et al., 2006). The linear system obtained is solved by using conjugate gradient method (Roussel et al., 2005).

When the global Maxwell-Boltzmann distribution is used, the electrons are described with a Maxwellian distributions. For this, the nonlinear version of the Poisson equation,

$$\nabla^2 \phi = -\frac{e(n_i - n_0 e^{e\phi/kT})}{\epsilon_0}, \quad (1.4)$$

---

<sup>2</sup>Centre national de la recherche scientifique, <http://www.cnrs.fr>

<sup>3</sup>Centre national d'études spatiales, <http://www.cnes.fr>

<sup>4</sup>Office national d'études et recherches aérospatiales, <http://www.onera.fr>

<sup>5</sup><http://www.artnum.com>

<sup>6</sup><http://dev.spis.org/projects/spine/home/spis>

<sup>7</sup><http://geuz.org/gmsh>

<sup>8</sup><http://www.paraview.org>

<sup>9</sup><http://www.artnum.com/en/products/cassandra.php>

where  $\phi$  is the potential,  $e$  is the elementary charge,  $n_i$  is the ion density,  $n_0$  is the undisturbed plasma density,  $k$  is the Boltzmann constant,  $T$  is the temperature, and  $\epsilon_0$  is the permittivity of vacuum, is used (Roussel et al., 2005).

Alltogether, SPIS is a really powerful software to be used when looking at spacecraft charging and similar problems, but one needs to be aware where problems may occur. In the next chapter it will be described how SPIS was used in the case of analyzing the Rosetta spacecraft and its surrounding plasma, first looking at the modelling of the spacecraft and thereafter all the simulation results together with parameters used. More details on the use of SPIS can also be found in Appendix B.

# 2

## SIMULATIONS AND RESULTS

The simulation process has been a bottom-up process, which means that as a first stage, simulation results for Rosetta in vacuum have been reproduced to agree with earlier results, obtained by other software. The plasma was then introduced, and finally also photoelectrons. For each step in the simulation process except the one with photoelectrons, two models have been used; Rosetta with cuboid shaped spacecraft body with booms for the Langmuir probes, and Rosetta with spherical shaped spacecraft body without the booms. The latter model, while simplified, has the advantage that there is no need for a separate simulation for each solar aspect angle (see Section 2.1).

The aim has been to study the most realistic case, which is the one where the photoelectrons are introduced. The most important results will therefore be found in Sections 2.4, 2.5, 2.6, and 2.7. The preceding sections reflect the way the work has been done and how the author introduced more parameters in the simulations. The results from the early sections (Section 2.2 and Section 2.3) will however help the reader in the understanding of the final results and conclusions.

The results are presented as plots of potential at probe positions versus solar aspect angle. Images showing how the potential and the particle density vary around Rosetta are also presented in order to give the reader a qualitative perspective of the plasma behaviour. All these images are taken from simulations where the solar aspect angle is in between  $140^\circ$  and  $150^\circ$ . In some of the simulations where one parameter has been varied, the difference in the result can only be seen by comparing the plots, no difference is seen in the images showing a plane in the plasma. For these cases, the images of the potential or particle density will not be presented.

A complete list of all simulations together with parameters for the simulations is presented in Appendix A. If the simulations are going to be rerun at anytime, it might be useful to have an idea of the simulation times needed. The order of time needed for the simulations presented in this chapter are as follows, for a Linux system running on an AMD dual core 875 2.2 GHz, with 8.2 GB of RAM-memory and 8 GB of swap memory:

- Vacuum: 10 minutes
- Plasma ( $eS U = 40^1$ ): 3-5 hours
- Plasma ( $eS U = 1^1$ ): 10 hours

---

<sup>1</sup>see Appendix D

- Plasma with photoelectrons ( $eSU = 40^1$ ): 5 hours
- Plasma with photoelectrons ( $eSU = 1^1$ ): 24 hours

It should be noted that these times are extremely approximate, and could vary a lot also for the same type of computer. They might however give a hint about the order of time needed.

## 2.1 Geometry

The two models of Rosetta are shown in Figure 2.1 (cuboid) and Figure 2.2 (spherical). The Langmuir probes themselves are not introduced in the models, instead the potential at the point where the probe centers would have been is examined. The models may look simple at a first glance, but when looking at the potential and its behaviour, the models do not need to be very detailed. This would just increase the simulation time, and therefore the models consist only of the spacecraft body, solar panels, and for the cuboid Rosetta also the booms are introduced.

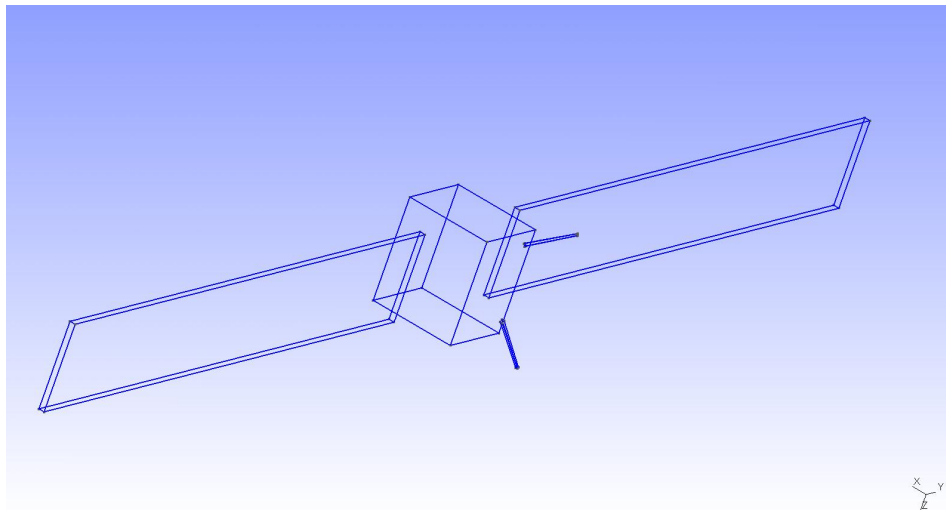


**Figure 2.1:** *The cuboid Rosetta model, with booms.*

The models of Rosetta is put inside a simulation box, with varying dimensions for the different types of simulations. Typical dimensions of the sides are on the order of 30-60 meters, which is chosen so that the boundaries of the box should be at least one or a couple of Debye lengths away from every spacecraft surface. Nested volumes (see Appendix B) have been used to make the meshing tuned to the specific simulation task. An example of the Rosetta model together with simulation box is shown in Figure 2.3.

As the goal is to find how the probes are affected by the spacecraft potential and photoelectron cloud, an angular dependence will be seen. The solar panels and spacecraft body can be rotated independently around the axis following the length of the solar panels. The Sun is in the positive  $x$ -direction and the solar panels will always face the Sun. The

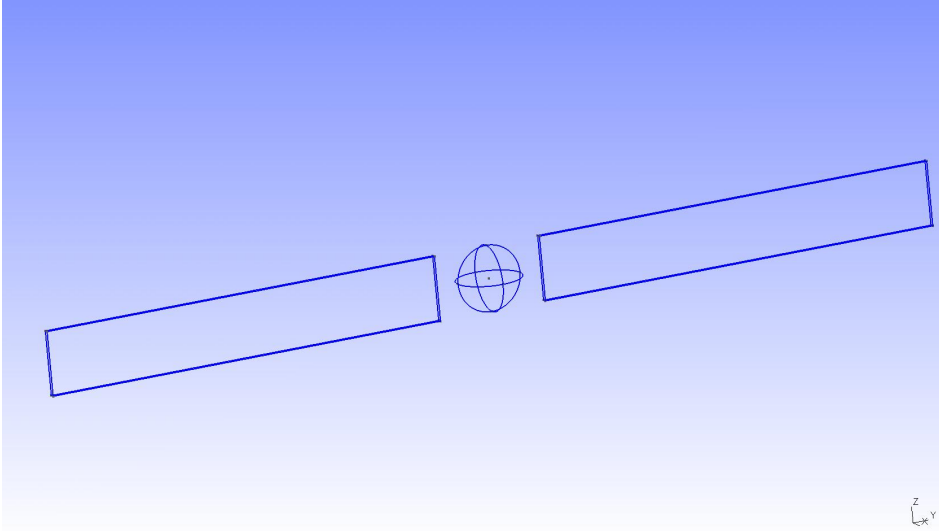


**Figure 2.2:** *The spherical Rosetta model, without booms.*

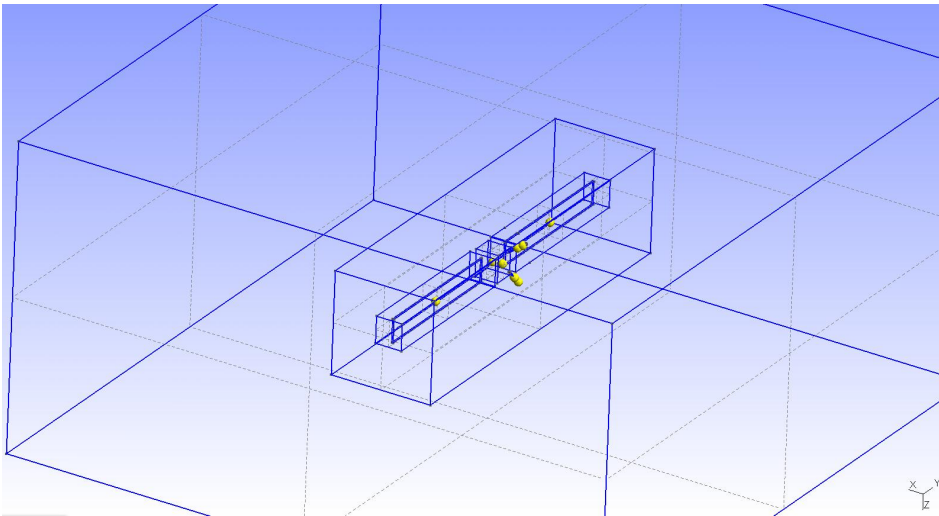


**Figure 2.3:** *The cuboid Rosetta model inside the simulation box.*

solar aspect angle is then defined as the angle the normal of the  $+x$ -axis of the spacecraft body makes with the positive  $x$ -axis, counted clockwise. This is also shown in Figure 2.4.

For the spherical Rosetta, only one simulation is needed in order to know the probe potentials at different solar aspect angles thanks to symmetry. For the cuboid shaped Rosetta, one simulation is needed for each angle. The drawback of the spherical model is when it comes to the photoelectrons. As the booms behave as ‘grounding’ the plasma to spacecraft potential, almost all the way to the probe centers, they will attract photoelectrons from the surrounding photoelectron cloud. Therefore the booms play an important

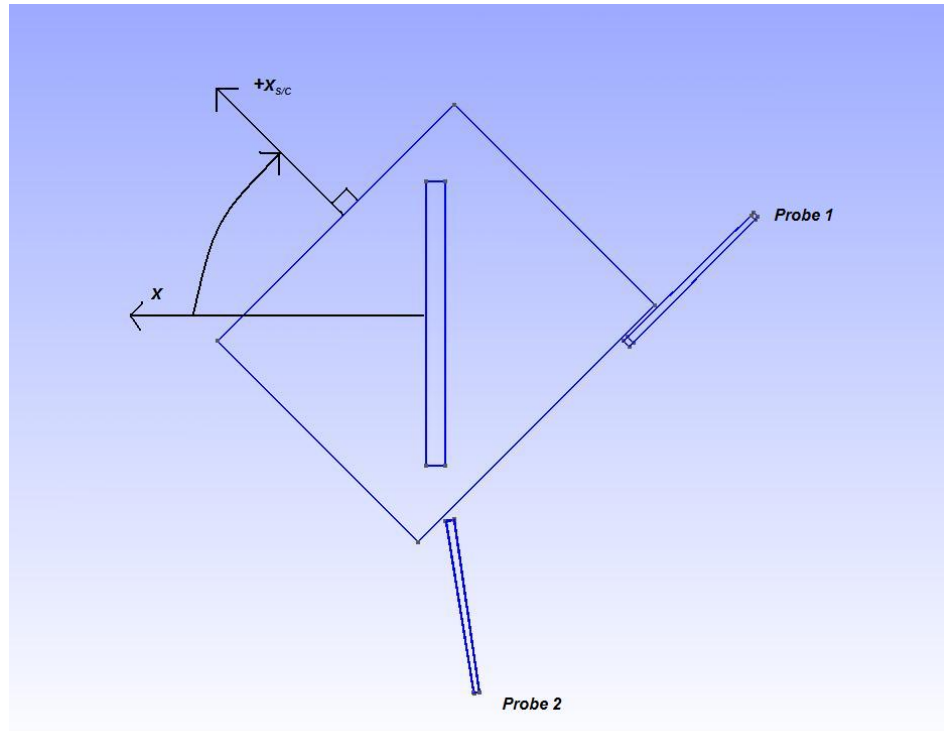


**Figure 2.4:** The solar aspect angle is defined as the angle the normal of the '+x' surface of the spacecraft body makes with the positive x-axis (direction of the Sun), counted clockwise. In this picture this angle is about 45°.

role in the simulation where photoelectrons are included (as they do in reality), and the spherical model is not used in these simulations as it lacks this feature.

In all the simulations, the spacecraft potential is locked at a given value, which has been set to either 0, 5, or 10 V. Various parameters have then been changed and results are compared to see the effect of the parameters.

For the simulations done, the description together with the results, usually a plot of the potential for various solar aspect angles, will be presented first. After that the results will be compared with applicable data and an interpretation will be done of the differences or similarities in the comparison.

## 2.2 Vacuum

### 2.2.1 Previous Work

For the vacuum case, earlier simulations have been done on Rosetta. It has been simulated with a vacuum code, both for the spherical and cuboid case by Chris Cully at IRF in Uppsala using a completely different numerical code, described in Cully et al. (2007). For the cuboid case, the potential against solar aspect angle is shown in Figure 2.5 and the same plot for the spherical case, without booms, is seen in Figure 2.6. As expected, the probe potentials show a  $180^\circ$  periodic behaviour, as there is no plasma flowing and the largest contribution to the variations is the potential from the solar panels. The first step is now to create similar plots with SPIS, which is done in the two following subsections.

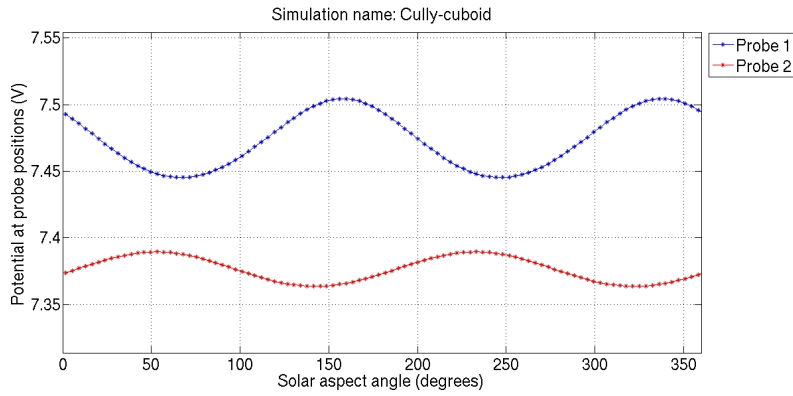


**Figure 2.5:** Cully cuboid; potential at probe positions as a function of solar aspect angle in vacuum. Chris Cully (IRF Uppsala) simulation of a cuboid Rosetta with booms. Parameters: No plasma,  $V_{S/C} = 10$  V. Simulation name: Cully Cuboid.

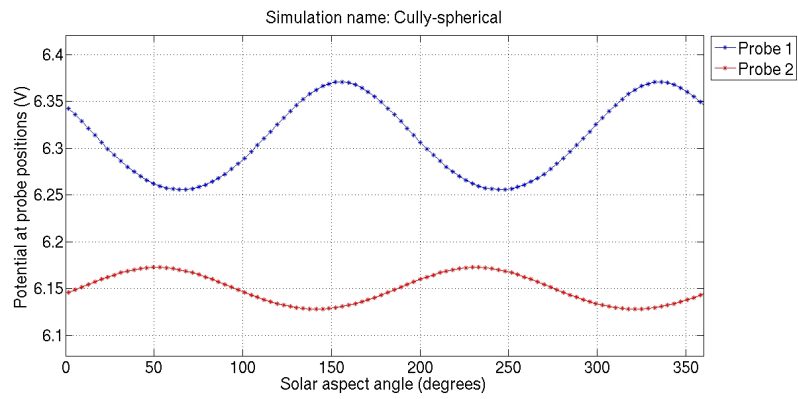


**Figure 2.6:** *Cully spherical; potential at probe positions as a function of solar aspect angle in vacuum. Chris Cully (IRF Uppsala) simulation of a spherical Rosetta without booms. Parameters: No plasma,  $V_{S/C} = 10$  V. Simulation name: Cully Spherical.*

### 2.2.2 Cuboid Shaped Rosetta

To be able to look at the potential at the probe positions for varying solar aspect angles with the cuboid Rosetta, one simulation is needed for each angle. In the case of vacuum, the simulations were done with a  $10^\circ$  interval. The result is shown in Figure 2.7. The potential at the probe positions peak at  $150^\circ$  and  $330^\circ$  for probe 1, which are the angles when this probe is closest to the solar panels. The same behaviour, with smaller amplitude, can be seen for probe 2. The reason for the smaller amplitude can be understood from that this probe is further away from the solar panels and the effect therefore diminishes.

In the case of vacuum, the plot should show a  $180^\circ$  periodical behaviour. This periodicity is not clear in the plots presented, which shows the numerical uncertainties in the simulations.

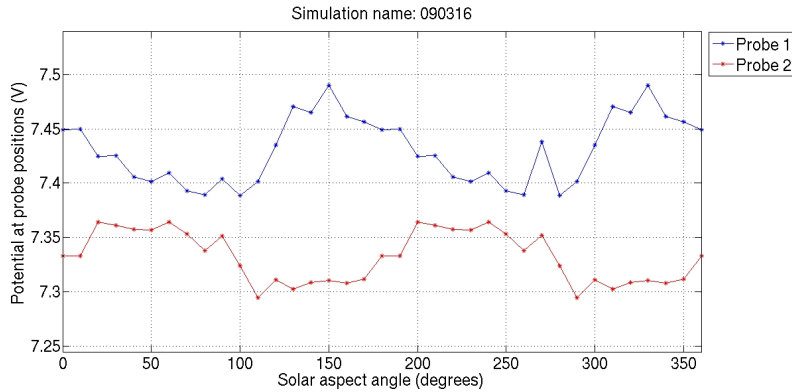


**Figure 2.7:** Cuboid Rosetta in vacuum; potential at probe positions as a function of solar aspect angle in vacuum. Simulation of a cuboid Rosetta with booms. Parameters: No plasma,  $V_{S/C} = 10$  V. Simulation name: 090316.

In Figure 2.8 the SPIS simulation is shown on top of the plot from the Cully simulation. To be able to compare amplitudes, the values from the SPIS simulation are shifted  $+0.04$  V to get a similar DC-level as the Cully simulation. The difference of  $0.04$  V is lower than  $1\%$  of the DC-values, and small errors like this could have reasons such as meshing.

The potential around Rosetta in vacuum is shown in Figure 2.9 (XY-plane), Figure 2.10 (XZ-plane), and Figure 2.11 (YZ-plane). In these cases, the solar aspect angle is  $150^\circ$ . For reasons that has to do with simulation settings, the solar panels were rotated instead of the spacecraft body when varying the solar aspect angle, which gives the same result as this is a vacuum simulation where the solar direction is irrelevant. Hence, in Figure 2.10 it looks like the solar aspect angle, as defined in section 2.1, is at  $0^\circ$ , which is not the case. For the spherical Rosetta, which is the next section, no rotation at all is needed as mentioned before, one simulation gives the results.

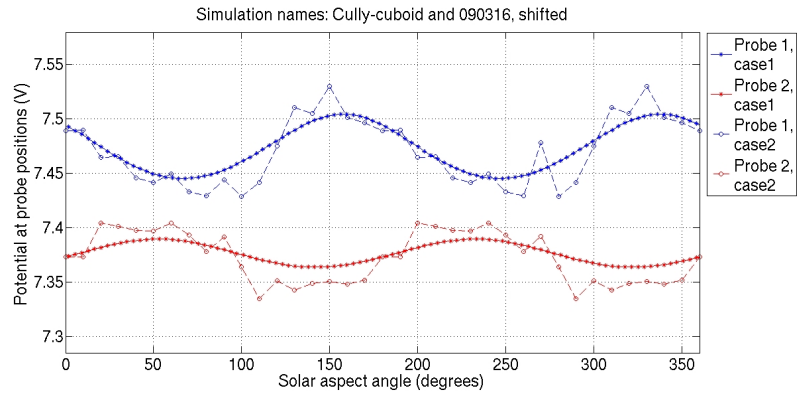


**Figure 2.8:** Different models in vacuum; potential at probe positions as a function of solar aspect angle in vacuum for two cases: 1) Cully cuboid simulation, 2) SPIS cuboid simulation (shifted +0.04 V). Parameters: No plasma,  $V_{S/C} = 10$  V. Simulation names: Cully Cuboid and 090316.

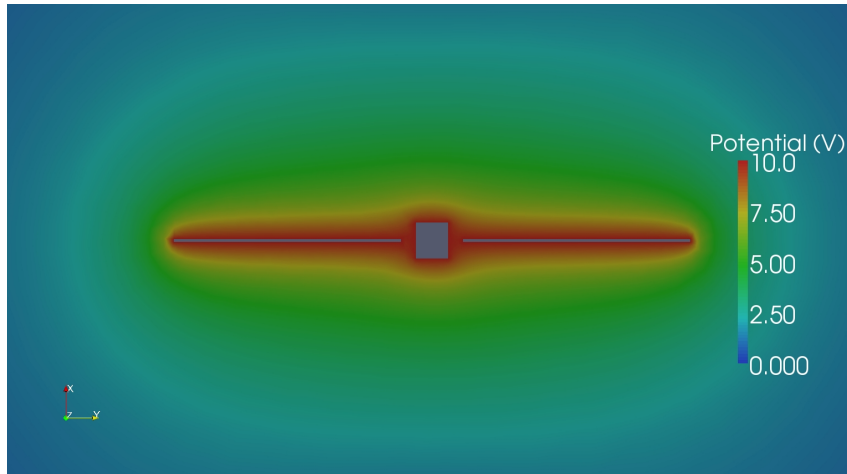


**Figure 2.9:** Cuboid Rosetta in vacuum; potential in V around Rosetta in the XY-plane. The solar aspect angle for this model is 150°. In this simulation the solar panels were rotated instead of the spacecraft body, which gives the same result as there is no plasma. Parameters: No plasma,  $V_{S/C} = 10$  V. Simulation name: 090316

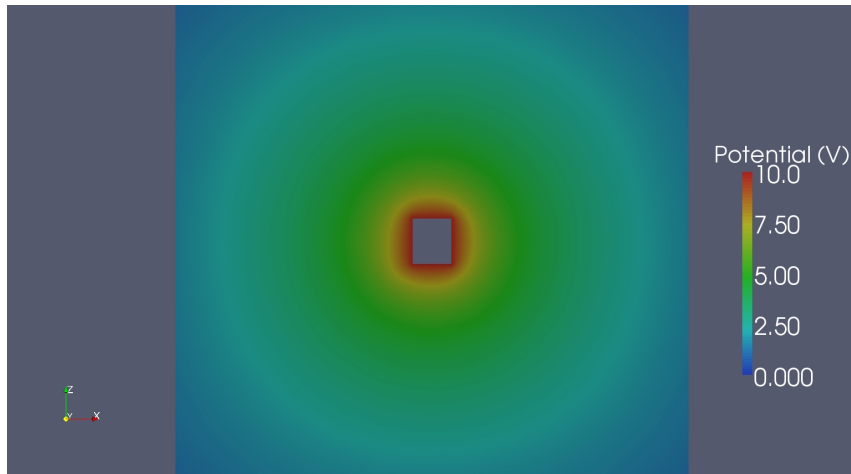


**Figure 2.10:** *Cuboid Rosetta in vacuum; potential in V around Rosetta in the XZ-plane. Parameters: No plasma,  $V_{S/C} = 10$  V. Simulation name: 090316*

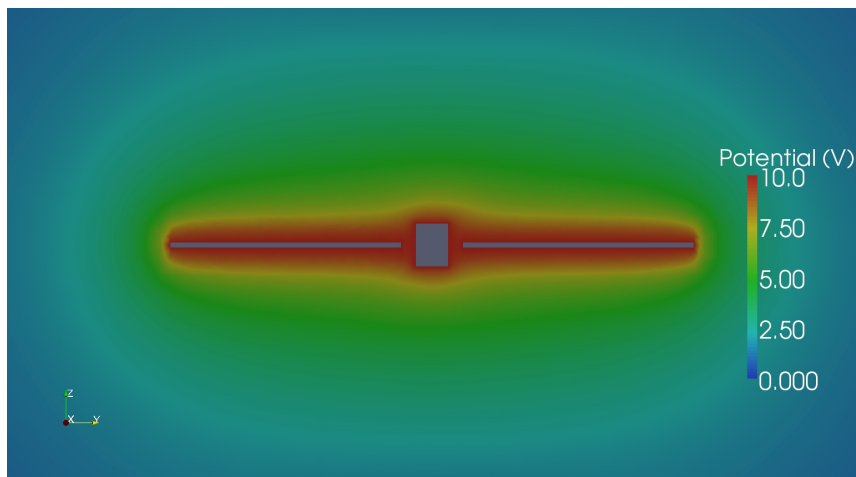


**Figure 2.11:** *Cuboid Rosetta in vacuum; potential in V around Rosetta in the YZ-plane. Parameters: No plasma,  $V_{S/C} = 10$  V. Simulation name: 090316*

### 2.2.3 Spherical Rosetta

For the spherical Rosetta, the vacuum simulation has been done in two cases; one with spacecraft potential at 10 V, see Figure 2.12 and one with spacecraft potential at 5 V, see Figure 2.13. As can be seen, the amplitude of the potential change due to the solar panels seems to scale linearly with the spacecraft potential, which is expected for a vacuum simulation where the only non-homogeneous boundary condition is the spacecraft potential. The DC-level of the potential at the probe positions differs of course. Other than that, the two plots behave similar.

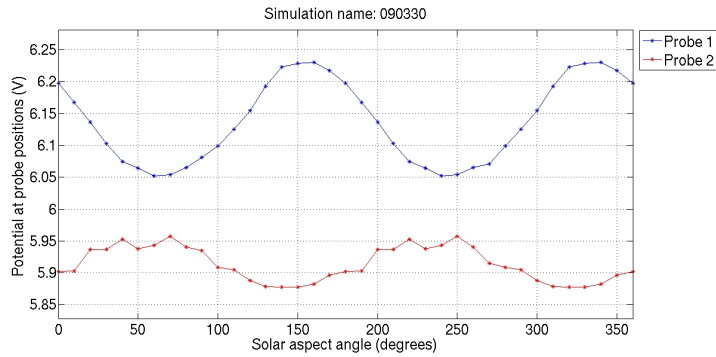


**Figure 2.12:** Spherical Rosetta in vacuum; potential at probe positions as a function of solar aspect angle in vacuum. Simulation of a spherical Rosetta without booms. Parameters: No plasma,  $V_{S/C} = 10$  V. Simulation name: 090330.

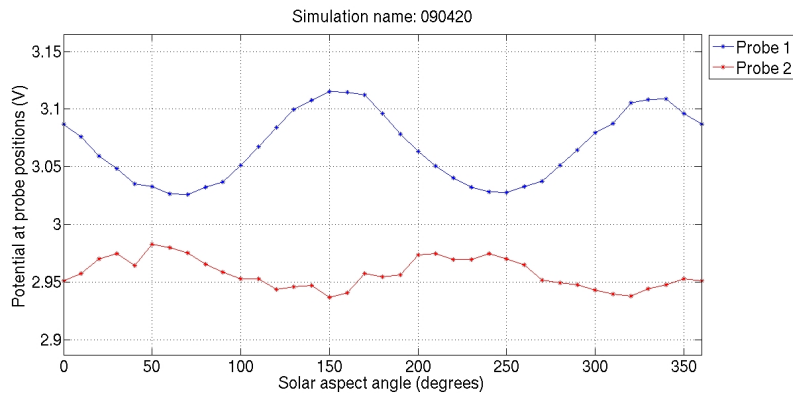


**Figure 2.13:** Spherical Rosetta in vacuum; potential at probe positions as a function of solar aspect angle in vacuum. Simulation of a spherical Rosetta without booms. Parameters: No plasma,  $V_{S/C} = 5$  V. Simulation name: 090420.

To examine if the potential around Rosetta scales linearly, the two simulation results are plotted together in Figure 2.14, where the potential values for the 10 V simulation have been divided by 2. This plot clearly shows that the potential at the position of the probes scales linearly with the spacecraft potential in the case of vacuum, so the simulation passes this first sanity check.

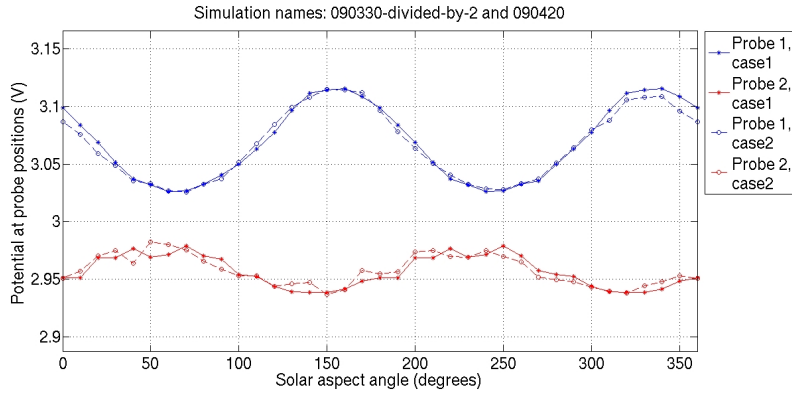


**Figure 2.14:** Varying spacecraft potential in vacuum; potential at probe positions as a function of solar aspect angle in vacuum for two cases; 1)  $V_{S/C}$  is 10 V, potentials at probe positions in the result is divided by two, 2)  $V_{S/C}$  is 5 V. The plot shows that the potential at probe positions scales linearly with the spacecraft potential in vacuum. Parameters: No plasma. Simulation names: 090330 and 090420.

In Figure 2.15, the spherical Rosetta simulation in vacuum is plotted together with the Cully simulation for the spherical Rosetta. For the SPIS simulation, potentials for probe 1 is shifted +0.17 V and values for probe 2 is shifted +0.23 V, so that the two simulations vary around the same DC-level. The amplitude in the SPIS simulations is larger than in the Cully simulation. The reason for this could be due to differences in how the solar panels are modelled. In the SPIS simulation the solar panels are modelled with a thickness of 15 cm, whereas in the Cully simulation they are modelled as a 2-dimensional surface with surface potential.

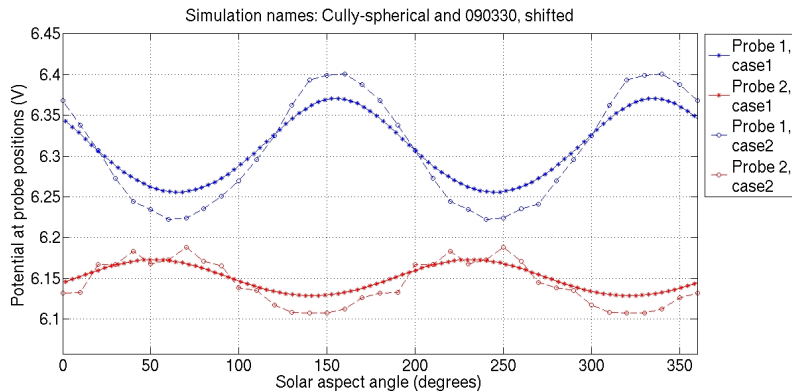


**Figure 2.15:** Different models in vacuum; potential at probe positions as a function of solar aspect angle in vacuum for two cases; 1) Cully simulation, 2) SPIS simulation (shifted +0.17 V for probe 1 and +0.23 V for probe 2). Parameters: No plasma,  $V_{S/C} = 10$  V. Simulation names: Cully and 090330.

The potential around Rosetta is shown in Figure 2.16 (XY-plane), Figure 2.17 (XZ-plane) and Figure 2.18 (YZ-plane). As it is earlier shown that the potential at the probe positions scales linearly with the spacecraft potential, the images showing how the vacuum potential varies around Rosetta for the case of 5 V spacecraft potential looks the same, but with a different scale of course. As there is no plasma flowing in any direction, the potential shows a symmetrical behaviour in front of and behind the spacecraft. This will definitely not be the case for the simulations in the next section, where the solar wind will be flowing from the Sun direction, creating a wake behind the spacecraft.

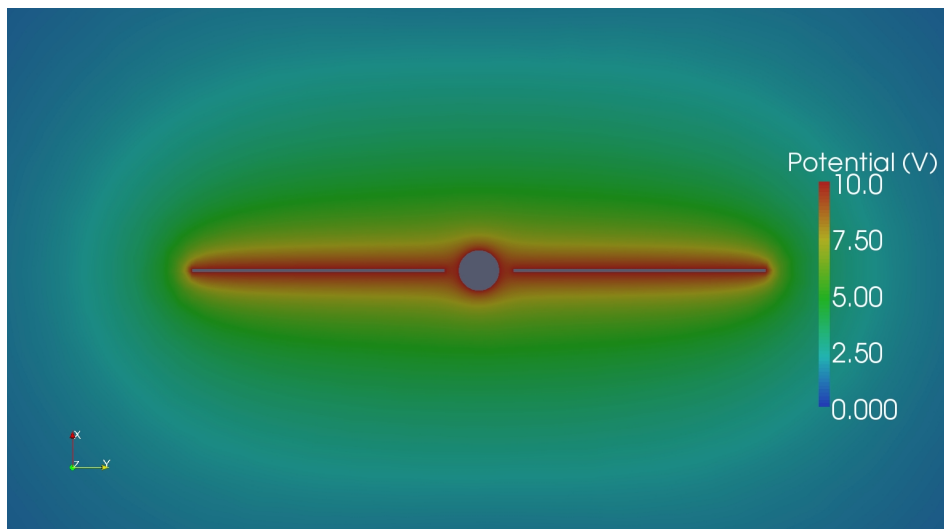


**Figure 2.16:** Spherical Rosetta in vacuum; potential in V around Rosetta in the XY-plane. Parameters: No plasma  $V_{S/C} = 10$  V. Simulation name: 090330

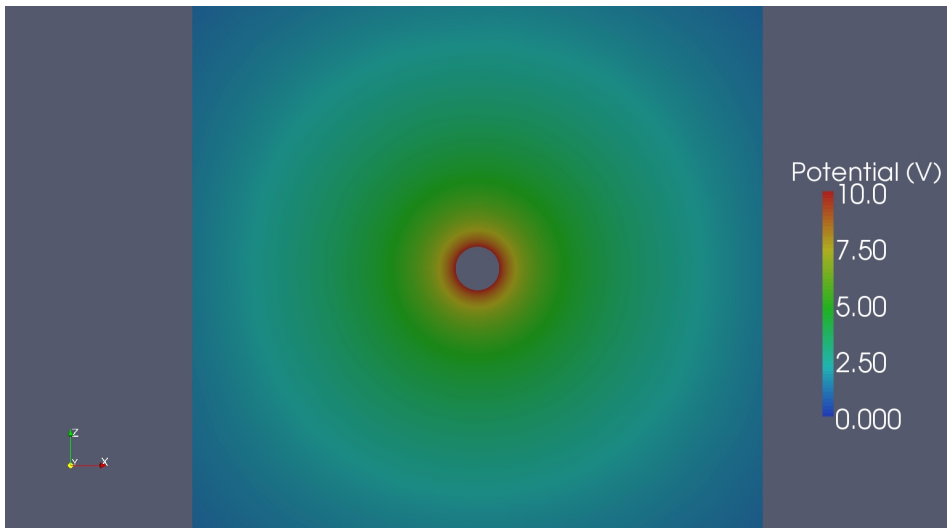


**Figure 2.17:** Spherical Rosetta in vacuum; potential in V around Rosetta in the XZ-plane. Parameters: No plasma,  $V_{SJC} = 10$  V. Simulation name: 090330

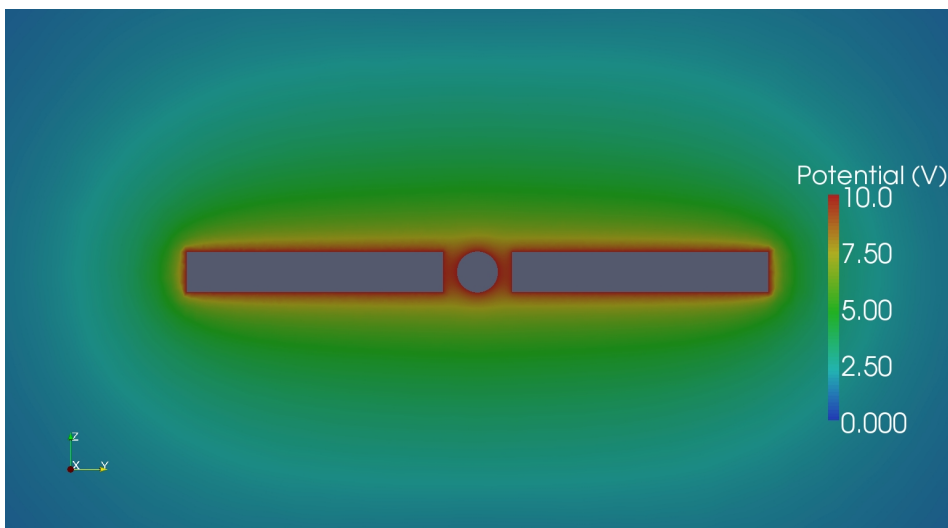


**Figure 2.18:** Spherical Rosetta in vacuum; potential in V around Rosetta in the YZ-plane. Parameters: No plasma,  $V_{SJC} = 10$  V. Simulation name: 090330.

### 2.3 Plasma without Photoelectrons

The simulations in plasma have been done in order to examine how big the drop in potential is inside the wake created behind the spacecraft, and to examine how the wake signature scales with electron and ion temperatures. No photoelectrons are introduced in any of the simulations in this section. As the probes are sometimes blocked from the flowing solar wind by the spacecraft body or solar panels, they will for some angles be inside the wake. In the simulations, the two earlier models of Rosetta (cuboid and spherical) have been used. It has also been examined how much these two models differ.

In order to speed up the simulations there is a parameter called *electronSpeedUp*, which if set to a value  $p$  causes SPIS to only track the electrons during a fraction  $\frac{1}{p}$  of the time step used for the ions, which is a useful approximation under certain circumstances. When introducing the photoelectrons, it can be shown that the result of the simulations differ when varying the *electronSpeedUp*, but this has not been the case when simulations are done with flowing plasma but without photoelectrons. Therefore, a different value of this parameter has been used in the non-photoelectron case and the photoelectron case. A more detailed description of this parameter and its effects is presented in Appendix D.

The parameters for the solar wind that are used as ‘reference’ parameters, and then sometimes varied, are:

- Electron temperature ( $T_e$ ): 12 eV
- Ion temperature ( $T_i$ ): 5 eV
- Density ( $n$ ):  $5 \text{ cm}^{-3}$
- Ion flow speed ( $v_i$ ): 400 km/s (flowing in negative  $x$ -direction)
- Spacecraft potential ( $V_{S/C}$ ): 10 V
- *electronSpeedUp* ( $eSU$ ): 40

#### 2.3.1 Cuboid Shaped Rosetta

For the cuboid Rosetta, the result of the simulations with solar wind parameters as above is shown in Figure 2.19. It is clearly visible how probe 1 enters the wake at around  $340^\circ$ , and the lowest potential measured will be at about  $60^\circ$ , which is the angle where probe 1 is right behind the solar panel with respect to the Sun. For probe 2, the lowest potential is at about  $330^\circ$ , which is the point where the probe is behind the spacecraft body, with respect to the Sun. The amplitude on the variations are similar for the two probes, which could be explained as they will be on a similar depth inside the wake, with respect to the solar panel for probe 1 and spacecraft body for probe 2. The large plateaus, between  $150^\circ$  and  $340^\circ$  for probe 1 and between  $80^\circ$  and  $200^\circ$  for probe 2, are partly due to effects already visible in the vacuum simulations and will be further explained in the next section, where the effects are even more clear.

The potential around Rosetta is shown in Figure 2.20 (XY-plane), Figure 2.21 (XZ-plane), and Figure 2.22 (YZ-plane). The Sun is always in the positive  $x$ -direction. In Figure 2.20, the wake can be seen as the dark blue field behind the spacecraft, which also cancels out the potential from the spacecraft itself at a closer distance behind the spacecraft, compared to how the potential behaves in front of the spacecraft. This behaviour

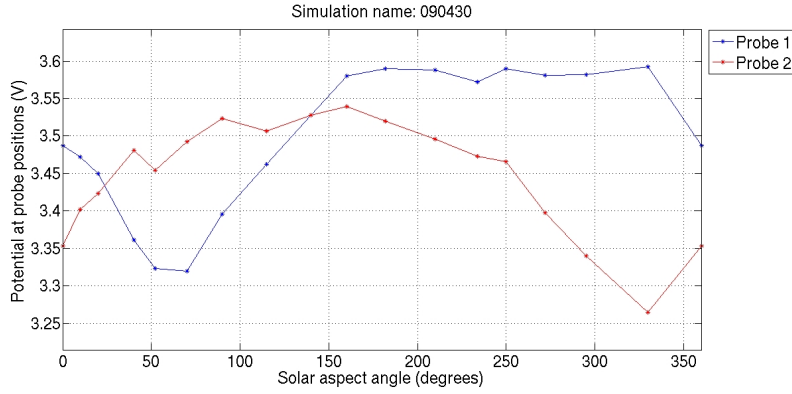


**Figure 2.19:** Cuboid Rosetta reference simulation in plasma without photoelectrons; potential at probe positions as a function of solar aspect angle. Parameters:  $T_e = 12 \text{ eV}$ ,  $T_i = 5 \text{ eV}$ ,  $n = 5 \text{ cm}^{-3}$ ,  $v_i = 400 \text{ km/s}$ ,  $V_{S/C} = 5 \text{ V}$ . Simulation name: 090430

is also seen in Figure 2.21. In Figure 2.22, the wake is not visible as the view is in the direction of the flowing plasma. Therefore, only the symmetrical potential around the spacecraft, due to the spacecraft potential, is visible.

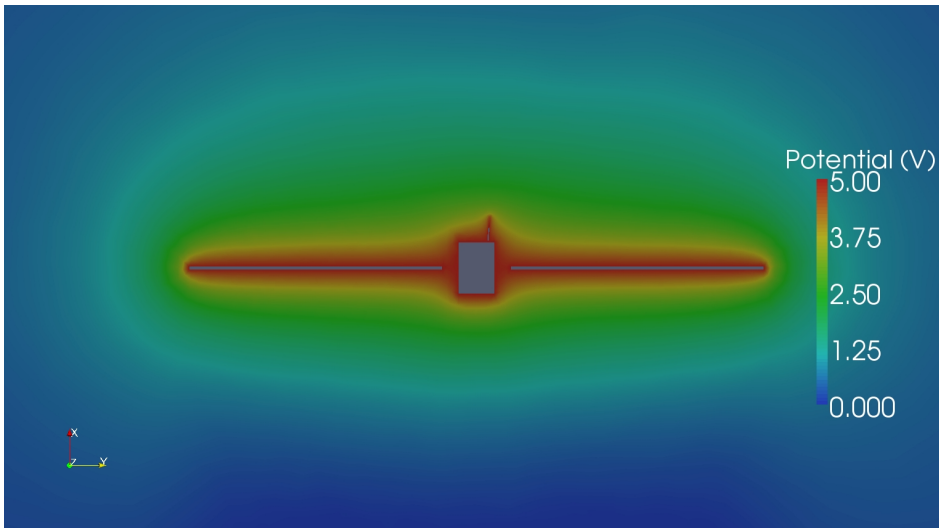


**Figure 2.20:** Cuboid Rosetta reference simulation in plasma without photoelectrons; potential in V around Rosetta in the XY-plane. Parameters:  $T_e = 12 \text{ eV}$ ,  $T_i = 5 \text{ eV}$ ,  $n = 5 \text{ cm}^{-3}$ ,  $v_i = 400 \text{ km/s}$ ,  $V_{S/C} = 5 \text{ V}$ . Simulation name: 090430

Figure 2.23 shows the ion density in the XY-plane. The picture shows that the ion density will be almost zero at the positions of the probes when they are in the middle of the wake (the length of boom 2, which gives a hint of the probe's position in the wake, can be seen in this picture as pointing towards the Sun from the spacecraft body). In Figure

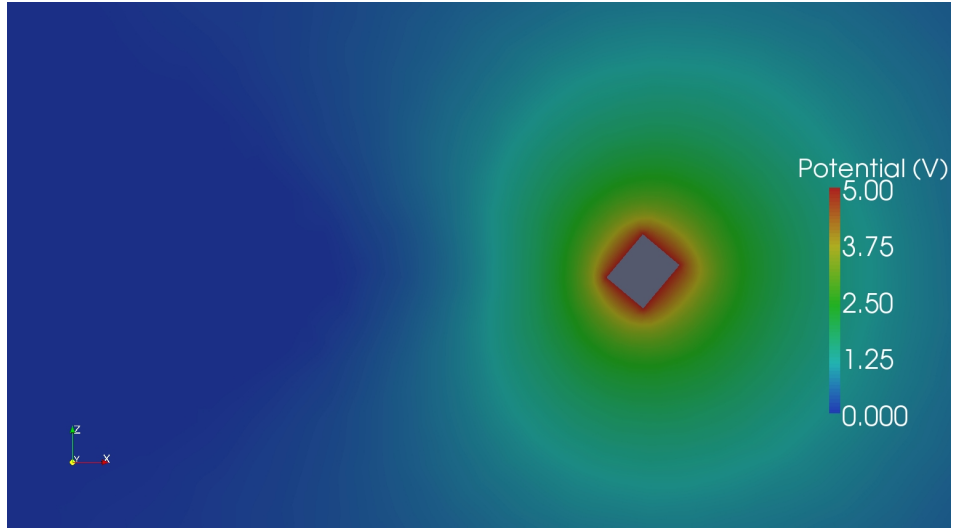


**Figure 2.21:** *Cuboid Rosetta reference simulation in plasma without photoelectrons; potential in V around Rosetta in the XZ-plane. Parameters:  $T_e = 12$  eV,  $T_i = 5$  eV,  $n = 5$  cm<sup>-3</sup>,  $v_i = 400$  km/s,  $V_{S/C} = 5$  V. Simulation name: 090430*

2.24 the wake is seen in another plane (XZ), where the low ion density is clearly visible as the blue part. The density in the YZ-plane is not shown as the density is homogenous in this plane, because the solar wind flows radially out from the Sun.

In order to examine how the electron temperature affects the wake, simulations were made similar to the one in Figure 2.19, but with electron temperature at 6 eV instead of 12 eV. The result is shown in 2.25. By comparing the two cases of varying electron temperature, it can be seen that the difference in the temperature gives rise to a shift of the plot. The comparison is shown in Figure 2.26. The reason for this can be the shorter Debye length in the case of lower electron temperature (see equation 1.1). With the shorter Debye length, the potential from the booms drops off at a faster rate when moving further away from the booms. The amplitude of the wake does not change appreciably. The potential and ion density in the various planes in the case of electron temperature of 6 eV, are similar to the same figures for the 12 eV case, and will therefore not be presented.

A comparison of how the cuboid model of Rosetta differs from the spherical model will be presented in the next section, together with simulation results of the spherical model in a plasma.

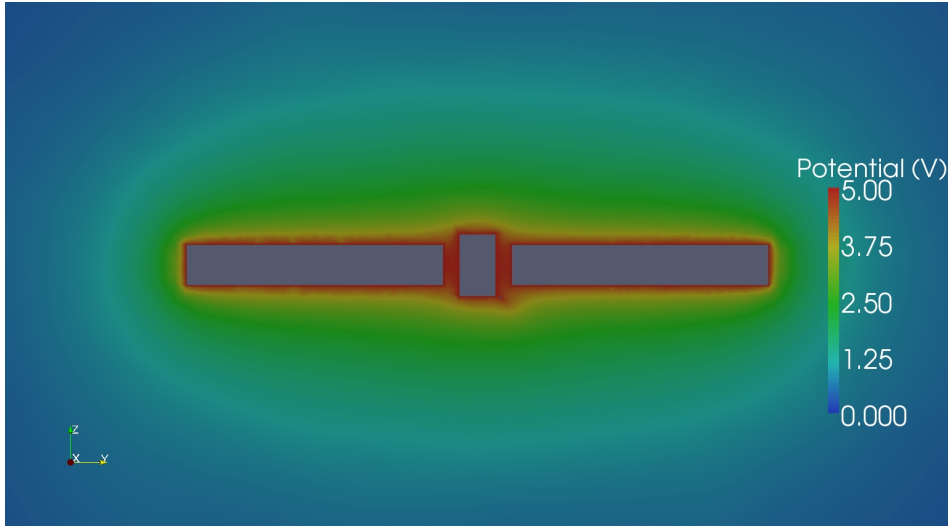


**Figure 2.22:** Cuboid Rosetta reference simulation in plasma without photoelectrons; potential in V around Rosetta in the YZ-plane. Parameters:  $T_e = 12$  eV,  $T_i = 5$  eV,  $n = 5$  cm<sup>-3</sup>,  $v_i = 400$  km/s,  $V_{S/C} = 5$  V. Simulation name: 090430

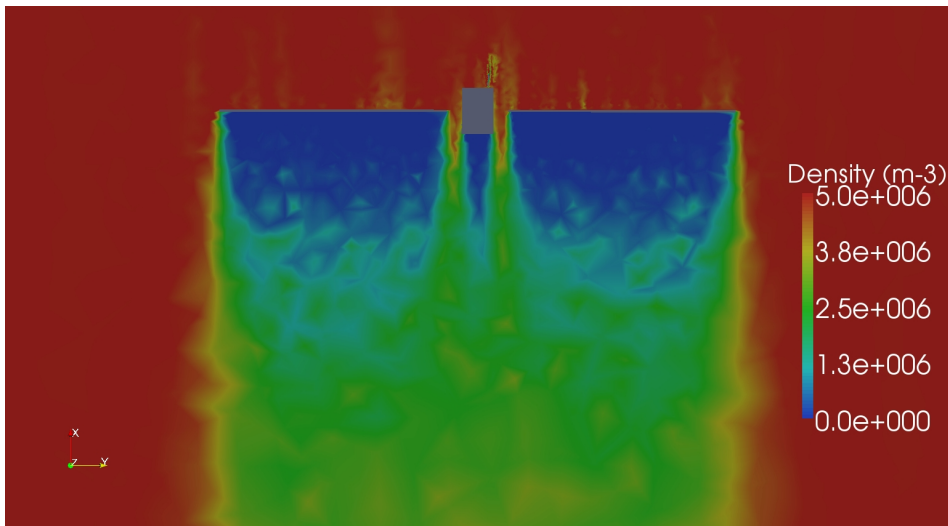


**Figure 2.23:** Cuboid Rosetta reference simulation in plasma without photoelectrons; ion density in m<sup>-3</sup> around Rosetta in the XY-plane. Parameters:  $T_e = 12$  eV,  $T_i = 5$  eV,  $n = 5$  cm<sup>-3</sup>,  $v_i = 400$  km/s,  $V_{S/C} = 5$  V. Simulation name: 090430

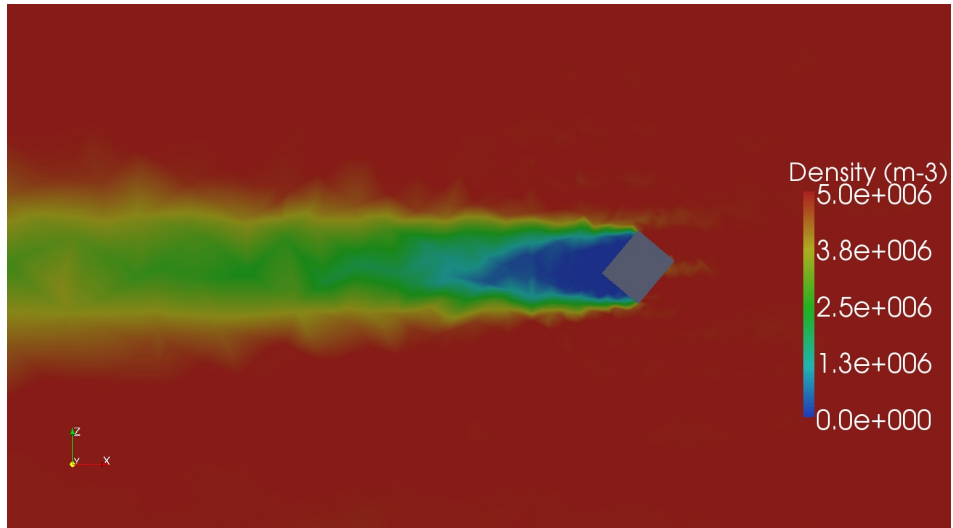


**Figure 2.24:** Cuboid Rosetta reference simulation in plasma without photoelectrons; ion density in  $m^{-3}$  around Rosetta in the XZ-plane. Parameters:  $T_e = 12$  eV,  $T_i = 5$  eV,  $n = 5$   $cm^{-3}$ ,  $v_i = 400$  km/s,  $V_{S/C} = 5$  V. Simulation name: 090430

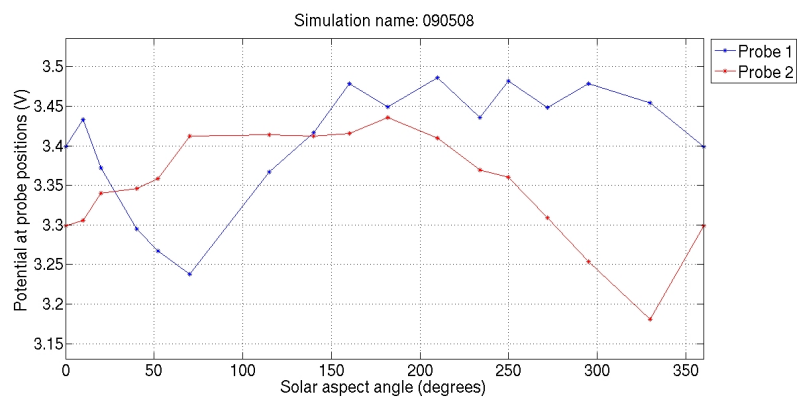


**Figure 2.25:** Low electron temperature; potential at probe positions as a function of solar aspect angle. Parameters:  $T_e = 6$  eV,  $T_i = 5$  eV,  $n = 5$   $cm^{-3}$ ,  $v_i = 400$  km/s,  $V_{S/C} = 5$  V. Simulation name: 090508

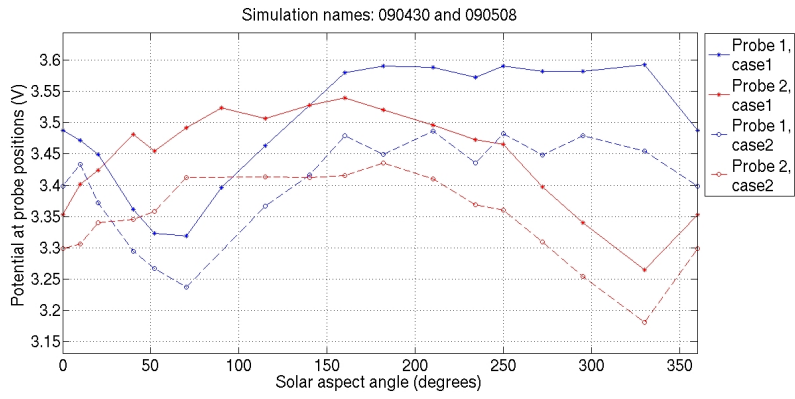


**Figure 2.26:** Varying electron temperature; potential at probe positions as a function of solar aspect angle for two cases; 1)  $T_e = 12$  eV, 2)  $T_e = 6$  eV. Parameters:  $T_i = 5$  eV,  $n = 5$  cm<sup>-3</sup>,  $v_i = 400$  km/s,  $V_{S/C} = 5$  V. Simulation names: 090430 and 090508

### 2.3.2 Spherical Rosetta

In the previous section it was shown how the electron temperature affects the results using the cuboid Rosetta model. In this section the effect of various ion temperature will be examined, using the spherical Rosetta model. Other than the reference ion temperature of 5 eV, also 12 eV has been used. The two ion temperatures were simulated with spacecraft potential of 0 V and 5 V in order to further examine the scaling due to various spacecraft potential.

The influence of the ion temperature was extremely small, so the results for the two different ion temperatures will therefore be presented in the same plots at once. For the case where the spacecraft potential was locked to 0 V, the result is shown in Figure 2.27. The only signature seen in the plot is from the wake, at  $60^\circ$  for probe 1 and  $330^\circ$  for probe 2, as noted in the previous section. The small positive potential showing up  $180^\circ$  from the wakes for the two probes, respectively, is most likely an effect of the code itself and has no physical meaning.

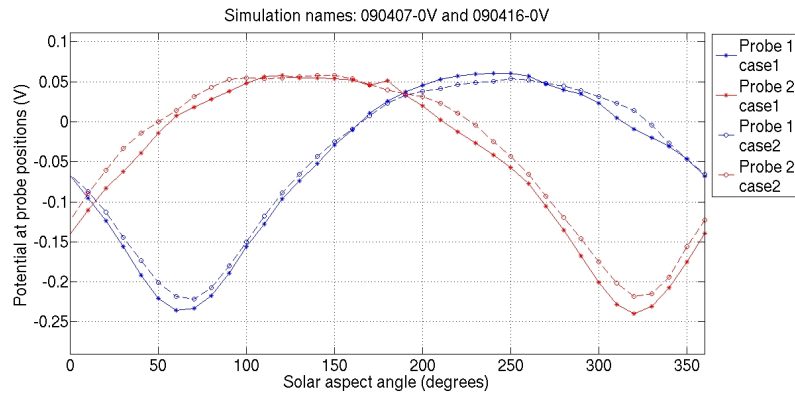


**Figure 2.27:** Varying ion temperature; potential at probe positions as a function of solar aspect angle for two cases; 1)  $T_i = 12$  eV, 2)  $T_i = 5$  eV. Parameters:  $T_e = 12$  eV,  $n = 5$   $\text{cm}^{-3}$ ,  $v_i = 400$  km/s,  $V_{S/C} = 0$  V. Simulation names: 090407 0V and 090416 0V

In the case of spacecraft potential at 5 V, the result is shown in Figure 2.28. One notable difference from the 0 V simulation in Figure 2.27 is the flattened part of the curve, between  $160^\circ$  and  $320^\circ$  for probe 1 and between  $50^\circ$  and  $210^\circ$  for probe 2. This flattening is due to the fact that the curve showing probe potential as a function of solar aspect angle in vacuum has a minimum for these angles, see for example Figure 2.12. The potential from the solar panels will increase the potential for all angles, compared to the 0 V simulation, but with varying amount due to the angular variations. A small drop in the potential is also visible in the middle of the flattened part of the curves, which is where the potential variations only due to the solar panel is at its absolute minimum.

The potential around the spherical Rosetta for the 5 V case is shown in Figure 2.29 (XY-plane), Figure 2.30 (XZ-plane), and Figure 2.31 (YZ-plane), the ion densities are shown in Figure 2.32 (XY-plane) and Figure 2.33 (XZ-plane). The same wake as in the case of a cuboid Rosetta is seen here. Please note that the Sun is in the negative  $x$ -direction here, which does not change any definitions thanks to the symmetry of the

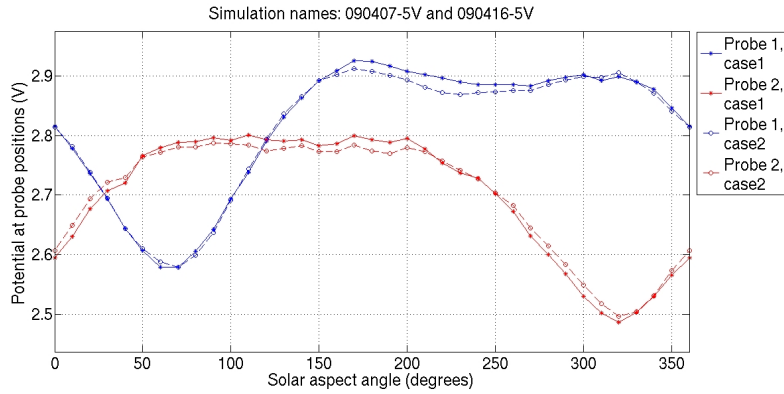


**Figure 2.28:** Varying ion temperature; potential at probe positions as a function of solar aspect angle, two cases; 1)  $T_i = 12$  eV, 2)  $T_i = 5$  eV. Parameters:  $T_e = 12$  eV,  $n = 5$  cm<sup>-3</sup>,  $v_i = 400$  km/s,  $V_{S/C} = 5$  V. Simulation names: 090407 5V and 090416 5V

spherical model.

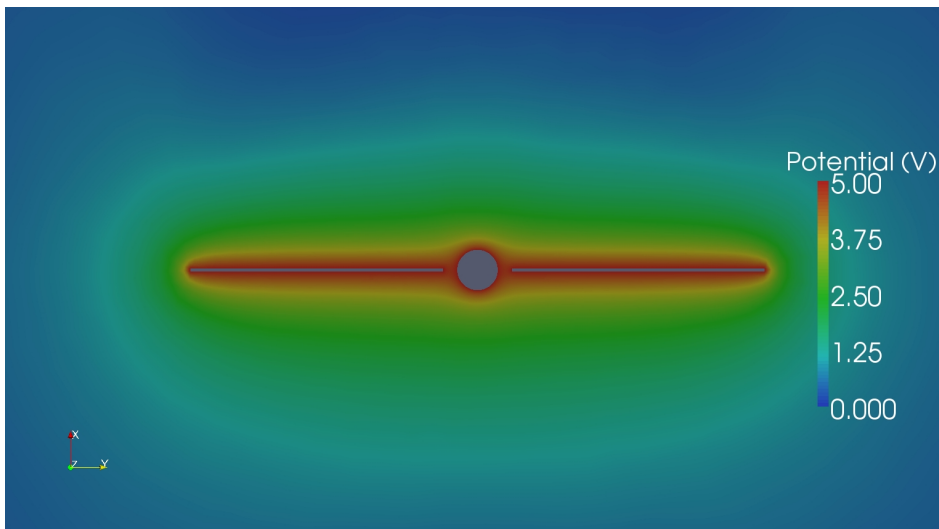


**Figure 2.29:** Low spacecraft potential without photoelectrons; potential in V around Rosetta in the XY-plane. Parameters:  $T_e = 12$  eV,  $T_i = 5$  eV,  $n = 5$  cm<sup>-3</sup>,  $v_i = 400$  km/s,  $V_{S/C} = 5$  V. Simulation name: 090416 5V

It was examined if the added effect of solar panel potential together with the wake was a linear superposition. This was done by plotting a superposition of the 0 V plasma simulation (named 090416 0V) and the vacuum simulation for spacecraft potential at 5 V (named 090420) together with the 5 V plasma simulation (named 090416 5V). The result is shown in Figure 2.34, where superpositioned simulations are shifted -0.2 V. This shows that to good approximation, this actually is a linear superposition, and the effects

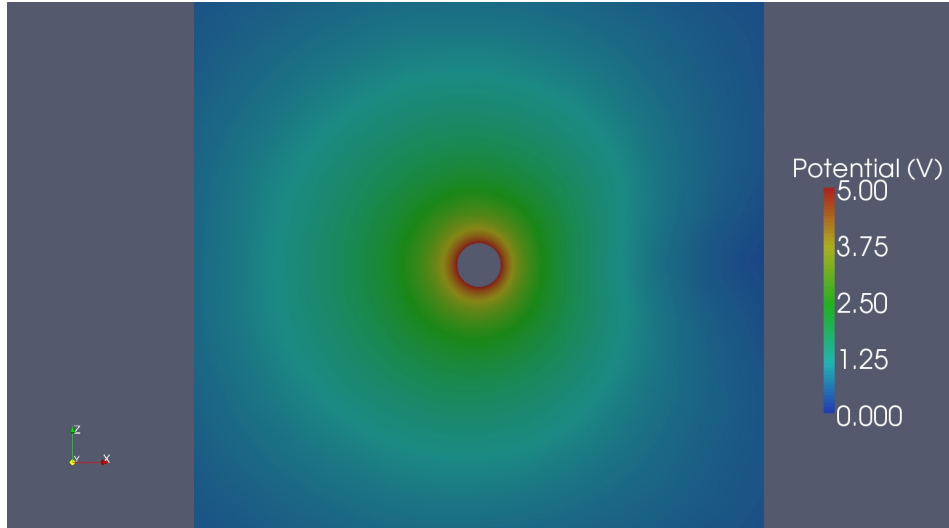


**Figure 2.30:** *Low spacecraft potential without photoelectrons; potential in V around Rosetta in the XZ-plane. Parameters:  $T_e = 12$  eV,  $T_i = 5$  eV,  $n = 5$  cm<sup>-3</sup>,  $v_i = 400$  km/s,  $V_{S/C} = 5$  V. Simulation name: 090416 5V*

of the wake and the solar panels can be modelled individually, and then added together. An explanation for the missing 0.2 V has not been found though, and might need more simulations to examine.

To be able to point out possible errors in any of the two models, it was examined how they relate to each other. This was done by using the reference values for the solar wind, as stated in the beginning of this chapter. The result is shown in Figure 2.35, where the potentials for the spherical model have been shifted +0.7 V. The lower potential for the spherical model at the probe positions is due to the lack of booms in that model, which will definitely lower the potential measured. Except for this variation, it is clear that the two models are quite consistent with each other and show a significant wake structure and also the flattened part of the curve, due to the potential of the solar panels as discussed earlier.

The signature from the wake structure is definitely found, and the question now is how big this effect is compared to the effect of photoelectrons from the spacecraft and solar panels. This is what will be examined in the next section.

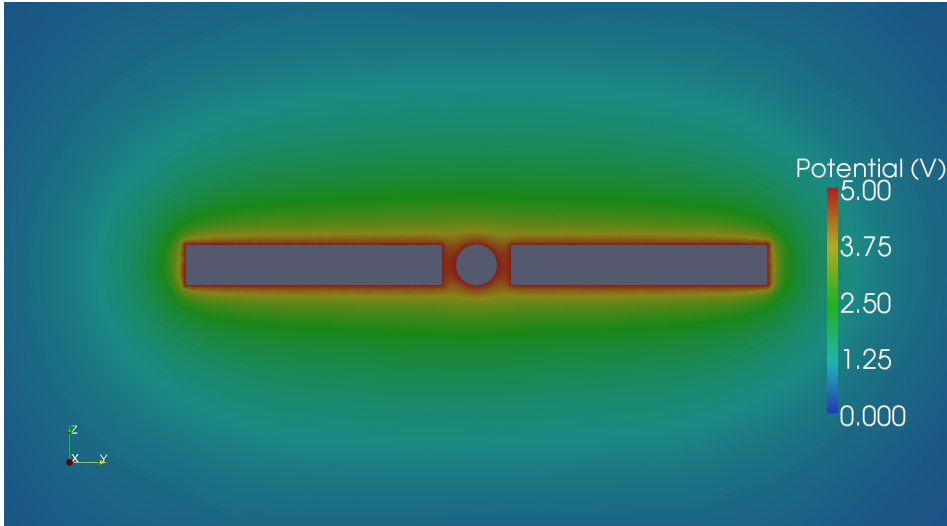


**Figure 2.31:** Low spacecraft potential without photoelectrons; potential in V around Rosetta in the YZ-plane. Parameters:  $T_e = 12$  eV,  $T_i = 5$  eV,  $n = 5$  cm<sup>-3</sup>,  $v_i = 400$  km/s,  $V_{S/C} = 5$  V. Simulation name: 090416 5V

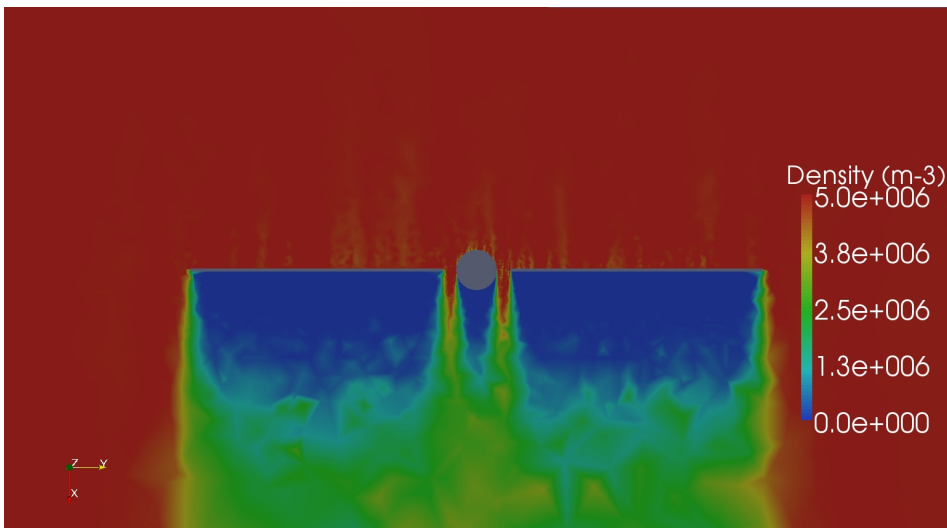


**Figure 2.32:** Low spacecraft potential without photoelectrons; ion density in m<sup>-3</sup> around Rosetta in the XY-plane. Parameters:  $T_e = 12$  eV,  $T_i = 5$  eV,  $n = 5$  cm<sup>-3</sup>,  $v_i = 400$  km/s,  $V_{S/C} = 5$  V. Simulation name: 090416 5V

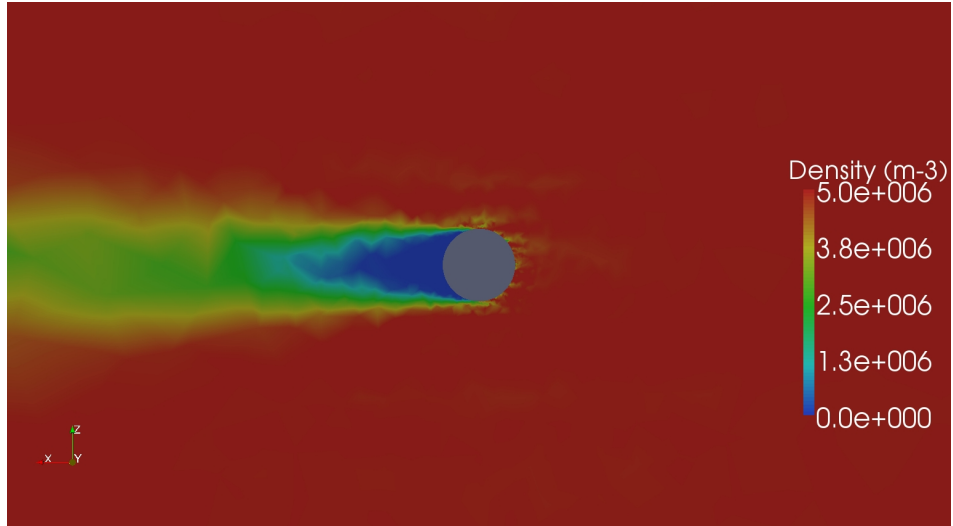


**Figure 2.33:** Low spacecraft potential without photoelectrons; ion density around Rosetta in the XZ-plane. Parameters:  $T_e = 12$  eV,  $T_i = 5$  eV,  $n = 5$   $\text{cm}^{-3}$ ,  $v_i = 400$  km/s,  $V_{S/C} = 5$  V. Simulation name: 090416 5V

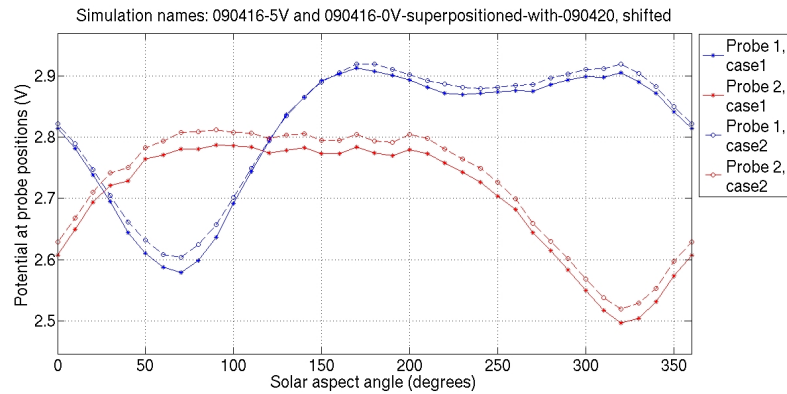


**Figure 2.34:** Superpositioning of various spacecraft potential; potential at probe positions as a function of solar aspect angle for two cases; 1)  $V_{S/C} = 5$  V in plasma, 2) Superposition of  $V_{S/C} = 0$  V in plasma and  $V_{S/C} = 5$  V in vacuum (shifted -0.2 V). The plot shows that the effect from the solar panels and the wake can be added linearly to see the combined effect. Parameters:  $T_e = 12$  eV,  $T_i = 5$  eV,  $n = 5$   $\text{cm}^{-3}$ ,  $v_i = 400$  km/s. Simulation names: 090416 5V and 090416 0V superpositioned with 090420 5V.

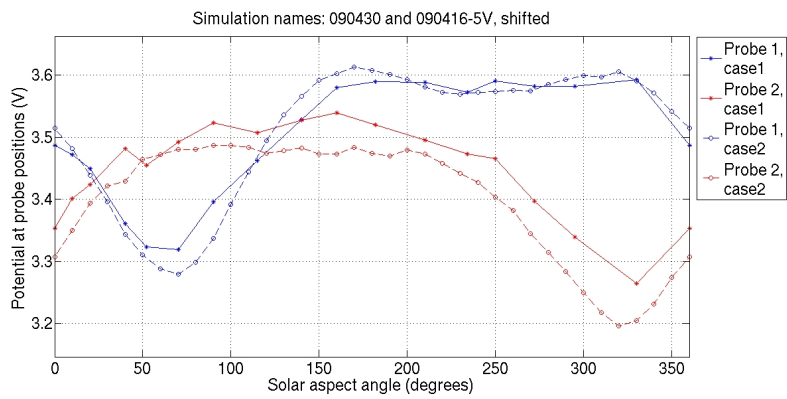


**Figure 2.35:** Different models in plasma; potential at probe positions as a function of solar aspect angle for two cases; 1) Cuboid Rosetta with booms, 2) Spherical Rosetta without booms (shifted +0.7 V). Parameters:  $T_e = 12$  eV,  $T_i = 5$  eV,  $n = 5$  cm<sup>-3</sup>,  $v_i = 400$  km/s,  $V_{S/C} = 5$  V. Simulation names: 090430 and 090416 5V.

## 2.4 Plasma and Photoelectrons - Reference Simulation

In order to get the most realistic case, the photoelectrons need to be introduced. As mentioned earlier, the spherical Rosetta is not a model to be used when photoelectrons are introduced, instead all the simulations are done with the cuboid Rosetta. For the photoelectron simulations, there is one reference simulation (named 090611) and other simulations are introduced and compared to the simulation 090611. Every sunlit surface emits photoelectrons according to the UV intensity of the sunlight. The intensity depends on the angle of the sunlit surface with respect to the Sun and the distance from the Sun. They are not all emitted from the spacecraft with the same energy, and are usually assumed to be Boltzmann distributed with characteristic temperature  $T_{ph}$ . The characteristic energy  $KT_{ph}$  determines the distance they can move away from the surface potential of the spacecraft.

There is however one drawback with SPIS when it comes to the photoelectrons. SPIS does not recognize whenever a surface that is pointing towards the Sun is in shadow. For Rosetta, this has been a problem whenever the booms are behind the spacecraft with respect to the Sun. In this case the surfaces of the boom facing towards the Sun are still modelled as emitting photoelectrons. It has however been examined if this type of modelling will affect the results of the simulations (see Appendix E). It is shown that this drawback could be neglected.

Together with the reference parameters presented in Section 2.3, the following parameters are used as reference parameters in the photoelectron case (the  $eSU$  is changed, see Appendix D):

- Photoelectron temperature ( $T_{ph}$ ): 2 eV
- Distance to the Sun ( $r$ ): 1 AU
- electronSpeedUp ( $eSU$ ): 1
- All surfaces of the spacecraft and solar panels are modelled as Indium Tin Oxide (ITO)<sup>2</sup>.

The result from the reference simulation, 090611, is shown in Figure 2.36. As can be seen, the amplitude of the drop in potential due to the photoelectron cloud is large compared to the drop due to the wake (see Figure 2.19). For probe 1, the maximum effect from the photoelectron cloud is at about  $250^\circ$ . This agrees well with the angle where the probe is in front of the solar panel, inside the photoelectron cloud. For probe 2, the photoelectron cloud is reached at  $150^\circ$ . The signature from the wake is still visible for the two probes, at about  $50^\circ$  for probe 1 and  $340^\circ$  for probe 2, but the effects are small compared to the effects of the photoelectrons. The difference in amplitude between the photoelectron cloud drop and wake drop is about a factor 7. Note also the short plateaus in the drop at about  $160^\circ$  for probe 1 and  $80^\circ$  for probe 2. These plateaus show up when the booms are in the planes of the solar panels, entering or leaving the photoelectron cloud and at the same time they are at their closest points to the solar panels, respectively. The angles for the plateaus agree with the maximum potential only due to the spacecraft potential, as shown in the vacuum simulations (see for example Figure 2.7).

---

<sup>2</sup>A typical value for the photoelectron emission saturation current density,  $j_{ph0}$ , for this type of material is  $30 \mu\text{A}/\text{m}^2$  (Hastings and Garret, 1996)

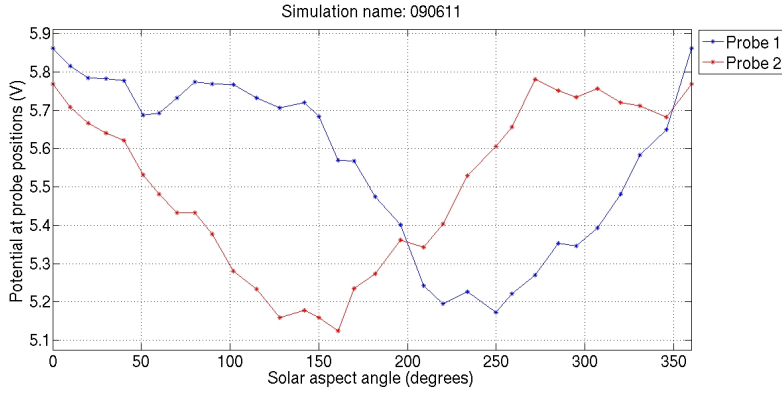


**Figure 2.36:** Reference simulation for plasma with photoelectrons; potential at probe positions as a function of solar aspect angle. Parameters:  $T_e = 12$  eV,  $T_i = 5$  eV,  $T_{ph} = 2$  eV,  $n = 5$  cm<sup>-3</sup>,  $v_i = 400$  km/s,  $V_{S/C} = 10$  V,  $r = 1$  AU. Simulation name: 090611.

The potential around Rosetta in the various planes is shown in Figure 2.37 to Figure 2.39. By comparing to the simulations without photoelectrons (for example Figure 2.20), it can be seen that the potential drops at a faster rate in front of Rosetta due to the photoelectron cloud. In Figure 2.40 and Figure 2.41 the ion density around Rosetta is shown (in the YZ-plane the ion density is homogenous and therefore is not shown). The images look almost identical to Figure 2.23 and Figure 2.24. This is as expected, as the solar wind ions have energies around 1 keV and should not much care about photoelectrons with an energy of a few eV. Figure 2.42 to Figure 2.44 show the photoelectron density. The scales in the density images are in elementary charge, hence the negative sign in the photoelectron density images. As expected, the photoelectron cloud is displaced toward the sunward (+x) side of the spacecraft.

The ion density in the case where photoelectrons are introduced looks similar to the case without photoelectrons, see for example Figure 2.23 and Figure 2.24. The density images of the photoelectrons are presented in order to be able to compare with the other photoelectron simulations, presented in the upcoming sections.

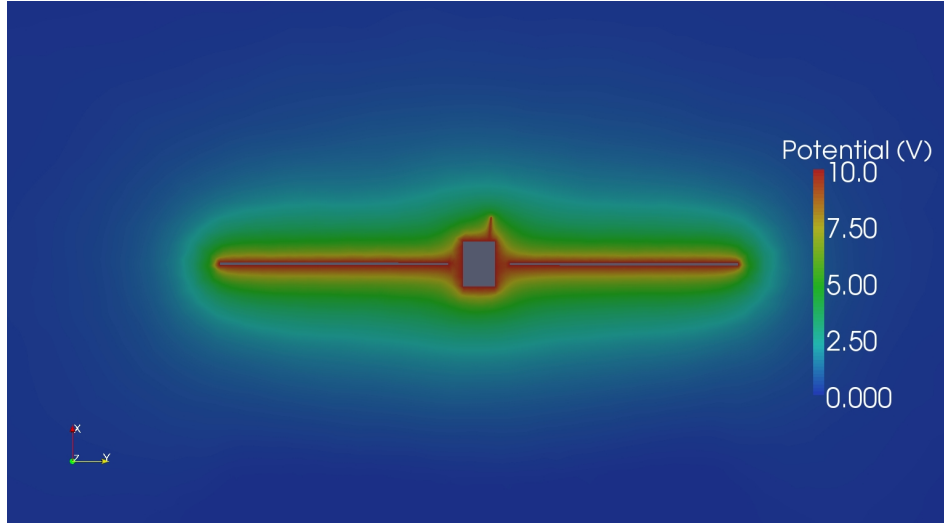


**Figure 2.37:** Reference simulation for plasma with photoelectrons; potential in  $V$  around Rosetta in the  $XY$ -plane. Parameters:  $T_e = 12$  eV,  $T_i = 5$  eV,  $T_{ph} = 2$  eV,  $n = 5$  cm<sup>-3</sup>,  $v_i = 400$  km/s,  $V_{S/C} = 10$  V,  $r = 1$  AU. Simulation name: 090611.

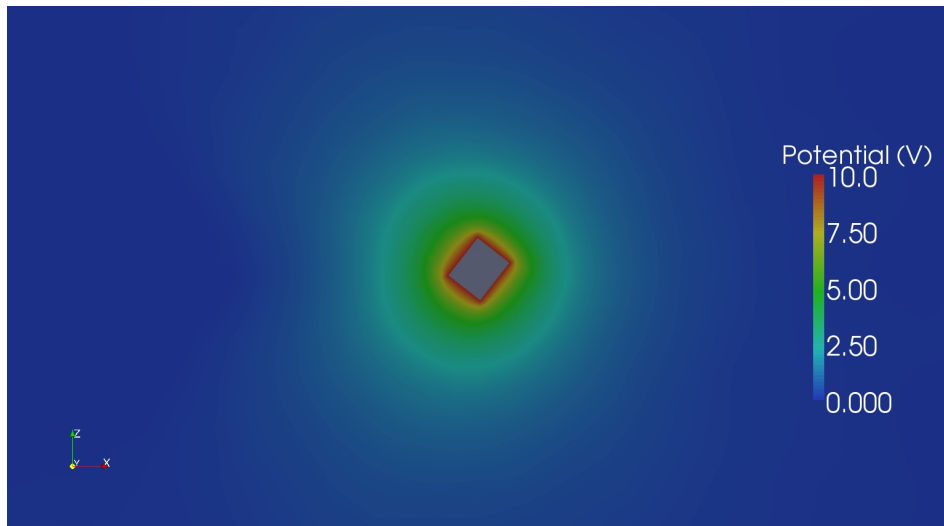


**Figure 2.38:** Reference simulation for plasma with photoelectrons; potential in  $V$  around Rosetta in the  $XZ$ -plane. Parameters:  $T_e = 12$  eV,  $T_i = 5$  eV,  $T_{ph} = 2$  eV,  $n = 5$  cm<sup>-3</sup>,  $v_i = 400$  km/s,  $V_{S/C} = 10$  V,  $r = 1$  AU. Simulation name: 090611.

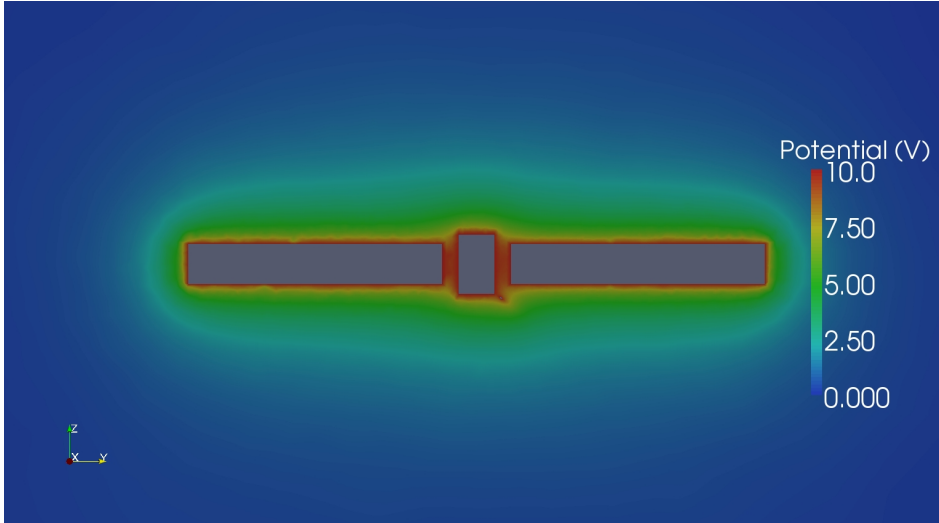


**Figure 2.39:** Reference simulation for plasma with photoelectrons; potential in V around Rosetta in the YZ-plane. Parameters:  $T_e = 12$  eV,  $T_i = 5$  eV,  $T_{ph} = 2$  eV,  $n = 5$  cm<sup>-3</sup>,  $v_i = 400$  km/s,  $V_{S/C} = 10$  V,  $r = 1$  AU. Simulation name: 090611.

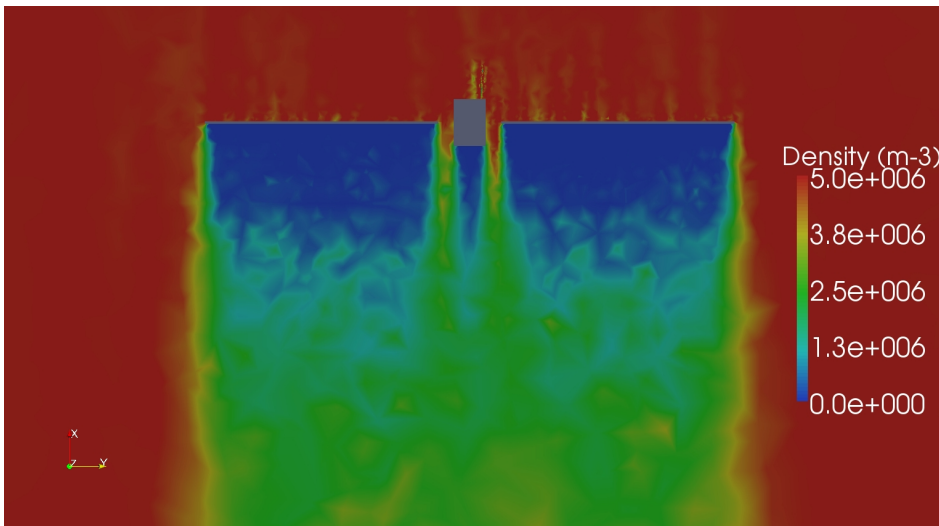


**Figure 2.40:** Reference simulation for plasma with photoelectrons; ion density in m<sup>-3</sup> around Rosetta in the XY-plane. Parameters:  $T_e = 12$  eV,  $T_i = 5$  eV,  $T_{ph} = 2$  eV,  $n = 5$  cm<sup>-3</sup>,  $v_i = 400$  km/s,  $V_{S/C} = 10$  V,  $r = 1$  AU. Simulation name: 090611.

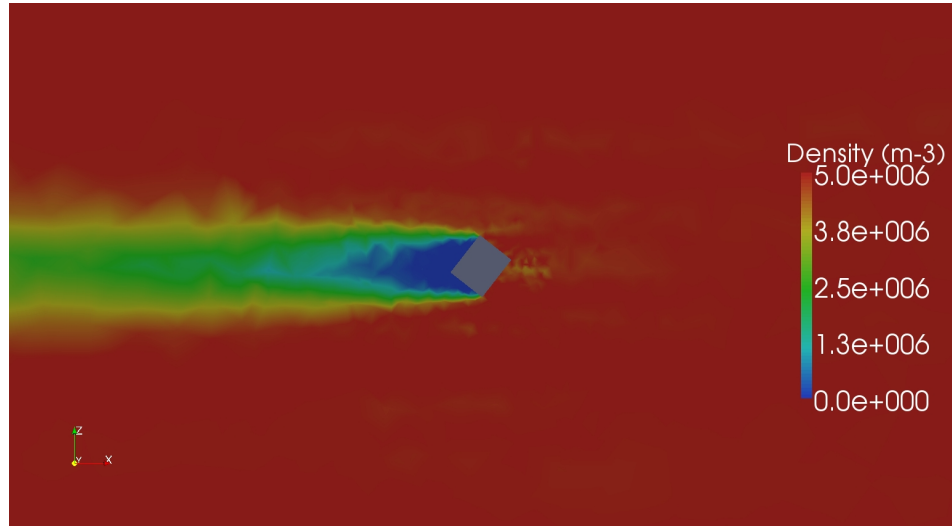


**Figure 2.41:** Reference simulation for plasma with photoelectrons; ion density in  $m^{-3}$  around Rosetta in the XZ-plane. Parameters:  $T_e = 12$  eV,  $T_i = 5$  eV,  $T_{ph} = 2$  eV,  $n = 5$   $cm^{-3}$ ,  $v_i = 400$  km/s,  $V_{S/JC} = 10$  V,  $r = 1$  AU. Simulation name: 090611.

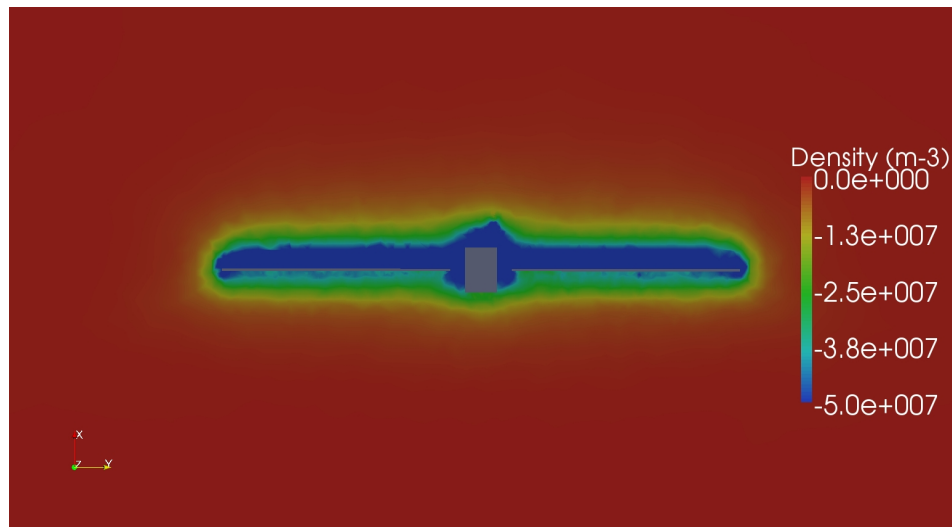


**Figure 2.42:** Reference simulation for plasma with photoelectrons; photoelectron density in  $m^{-3}$  around Rosetta in the XY-plane. Parameters:  $T_e = 12$  eV,  $T_i = 5$  eV,  $T_{ph} = 2$  eV,  $n = 5$   $cm^{-3}$ ,  $v_i = 400$  km/s,  $V_{S/JC} = 10$  V,  $r = 1$  AU. Simulation name: 090611.

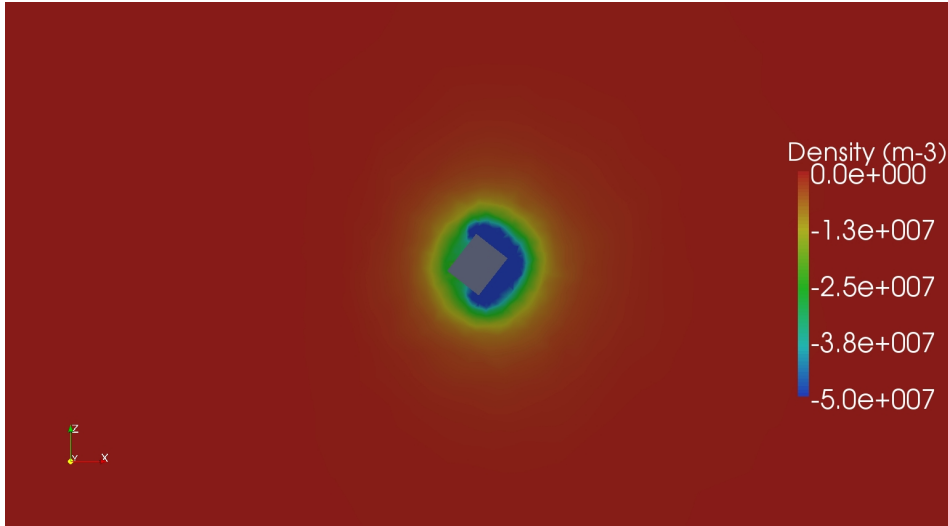


**Figure 2.43:** Reference simulation for plasma with photoelectrons; photoelectron density in  $m^{-3}$  around Rosetta in the XZ-plane. Parameters:  $T_e = 12$  eV,  $T_i = 5$  eV,  $T_{ph} = 2$  eV,  $n = 5$   $cm^{-3}$ ,  $v_i = 400$  km/s,  $V_{S/C} = 10$  V,  $r = 1$  AU. Simulation name: 090611.

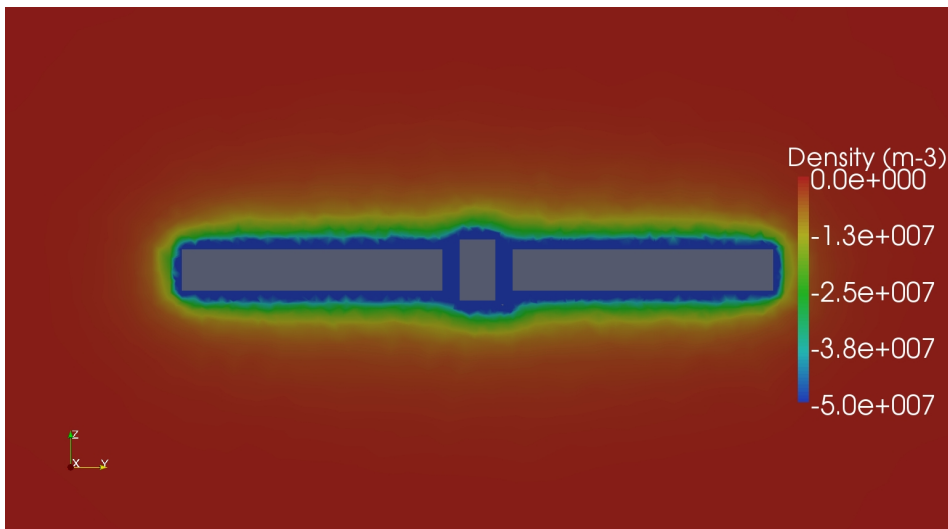


**Figure 2.44:** Reference simulation for plasma with photoelectrons; photoelectron density in  $m^{-3}$  around Rosetta in the YZ-plane. Parameters:  $T_e = 12$  eV,  $T_i = 5$  eV,  $T_{ph} = 2$  eV,  $n = 5$   $cm^{-3}$ ,  $v_i = 400$  km/s,  $V_{S/C} = 10$  V,  $r = 1$  AU. Simulation name: 090611.

## 2.5 Plasma and Photoelectrons - Various Distance from the Sun

On Rosetta's journey through the solar system, the solar UV flux will decrease with the square of the heliocentric distance, which will lead to a smaller amount of emitted photoelectrons. Simulations have therefore been done in order to see the effects of various solar UV flux on the potential at probe positions. It should be noted that only the solar UV flux is varied in these simulations, not the plasma (solar wind) density as is the true case in space.

At a distance 2 AU from the Sun, the result of the simulation is shown in Figure 2.45. The magnitude of the potential drop due to the photoelectron cloud is smaller, the 'depth' of the drop is 0.3 V instead of 0.6 V for the reference case (see Figure 2.36). Because of this, the potential drop due to the wake formed behind the spacecraft is more visible in the case of Rosetta at 2 AU than at 1 AU - the ratio between the two drops for probe 1 is a factor 3 instead of a factor 7 for the 1 AU case.

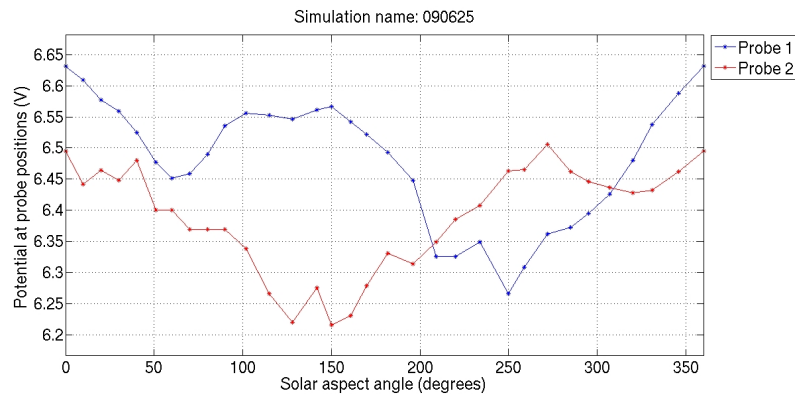


**Figure 2.45:** Rosetta at 2 AU; potential at probe positions as a function of solar aspect angle. Parameters:  $T_e = 12$  eV,  $T_i = 5$  eV,  $T_{ph} = 2$  eV,  $n = 5$  cm<sup>-3</sup>,  $v_i = 400$  km/s,  $V_{S/C} = 10$  V,  $r = 2$  AU. Simulation name: 090625.

The result of the simulation of Rosetta at 3 AU from the Sun is shown in Figure 2.46. The potential drop from the photoelectron cloud is on the same size as the drop from the wake in this case. For probe 1, the photoelectron cloud only brings the potential down when it is almost straight in front of the solar panels (at 250°), the plot could actually be compared to the case of no photoelectrons, see Figure 2.19.

In Figure 2.47 the three cases, 1 AU, 2 AU, and 3 AU, are presented in the same plot, where the 2 AU and 3 AU simulation results have been shifted in order to start at the same voltages as the reference case. This plot shows that the potential drops due to the photoelectron cloud scale approximately linearly with the distance from the Sun.

The potential around Rosetta for the various distances from the Sun in every plane is presented in Figure 2.48 to Figure 2.53. It can be seen how the potential drops at a faster rate, both in front and behind the spacecraft, for shorter distance from the Sun, as has been discussed earlier. In the YZ-plane no big differences are visible as the variations in sunflux is only creating differences along the  $x$ -axis.

The images of ion densities in the various planes look the same as for the reference case, and need not to be presented. The more interesting part is how the photoelectron

## 2.5. PLASMA AND PHOTOELECTRONS - VARIOUS DISTANCE FROM THE SUN

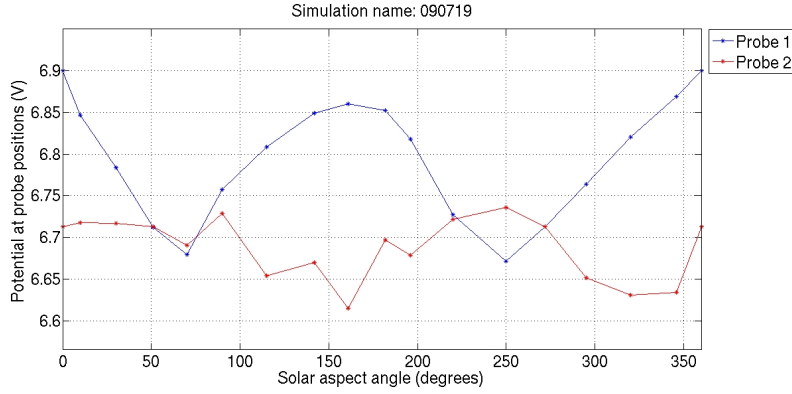


**Figure 2.46:** Rosetta at 3 AU; potential at probe positions as a function of solar aspect angle. Parameters:  $T_e = 12$  eV,  $T_i = 5$  eV,  $T_{ph} = 2$  eV,  $n = 5$  cm<sup>-3</sup>,  $v_i = 400$  km/s,  $V_{S/C} = 10$  V,  $r = 3$  AU. Simulation name: 090719.

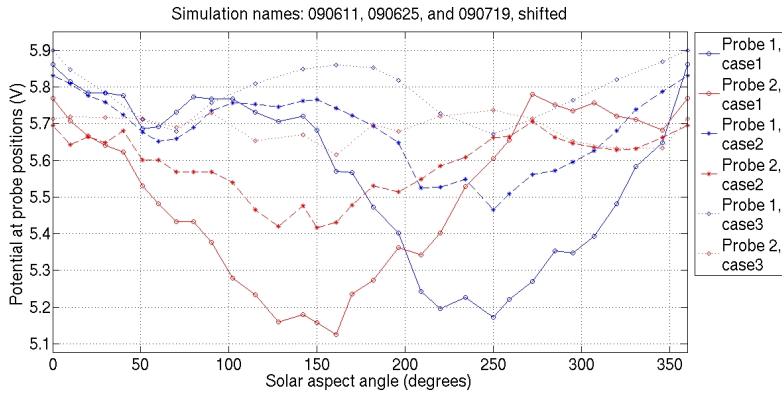


**Figure 2.47:** Rosetta at various distance from the sun; potential at probe positions as a function of solar aspect angle for three cases: 1)  $r = 1$  AU, 2)  $r = 2$  AU (shifted  $-0.8$ ), 3)  $r = 3$  AU (shifted  $-1.0$  V). Parameters:  $T_e = 12$  eV,  $T_i = 5$  eV,  $T_{ph} = 2$  eV,  $n = 5$  cm<sup>-3</sup>,  $v_i = 400$  km/s,  $V_{S/C} = 10$  V. Simulation names: 090611, 090625, 090719.

cloud around Rosetta looks at various distances. The photoelectron density for varying distances is shown in Figure 2.54 to Figure 2.59. It is clearly visible how the photoelectron cloud gets smaller with varying distance. In the case of 3 AU, it can be seen that the photoelectron cloud is almost not present behind the spacecraft (see for example Figure 2.57), which is why the potential could increase at such a fast rate when leaving the wake, as discussed when analyzing Figure 2.46.

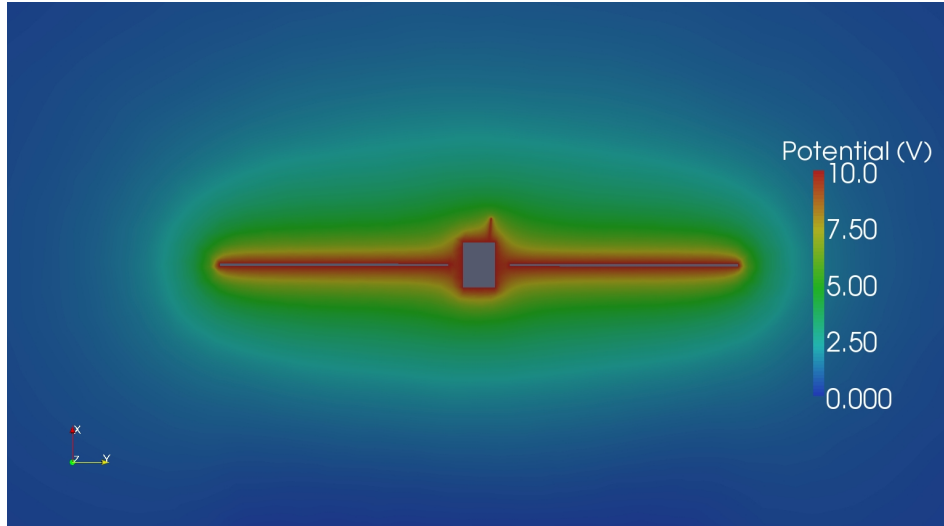


**Figure 2.48:** *Rosetta at 2 AU; potential in V around Rosetta in the XY-plane. Parameters:  $T_e = 12$  eV,  $T_i = 5$  eV,  $T_{ph} = 2$  eV,  $n = 5$  cm<sup>-3</sup>,  $v_i = 400$  km/s,  $V_{S/C} = 10$  V,  $r = 2$  AU. Simulation name: 090625.*

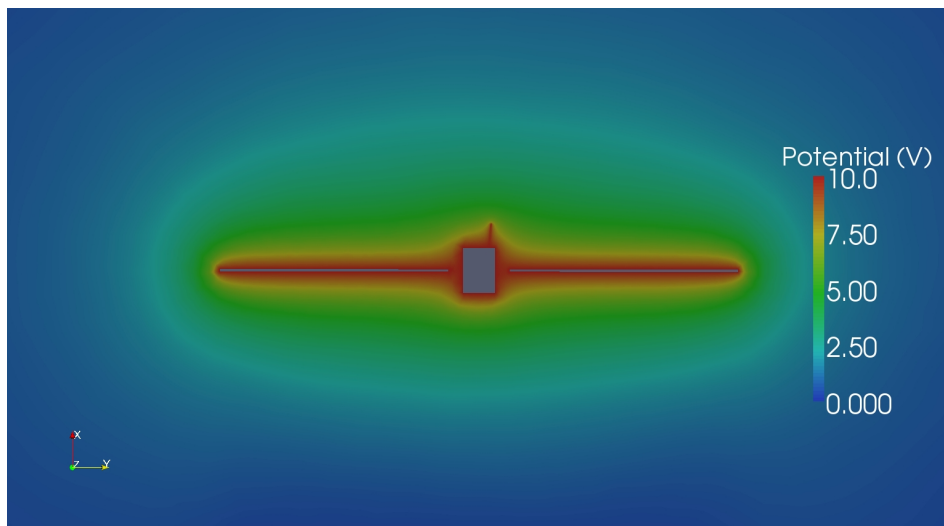


**Figure 2.49:** *Rosetta at 3 AU; potential in V around Rosetta in the XY-plane. Parameters:  $T_e = 12$  eV,  $T_i = 5$  eV,  $T_{ph} = 2$  eV,  $n = 5$  cm<sup>-3</sup>,  $v_i = 400$  km/s,  $V_{S/C} = 10$  V,  $r = 3$  AU. Simulation name: 090719.*

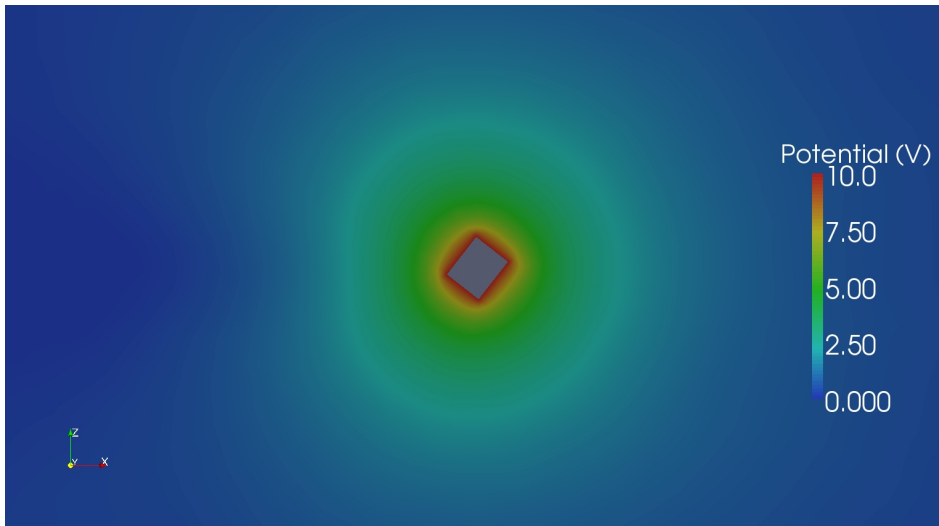


**Figure 2.50:** Rosetta at 2 AU; potential in V around Rosetta in the XZ-plane. Parameters:  $T_e = 12$  eV,  $T_i = 5$  eV,  $T_{ph} = 2$  eV,  $n = 5$  cm<sup>-3</sup>,  $v_i = 400$  km/s,  $V_{S/C} = 10$  V,  $r = 2$  AU. Simulation name: 090625.

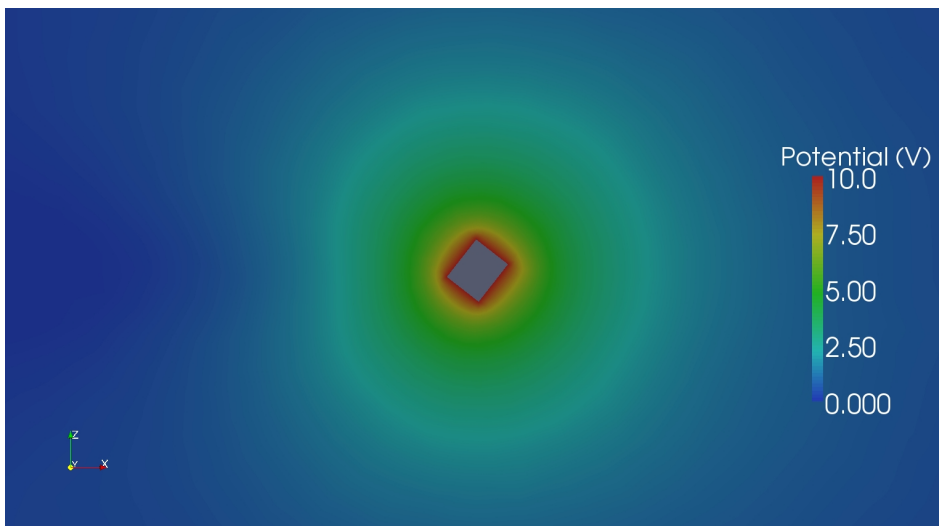


**Figure 2.51:** Rosetta at 3 AU; potential in V around Rosetta in the XZ-plane. Parameters:  $T_e = 12$  eV,  $T_i = 5$  eV,  $T_{ph} = 2$  eV,  $n = 5$  cm<sup>-3</sup>,  $v_i = 400$  km/s,  $V_{S/C} = 10$  V,  $r = 3$  AU. Simulation name: 090719.

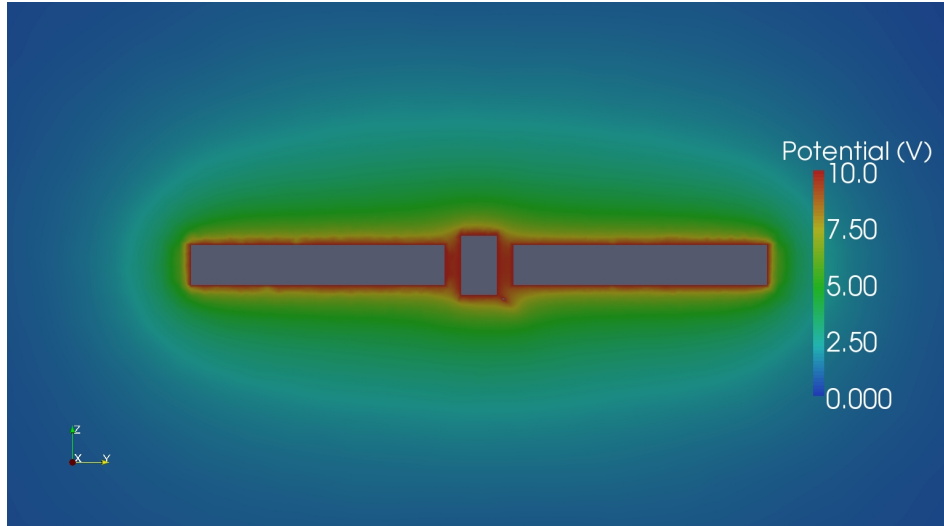


**Figure 2.52:** *Rosetta at 2 AU; potential in V around Rosetta in the YZ-plane. Parameters:  $T_e = 12$  eV,  $T_i = 5$  eV,  $T_{ph} = 2$  eV,  $n = 5$  cm<sup>-3</sup>,  $v_i = 400$  km/s,  $V_{S/C} = 10$  V,  $r = 2$  AU. Simulation name: 090625.*

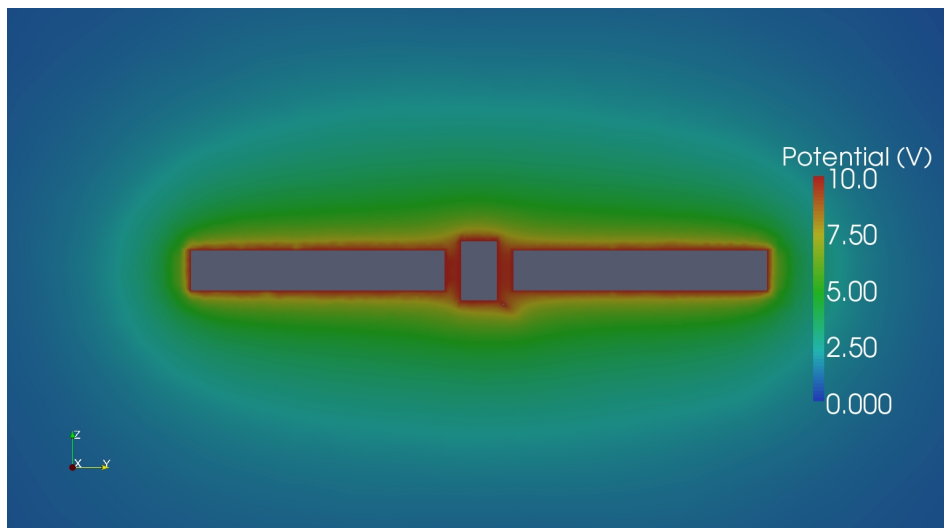


**Figure 2.53:** *Rosetta at 3 AU; potential in V around Rosetta in the YZ-plane. Parameters:  $T_e = 12$  eV,  $T_i = 5$  eV,  $T_{ph} = 2$  eV,  $n = 5$  cm<sup>-3</sup>,  $v_i = 400$  km/s,  $V_{S/C} = 10$  V,  $r = 3$  AU. Simulation name: 090719.*

2.5. PLASMA AND PHOTOELECTRONS - VARIOUS DISTANCE FROM THE SUN

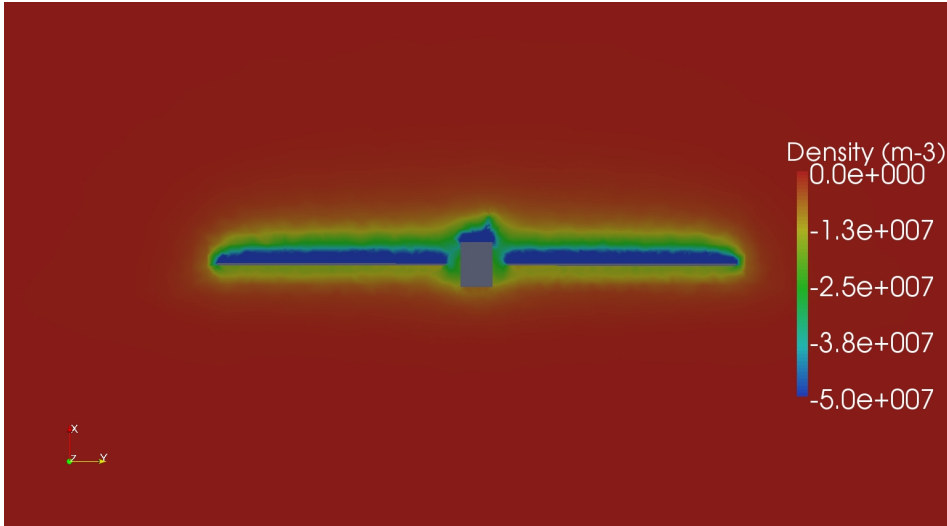


**Figure 2.54:** Rosetta at 2 AU; photoelectron density in  $m^{-3}$  around Rosetta in the XY-plane. Parameters:  $T_e = 12$  eV,  $T_i = 5$  eV,  $T_{ph} = 2$  eV,  $n = 5$   $cm^{-3}$ ,  $v_i = 400$  km/s,  $V_{S/C} = 10$  V,  $r = 2$  AU. Simulation name: 090625.

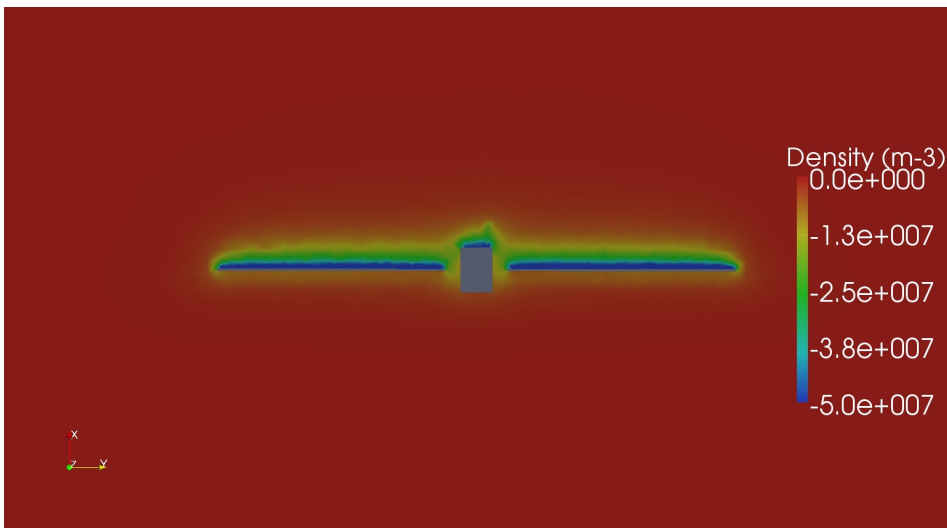


**Figure 2.55:** Rosetta at 3 AU; photoelectron density in  $m^{-3}$  around Rosetta in the XY-plane. Parameters:  $T_e = 12$  eV,  $T_i = 5$  eV,  $T_{ph} = 2$  eV,  $n = 5$   $cm^{-3}$ ,  $v_i = 400$  km/s,  $V_{S/C} = 10$  V,  $r = 3$  AU. Simulation name: 090719.

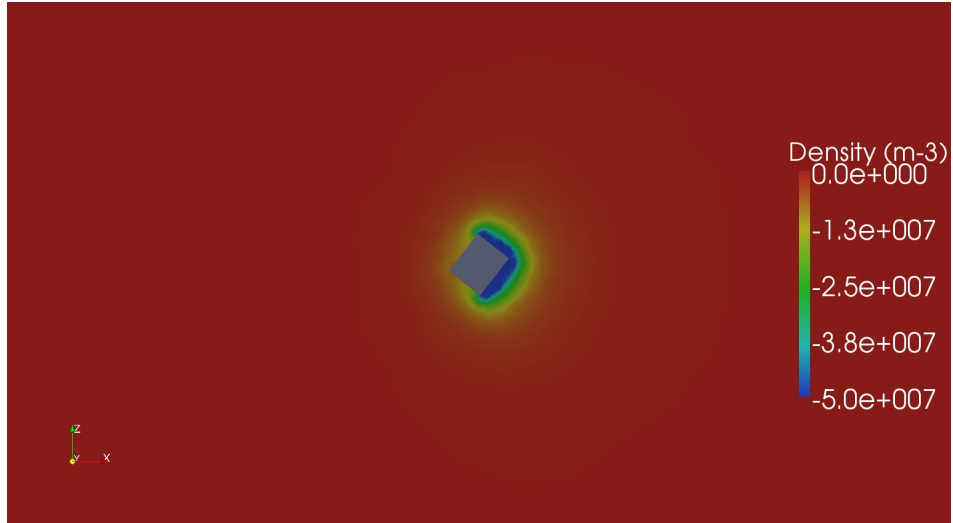


**Figure 2.56:** Rosetta at 2 AU; photoelectron density in  $m^{-3}$  around Rosetta in the XZ-plane. Parameters:  $T_e = 12$  eV,  $T_i = 5$  eV,  $T_{ph} = 2$  eV,  $n = 5$   $cm^{-3}$ ,  $v_i = 400$  km/s,  $V_{S/C} = 10$  V,  $r = 2$  AU. Simulation name: 090625.

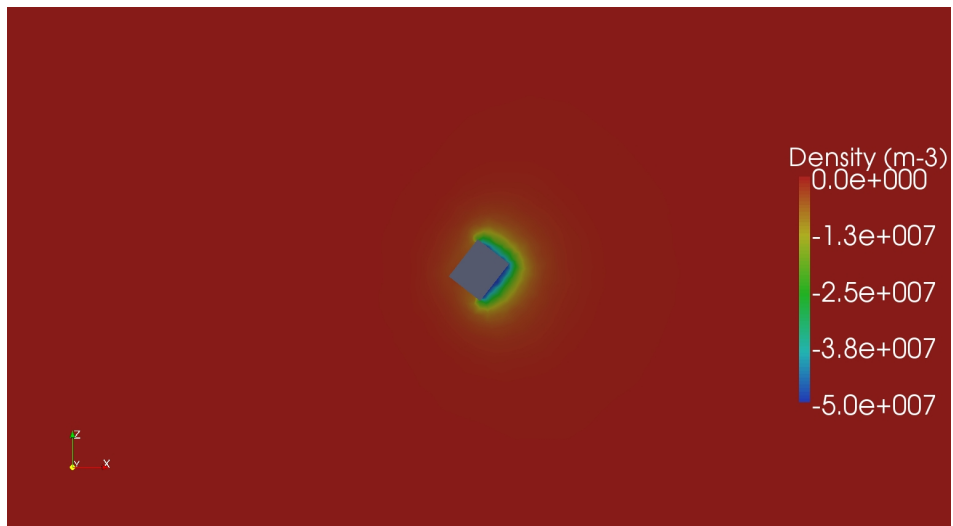


**Figure 2.57:** Rosetta at 3 AU; photoelectron density in  $m^{-3}$  around Rosetta in the XZ-plane. Parameters:  $T_e = 12$  eV,  $T_i = 5$  eV,  $T_{ph} = 2$  eV,  $n = 5$   $cm^{-3}$ ,  $v_i = 400$  km/s,  $V_{S/C} = 10$  V,  $r = 3$  AU. Simulation name: 090719.

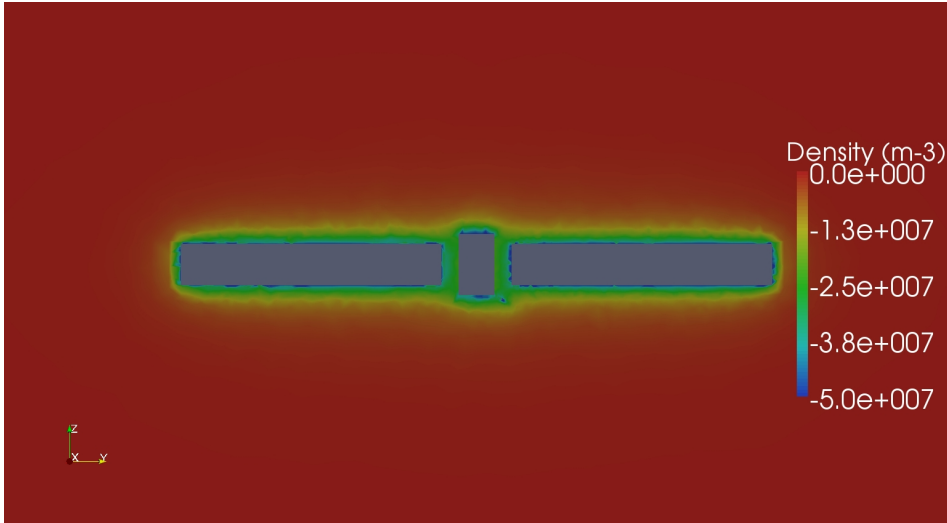


**Figure 2.58:** Rosetta at 2 AU; photoelectron density in  $m^{-3}$  around Rosetta in the YZ-plane. Parameters:  $T_e = 12$  eV,  $T_i = 5$  eV,  $T_{ph} = 2$  eV,  $n = 5$   $cm^{-3}$ ,  $v_i = 400$  km/s,  $V_{S/C} = 10$  V,  $r = 2$  AU. Simulation name: 090625.

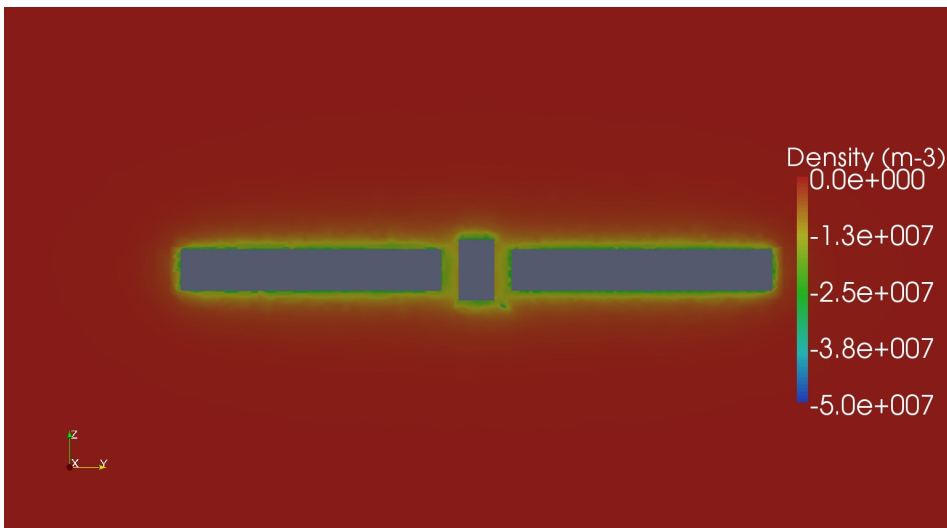


**Figure 2.59:** Rosetta at 3 AU; photoelectron density in  $m^{-3}$  around Rosetta in the YZ-plane. Parameters:  $T_e = 12$  eV,  $T_i = 5$  eV,  $T_{ph} = 2$  eV,  $n = 5$   $cm^{-3}$ ,  $v_i = 400$  km/s,  $V_{S/C} = 10$  V,  $r = 3$  AU. Simulation name: 090719.

## 2.6 Plasma and Photoelectrons - Various Spacecraft Potential

When lowering the spacecraft potential, there is less potential to hold back the photoelectrons emitted from the spacecraft surfaces. The photoelectrons can reach further out, with the same energy, compared to when the spacecraft potential is higher. As a result, the effect from the photoelectrons on the potential drop is even stronger with lower spacecraft potential, than in the reference case. The result of the simulation when the spacecraft potential is half of that in the reference case (5 V instead of 10 V), is presented in Figure 2.60. The DC-level of the potential at the probe positions is not scaling linearly with the spacecraft potential, which was the case for vacuum (see 2.14). The reference simulation together with the simulation of lower spacecraft potential are plotted in Figure 2.61, where the latter is shifted +4.0 V in order to get to the same DC-level. The potential drop due to wake formed behind the spacecraft is almost half the depth in the lower spacecraft potential case, which is seen in the plot.

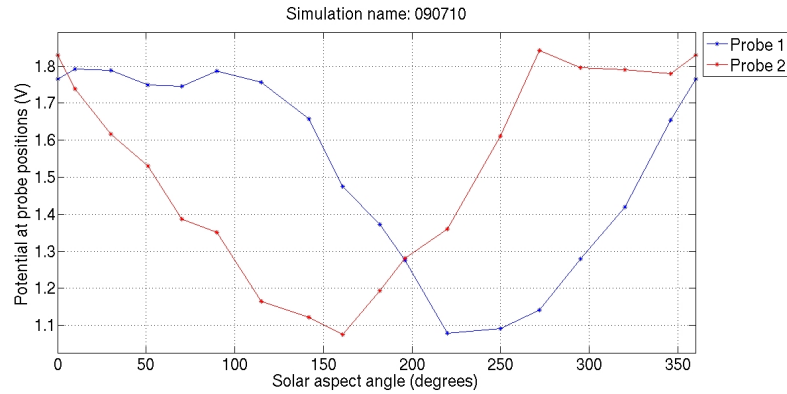


**Figure 2.60:** Rosetta at 5 V; potential at probe positions as a function of solar aspect angle. Parameters:  $T_e = 12$  eV,  $T_i = 5$  eV,  $T_{ph} = 2$  eV,  $n = 5$  cm<sup>-3</sup>,  $v_i = 400$  km/s,  $V_{S/C} = 5$  V,  $r = 1$  AU. Simulation name: 090710.

The potential around Rosetta in the various planes for the case of lower spacecraft potential is presented in Figure 2.62 to Figure 2.64. The same kind of images but with photoelectron density around Rosetta are presented in Figure 2.65 to Figure 2.67. As expected, the photoelectron cloud is increased in size compared to the reference case, compare for example to Figure 2.43.

## 2.6. PLASMA AND PHOTOELECTRONS - VARIOUS SPACECRAFT POTENTIAL

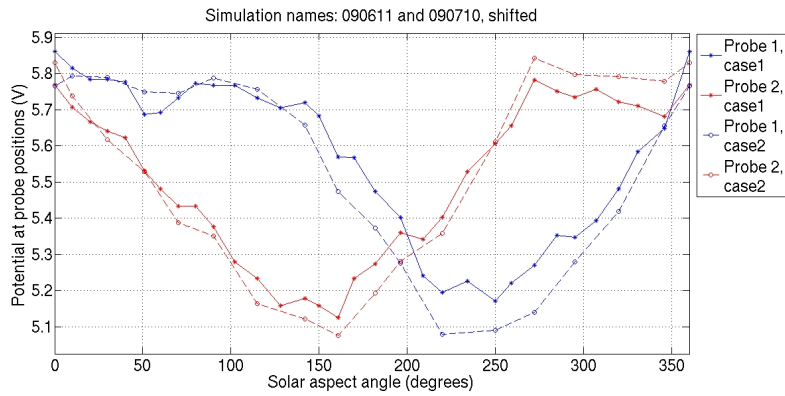


**Figure 2.61:** Rosetta at various spacecraft potential; potential at probe positions as a function of solar aspect angle for two cases: 1)  $V_{S/C} = 10$  V, 2)  $V_{S/C} = 5$  V (shifted +4.0 V). Parameters:  $T_e = 12$  eV,  $T_i = 5$  eV,  $T_{ph} = 2$  eV,  $n = 5$  cm<sup>-3</sup>,  $v_i = 400$  km/s,  $r = 1$  AU. Simulation names: 090611 and 090710.

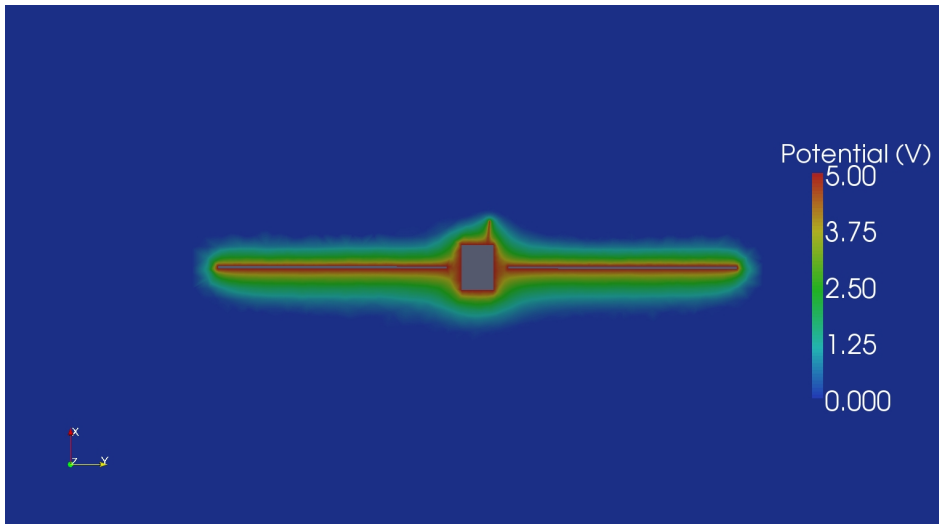


**Figure 2.62:** Rosetta at 5 V; potential in V around Rosetta in the XY-plane. Parameters:  $T_e = 12$  eV,  $T_i = 5$  eV,  $T_{ph} = 2$  eV,  $n = 5$  cm<sup>-3</sup>,  $v_i = 400$  km/s,  $V_{S/C} = 5$  V,  $r = 1$  AU. Simulation name: 090710.

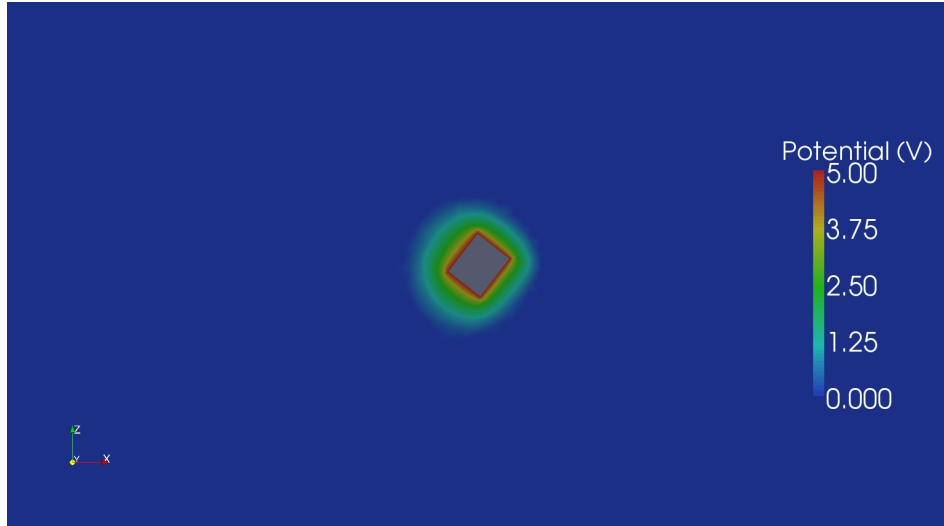


**Figure 2.63:** Rosetta at 5 V; potential in V around Rosetta in the XZ-plane. Parameters:  $T_e = 12$  eV,  $T_i = 5$  eV,  $T_{ph} = 2$  eV,  $n = 5$  cm<sup>-3</sup>,  $v_i = 400$  km/s,  $V_{S/C} = 5$  V,  $r = 1$  AU. Simulation name: 090710.

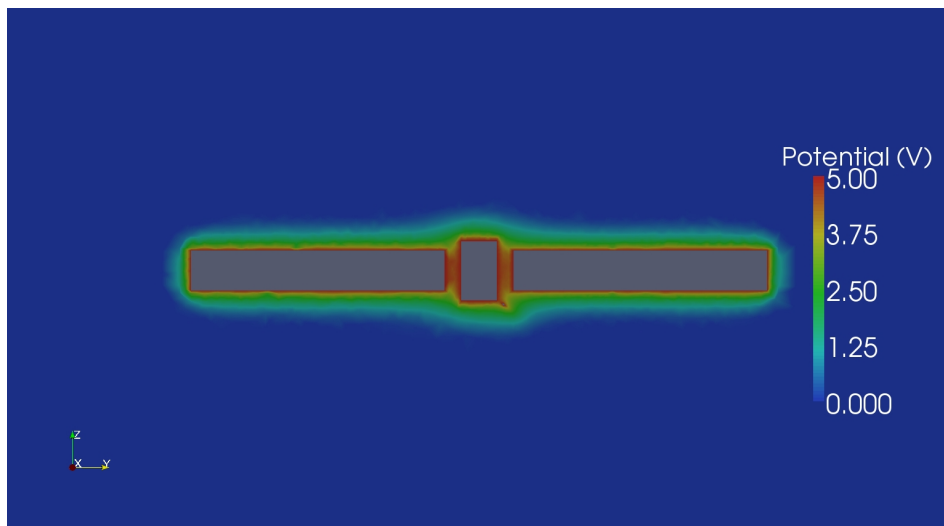


**Figure 2.64:** Rosetta at 5 V; potential in V around Rosetta in the YZ-plane. Parameters:  $T_e = 12$  eV,  $T_i = 5$  eV,  $T_{ph} = 2$  eV,  $n = 5$  cm<sup>-3</sup>,  $v_i = 400$  km/s,  $V_{S/C} = 5$  V,  $r = 1$  AU. Simulation name: 090710.

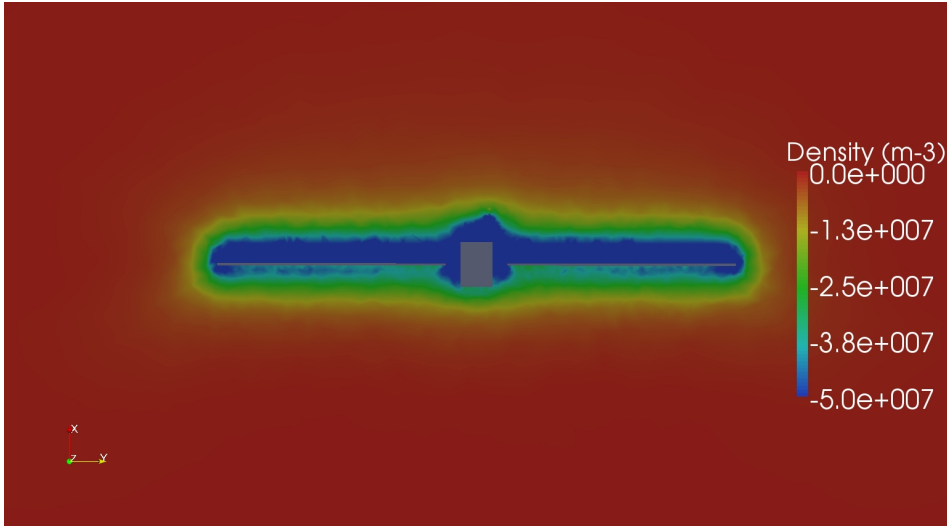


**Figure 2.65:** Rosetta at 5 V; photoelectron density in  $m^{-3}$  around Rosetta in the XY-plane. Parameters:  $T_e = 12$  eV,  $T_i = 5$  eV,  $T_{ph} = 2$  eV,  $n = 5$   $cm^{-3}$ ,  $v_i = 400$  km/s,  $V_{S/C} = 5$  V,  $r = 1$  AU. Simulation name: 090710.

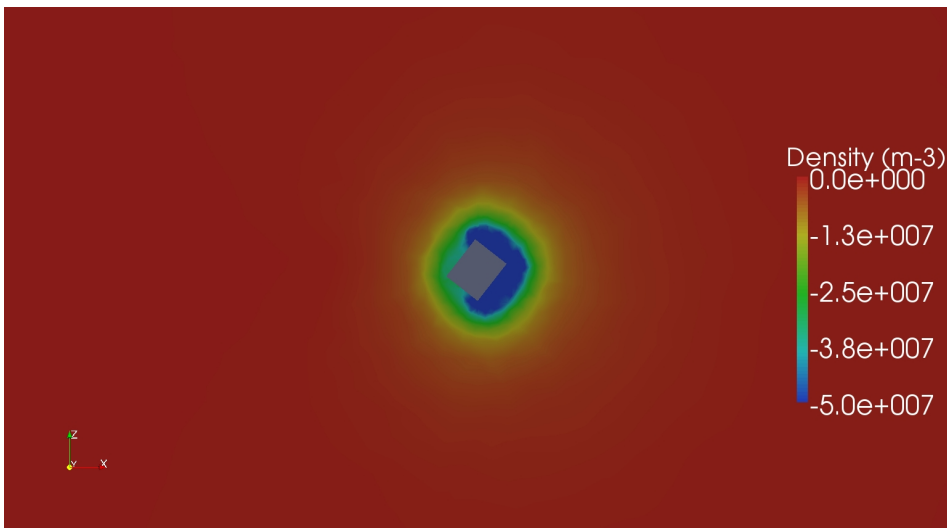


**Figure 2.66:** Rosetta at 5 V; photoelectron density in  $m^{-3}$  around Rosetta in the XZ-plane. Parameters:  $T_e = 12$  eV,  $T_i = 5$  eV,  $T_{ph} = 2$  eV,  $n = 5$   $cm^{-3}$ ,  $v_i = 400$  km/s,  $V_{S/C} = 5$  V,  $r = 1$  AU. Simulation name: 090710.

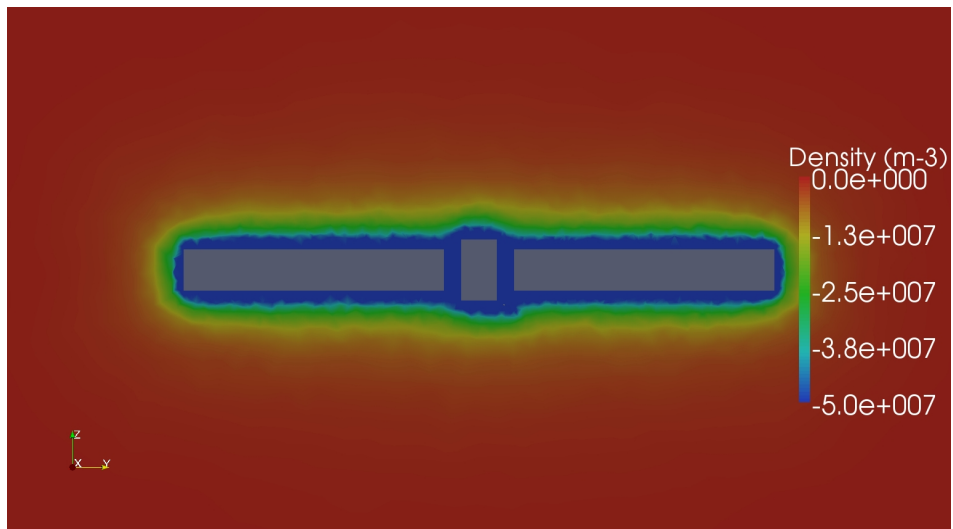


**Figure 2.67:** Rosetta at 5 V; photoelectron density in  $m^{-3}$  around Rosetta in the YZ-plane. Parameters:  $T_e = 12$  eV,  $T_i = 5$  eV,  $T_{ph} = 2$  eV,  $n = 5$   $cm^{-3}$ ,  $v_i = 400$  km/s,  $V_{S/C} = 5$  V,  $r = 1$  AU. Simulation name: 090710.

## 2.7 Plasma and Photoelectrons - Various Photoelectron Temperature

The exact distribution of emitted photoelectrons in energy and angle is not known. Their importance for the measurements is affected of what temperature they have when leaving the surface. In the reference case the photoelectron temperature was set to 2 eV, and it has been simulated how various photoelectron temperature would affect the result.

In Figure 2.68 the result shows the behaviour when the photoelectron temperature is set to 1 eV. This of course has the result that the photoelectrons can not escape as far as before from the spacecraft surface, simply because they have lower energy. This can be seen in the plot as the potential drop due to the photoelectrons is smaller than in the reference case. The ‘depth’ in the photoelectron drop is about 0.2 V in this case, compare to 0.6 V in the reference case. As a result, the plot takes a form similar to the one when Rosetta was simulated at a distance of 3 AU (see Figure 2.46).

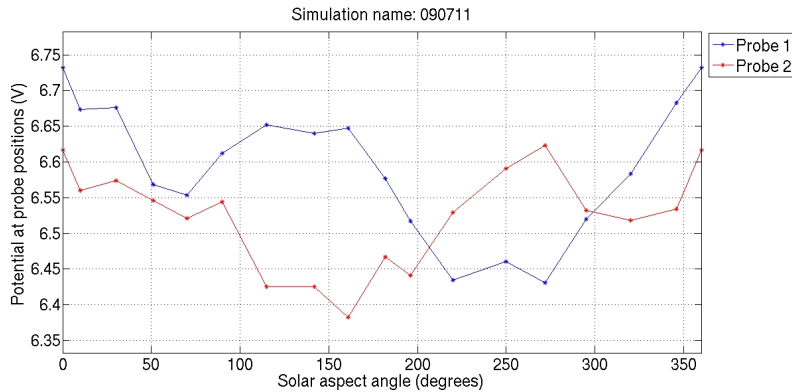


**Figure 2.68:** Photoelectron temperature at 1 eV; potential at probe positions as a function of solar aspect angle. Parameters:  $T_e = 12$  eV,  $T_i = 5$  eV,  $T_{ph} = 1$  eV,  $n = 5$  cm<sup>-3</sup>,  $v_i = 400$  km/s,  $V_{S/C} = 10$  V,  $r = 1$  AU. Simulation name: 090711.

For the case where the photoelectron temperature is increased to 4 eV instead of 2 eV, the result is shown in Figure 2.69. In this case the potential drop due to the photoelectron cloud is increased, reaching a value of 0.9 V compared to 0.6 V for the reference case. The effect from the wake formed behind the spacecraft seems to be decreased in the case of higher photoelectron temperature. This is most likely due to the fact that at the probe position where the wake effect is the strongest (50° for probe 1), the probes are actually in a strong photoelectron cloud, decreasing the potential with a higher magnitude than the wake does itself. Therefore the effect from the wake seems to be lowered.

In Figure 2.70 the reference case is plotted together with the various photoelectron temperature cases, where the two latter ones have been shifted in order to start at the same DC-level.

In Figure 2.71 to Figure 2.76 the potential around Rosetta is presented. It can be seen how the potential decreases at a higher rate outwards from the spacecraft in the case of higher photoelectron temperature. This is also comparable to the case of varying solar UV flux. The density of the photoelectrons is presented in Figure 2.77 to Figure 2.82. The bigger photoelectron cloud can be seen in the case of photoelectron temperature of 4 eV, giving rise to the increased effect from the photoelectrons on the probe measurements.

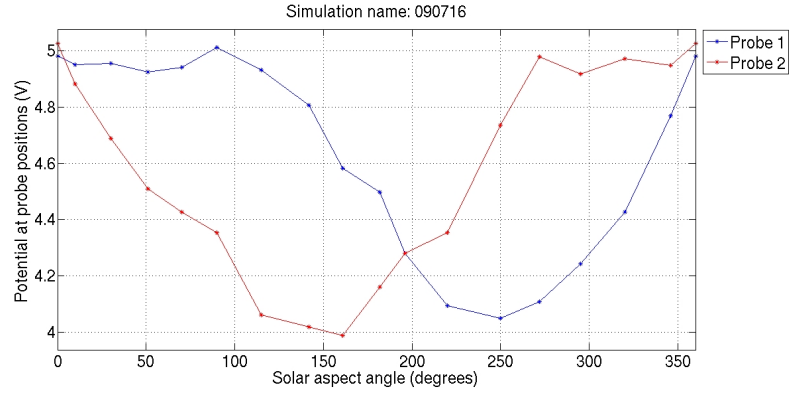


**Figure 2.69:** Photoelectron temperature at 4 eV; potential at probe positions as a function of solar aspect angle. Parameters:  $T_e = 12$  eV,  $T_i = 5$  eV,  $T_{ph} = 4$  eV,  $n = 5$  cm<sup>-3</sup>,  $v_i = 400$  km/s,  $V_{S/C} = 10$  V,  $r = 1$  AU. Simulation name: 090716.

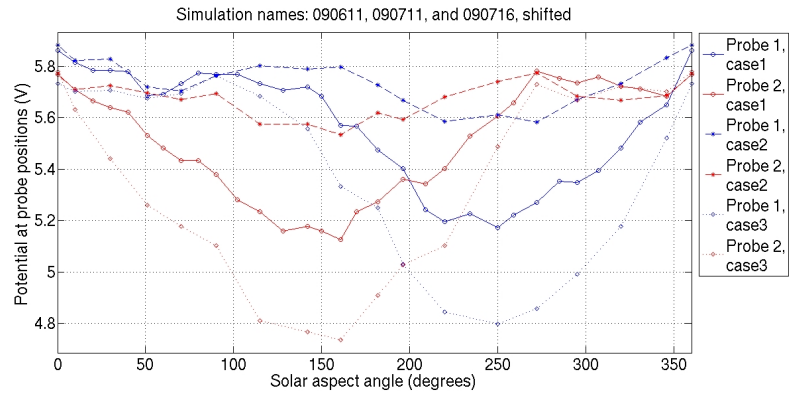


**Figure 2.70:** Various photoelectron temperature; potential at probe positions as a function of solar aspect angle for three cases: 1)  $T_{ph} = 2$  eV, 2)  $T_{ph} = 1$  eV (shifted -0.85 V), 3)  $T_{ph} = 4$  eV (shifted +0.75 V). Parameters:  $T_e = 12$  eV,  $T_i = 5$  eV,  $n = 5$  cm<sup>-3</sup>,  $v_i = 400$  km/s,  $V_{S/C} = 10$  V,  $r = 1$  AU. Simulation names: 090611, 090711, 090716.

2.7. PLASMA AND PHOTOELECTRONS - VARIOUS PHOTOELECTRON TEMPERATURE

---

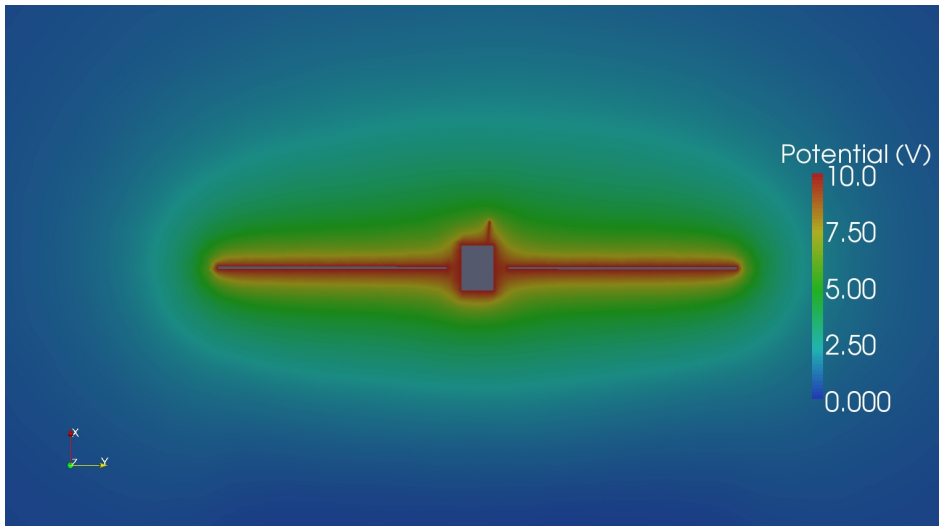


**Figure 2.71:** Photoelectron temperature at 1 eV; potential in V around Rosetta in the XY-plane. Parameters:  $T_e = 12$  eV,  $T_i = 5$  eV,  $T_{ph} = 1$  eV,  $n = 5$  cm<sup>-3</sup>,  $v_i = 400$  km/s,  $V_{S/C} = 10$  V,  $r = 1$  AU. Simulation name: 090711.

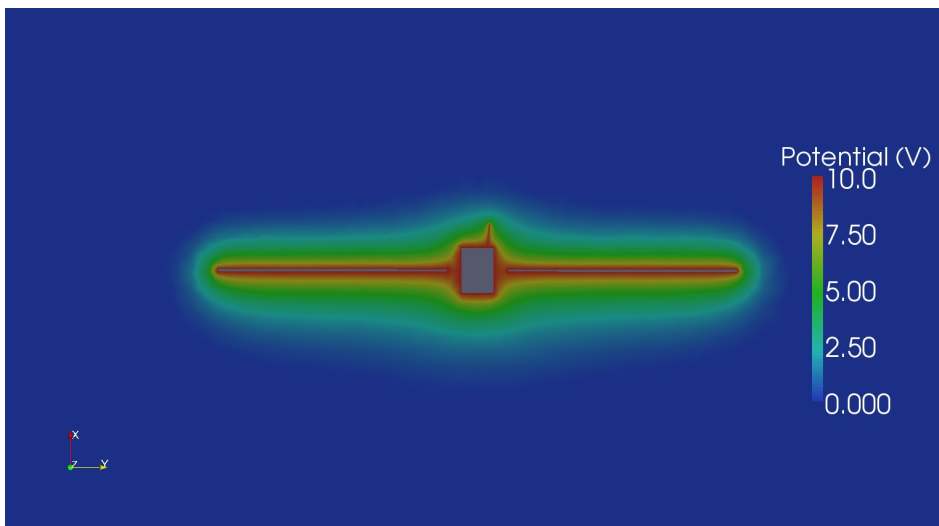


**Figure 2.72:** Photoelectron temperature at 4 eV; potential in V around Rosetta in the XY-plane. Parameters:  $T_e = 12$  eV,  $T_i = 5$  eV,  $T_{ph} = 4$  eV,  $n = 5$  cm<sup>-3</sup>,  $v_i = 400$  km/s,  $V_{S/C} = 10$  V,  $r = 1$  AU. Simulation name: 090716.

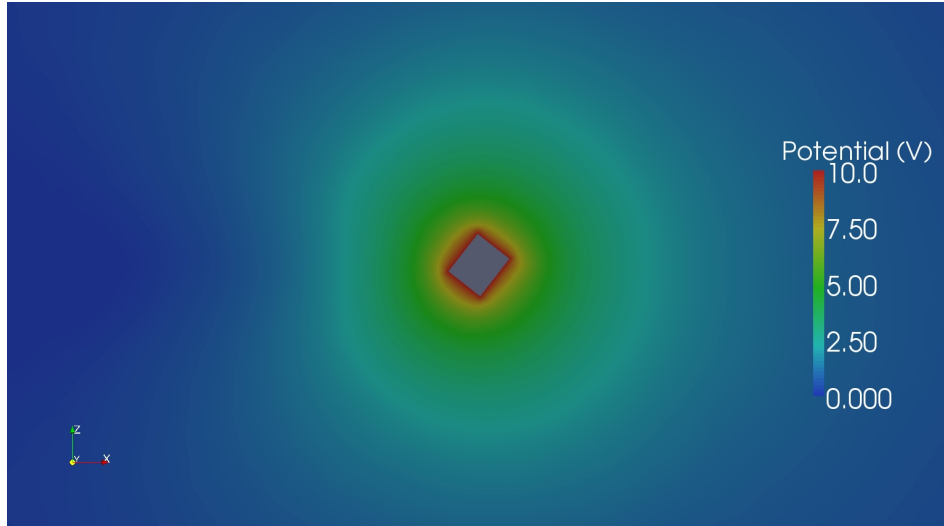


**Figure 2.73:** Photoelectron temperature at 1 eV; potential in V around Rosetta in the XZ-plane. Parameters:  $T_e = 12$  eV,  $T_i = 5$  eV,  $T_{ph} = 1$  eV,  $n = 5$  cm<sup>-3</sup>,  $v_i = 400$  km/s,  $V_{S/C} = 10$  V,  $r = 1$  AU. Simulation name: 090711.

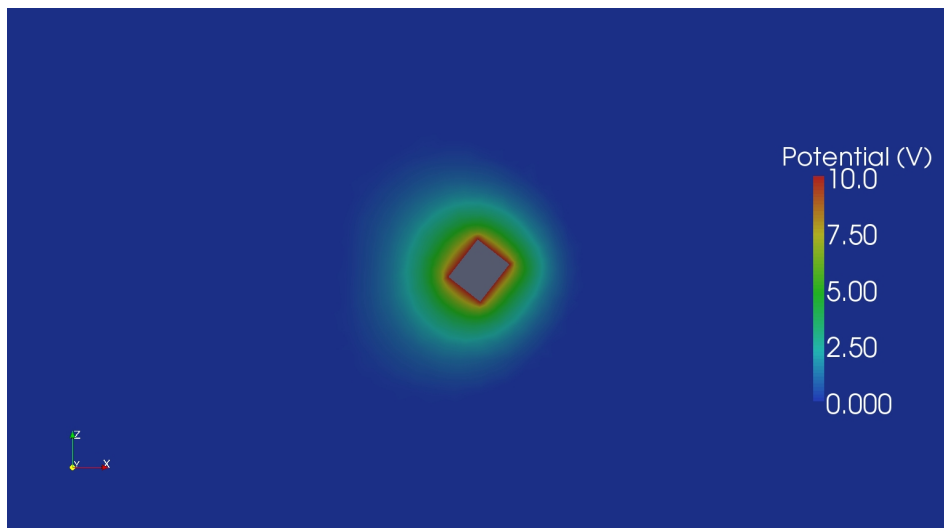


**Figure 2.74:** Photoelectron temperature at 4 eV; potential in V around Rosetta in the XZ-plane. Parameters:  $T_e = 12$  eV,  $T_i = 5$  eV,  $T_{ph} = 4$  eV,  $n = 5$  cm<sup>-3</sup>,  $v_i = 400$  km/s,  $V_{S/C} = 10$  V,  $r = 1$  AU. Simulation name: 090716.

2.7. PLASMA AND PHOTOELECTRONS - VARIOUS PHOTOELECTRON TEMPERATURE

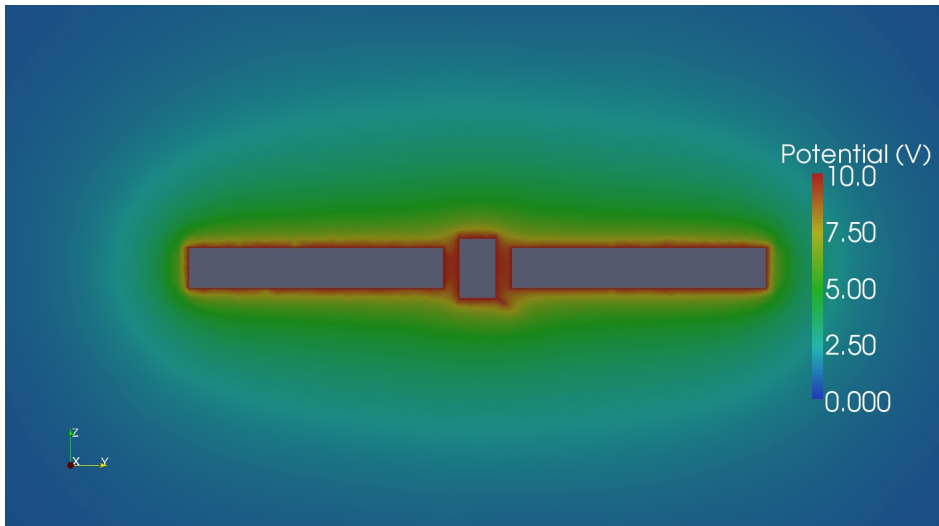


**Figure 2.75:** Photoelectron temperature at 1 eV; potential in V around Rosetta in the YZ-plane. Parameters:  $T_e = 12$  eV,  $T_i = 5$  eV,  $T_{ph} = 1$  eV,  $n = 5$  cm<sup>-3</sup>,  $v_i = 400$  km/s,  $V_{S/C} = 10$  V,  $r = 1$  AU. Simulation name: 090711.

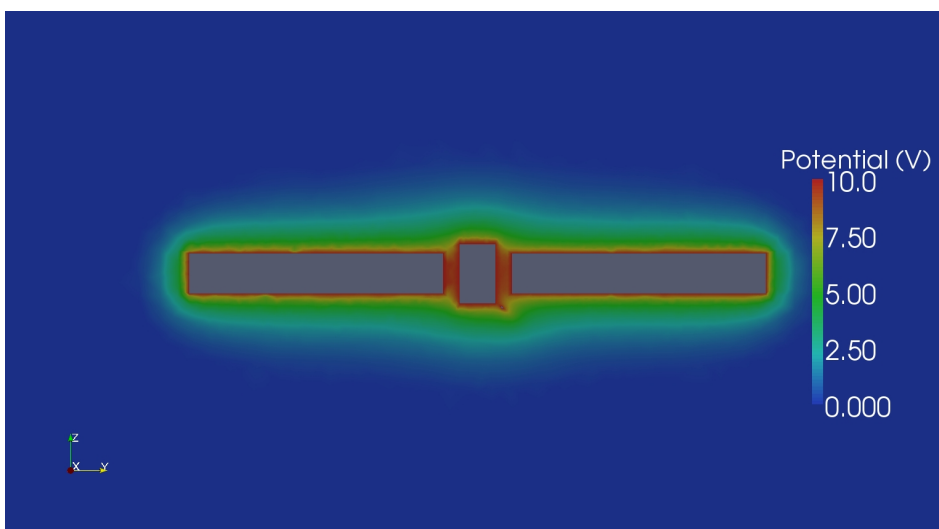


**Figure 2.76:** Photoelectron temperature at 4 eV; potential in V around Rosetta in the YZ-plane. Parameters:  $T_e = 12$  eV,  $T_i = 5$  eV,  $T_{ph} = 4$  eV,  $n = 5$  cm<sup>-3</sup>,  $v_i = 400$  km/s,  $V_{S/C} = 10$  V,  $r = 1$  AU. Simulation name: 090716.

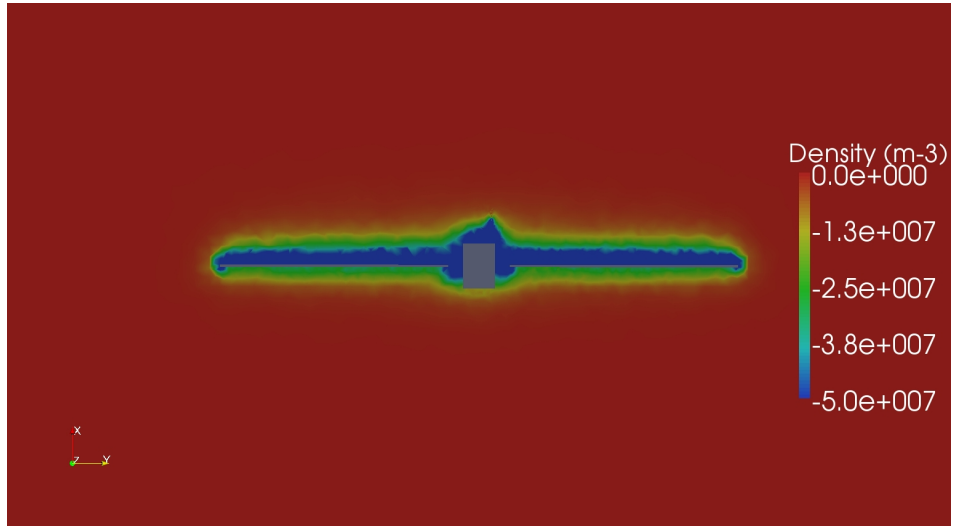


**Figure 2.77:** Photoelectron temperature at 1 eV; photoelectron density in  $m^{-3}$  around Rosetta in the XY-plane. Parameters:  $T_e = 12$  eV,  $T_i = 5$  eV,  $T_{ph} = 1$  eV,  $n = 5$   $cm^{-3}$ ,  $v_i = 400$  km/s,  $V_{S/C} = 10$  V,  $r = 1$  AU. Simulation name: 090711.

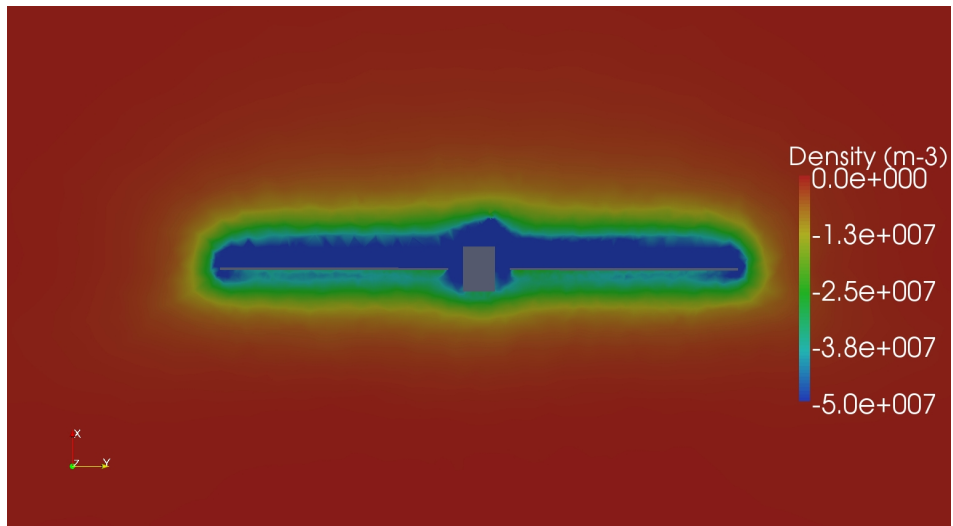


**Figure 2.78:** Photoelectron temperature at 4 eV; photoelectron density in  $m^{-3}$  around Rosetta in the XY-plane. Parameters:  $T_e = 12$  eV,  $T_i = 5$  eV,  $T_{ph} = 4$  eV,  $n = 5$   $cm^{-3}$ ,  $v_i = 400$  km/s,  $V_{S/C} = 10$  V,  $r = 1$  AU. Simulation name: 090716.

2.7. PLASMA AND PHOTOELECTRONS - VARIOUS PHOTOELECTRON TEMPERATURE

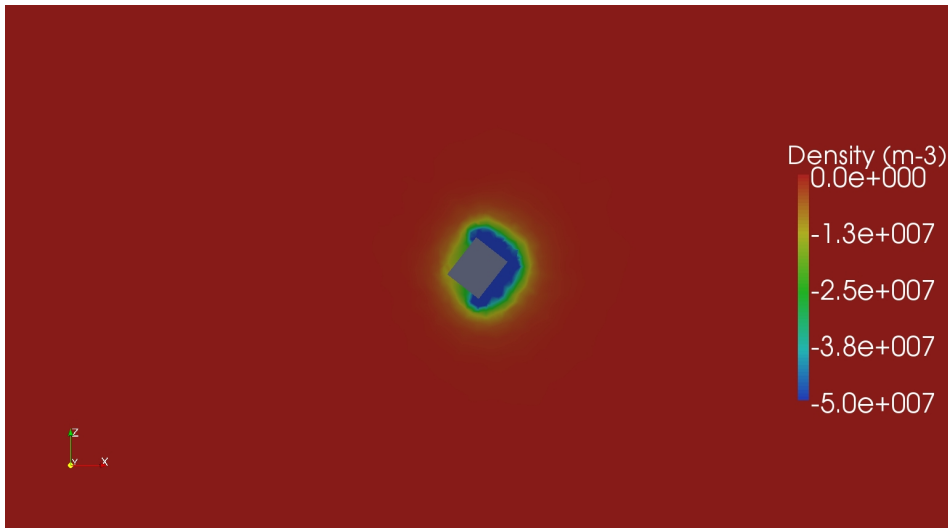


**Figure 2.79:** Photoelectron temperature at 1 eV; photoelectron density in  $m^{-3}$  around Rosetta in the XZ-plane. Parameters:  $T_e = 12$  eV,  $T_i = 5$  eV,  $T_{ph} = 1$  eV,  $n = 5$   $cm^{-3}$ ,  $v_i = 400$  km/s,  $V_{S/C} = 10$  V,  $r = 1$  AU. Simulation name: 090711.

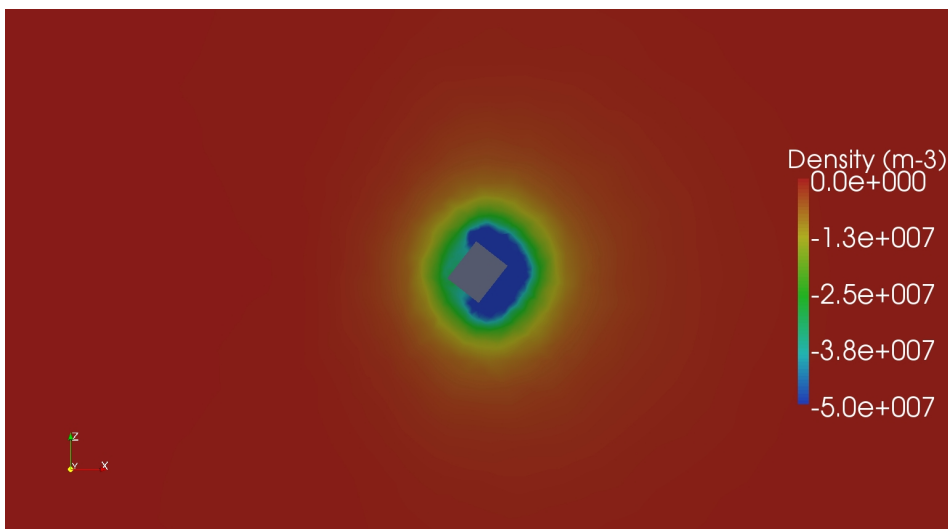


**Figure 2.80:** Photoelectron temperature at 4 eV; photoelectron density in  $m^{-3}$  around Rosetta in the XZ-plane. Parameters:  $T_e = 12$  eV,  $T_i = 5$  eV,  $T_{ph} = 4$  eV,  $n = 5$   $cm^{-3}$ ,  $v_i = 400$  km/s,  $V_{S/C} = 10$  V,  $r = 1$  AU. Simulation name: 090716.

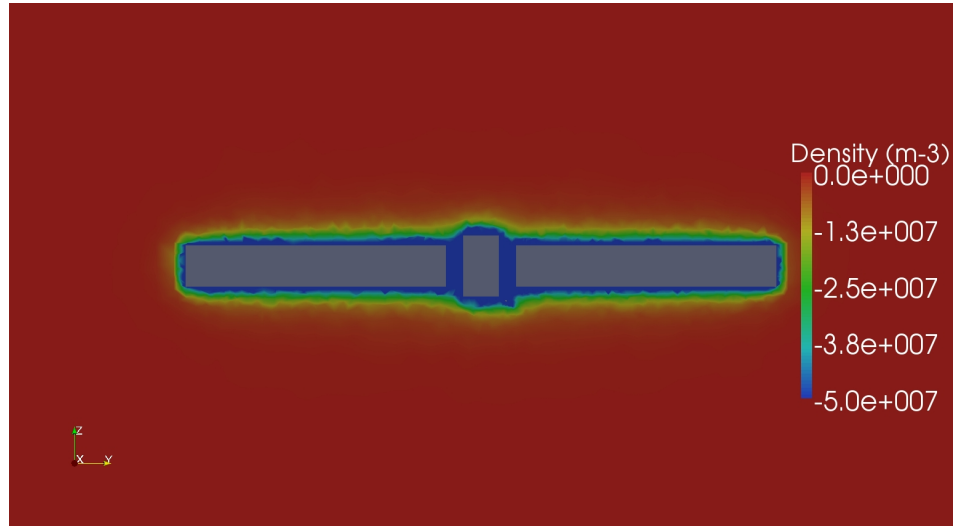


**Figure 2.81:** Photoelectron temperature at 1 eV; photoelectron density in  $m^{-3}$  around Rosetta in the YZ-plane. Parameters:  $T_e = 12$  eV,  $T_i = 5$  eV,  $T_{ph} = 1$  eV,  $n = 5$   $cm^{-3}$ ,  $v_i = 400$  km/s,  $V_{S/C} = 10$  V,  $r = 1$  AU. Simulation name: 090711.

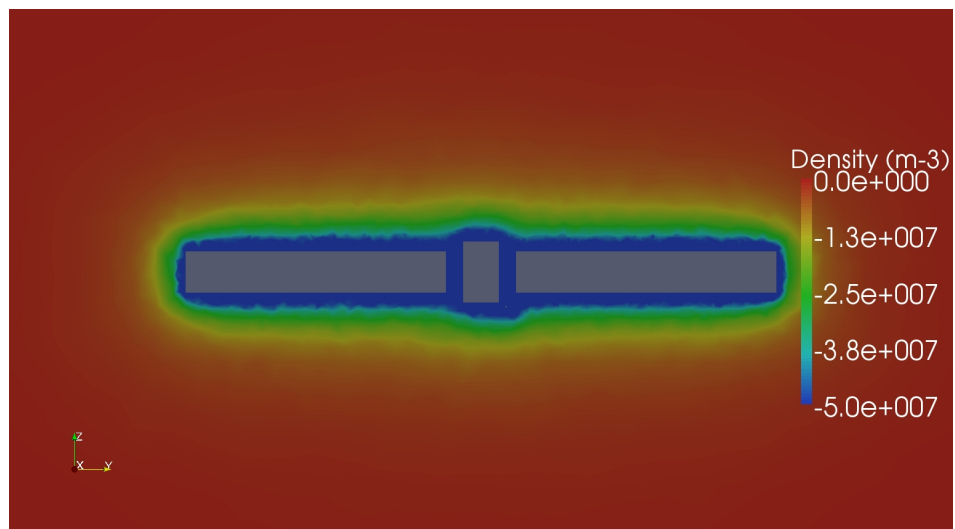


**Figure 2.82:** Photoelectron temperature at 4 eV; photoelectron density in  $m^{-3}$  around Rosetta in the YZ-plane. Parameters:  $T_e = 12$  eV,  $T_i = 5$  eV,  $T_{ph} = 4$  eV,  $n = 5$   $cm^{-3}$ ,  $v_i = 400$  km/s,  $V_{S/C} = 10$  V,  $r = 1$  AU. Simulation name: 090716.

# 3

## CONCLUSIONS

The simulations in the previous chapter show that there are three factors affecting what is measured with the probes on Rosetta:

- Photoelectrons emitted from the spacecraft.
- Wake forming behind the spacecraft.
- Potential from the solar panels.

The biggest impact on measurements is shown to be due to the photoelectron cloud. The potential drop in the plasma due to this cloud is on the order of 10% of the spacecraft potential for reasonable solar wind parameters.

The impact from the photoelectrons scales with varying properties such as distance from the Sun, spacecraft potential and photoelectron temperature. When these parameters vary, the size and the density of the photoelectron cloud will change and therefore the potential measured at the probe positions. For some cases, the probes will be inside the photoelectron cloud, for some cases the booms will be long enough so that the probes are outside of the dense part of the photoelectron cloud most of the time. A higher sunflux will have the same effect as higher photoelectron temperature, that is a denser and bigger photoelectron cloud. A higher spacecraft potential will have the opposite effect, as it will increase the amount of energy the photoelectrons need to escape the spacecraft surfaces.

The effect from the wake is much less than the effect from the photoelectrons, changing the potential on the order of a couple percents. The wake is however recognized in the results, as it by definition is on the opposite side of the photoelectron cloud.

The effects from the solar panels are small compared to the effects from the wake and photoelectron cloud. The effect from the solar panels can however be seen at some points, for example the case when the probes are in the plane of the solar panels, which is when the probes are at their closest point to the panels.

In Table 3.1, some of the potential values from the simulations of plasma with photoelectrons are shown, taken from the plots in the previous chapter. The table shows how the potential drops due to photoelectrons and wake formation compared to the case where the probe is undisturbed by these two effects. It is easy to see that the photoelectron drop is on the order of 10% and the wake drop is on the order of a couple percents of the undisturbed potential in the reference case, and then varying with the varying parameters.

<i>Simulation name</i>	<b>Probe 1</b>			<b>Probe 2</b>		
	<i>Angle<sup>a</sup></i>	<i><math>\phi^b</math></i>	<i><math>\phi - \phi_{undisturbed}^c</math></i>	<i>Angle<sup>a</sup></i>	<i><math>\phi^b</math></i>	<i><math>\phi - \phi_{undisturbed}^c</math></i>
<b>090611</b>						
Undisturbed <sup>d</sup>	0	5.86	-	272	5.78	-
Photoelectron minimum <sup>e</sup>	250	5.17	-0.69	161	5.13	-0.65
Wake minimum <sup>f</sup>	50	5.69	-0.17	346	5.68	-0.10
<b>090625</b>						
Undisturbed <sup>d</sup>	0	6.63	-	272	6.51	-
Photoelectron minimum <sup>e</sup>	250	6.27	-0.36	150	6.22	-0.29
Wake minimum <sup>f</sup>	60	6.45	-0.18	320	6.43	-0.08
<b>090710</b>						
Undisturbed <sup>d</sup>	10	1.79	-	272	1.84	-
Photoelectron minimum <sup>e</sup>	220	1.08	-0.71	161	1.08	-0.76
Wake minimum <sup>f</sup>	50	1.75	-0.04	346	1.78	-0.06
<b>090711</b>						
Undisturbed <sup>d</sup>	0	6.73	-	272	6.62	-
Photoelectron minimum <sup>e</sup>	272	6.43	-0.30	161	6.38	-0.24
Wake minimum <sup>f</sup>	70	6.55	-0.18	320	6.52	-0.10
<b>090716</b>						
Undisturbed <sup>d</sup>	0	4.98	-	272	4.98	-
Photoelectron minimum <sup>e</sup>	250	4.05	-0.93	161	3.99	-0.99
Wake minimum <sup>f</sup>	50	4.93	-0.05	346	4.95	-0.03
<b>090719</b>						
Undisturbed <sup>d</sup>	0	6.90	-	250	6.74	-
Photoelectron minimum <sup>e</sup>	250	6.67	-0.23	161	6.62	-0.12
Wake minimum <sup>f</sup>	70	6.68	-0.22	346	6.63	-0.11

<sup>a</sup>Solar aspect angle in degrees where the given values are taken from.

<sup>b</sup>Potential at probe position in V.

<sup>c</sup>How much the potential differs from the undisturbed potential in V.

<sup>d</sup>Values from the region in the plot where the measurement is least disturbed by photoelectrons and wake.

<sup>e</sup>Values from the point in the plot where the lowest potential due to the photoelectrons occurs.

<sup>f</sup>Values from the point in the plot where the lowest potential due to the wake occurs.

**Table 3.1:** Numerical results from plasma and photoelectrons simulations. Values shown are for the undisturbed part of the plot, the photoelectron drop minimum, and the wake drop minimum.

# 4

## FUTURE WORK

During the work, different thoughts about what should be investigated have come up. The work for this thesis had to be limited in order to complete the work and there are many ways to further build on the work done.

- **Scaling of the effects.** How does the potential at the probes scale with varying parameters? This has been a first study of such effects, and many more parameters could be varied.
- **Floating spacecraft potential.** In all the simulations done, the spacecraft potential has been locked to various values. The potential could be set floating to analyze what the spacecraft potential should actually be in various plasma surroundings, though this will depend on the photoelectron temperature which is uncertain.
- **Analytical model.** Derive an analytical model of the effects to be used when analyzing data.
- **Compare with measurements.** By comparing the results of the simulations with the measurements done, it could be understood if the simulations and numerical data from the probes agree.



## REFERENCES

- Berthelier, J.-J. and Roussel, J.-F. (2004). A study of the electrical charging of the Rosetta orbiter: 2. Experimental tests in a laboratory plasma. *Journal of Geophysical Research (Space Physics)*, 109:1105–+.
- Bond, P. (2001). *Rosetta Europe's Comet Chaser*. ESA Publications Division.
- Chen, F. F. (1984). *Introduction to Plasma Physics and Controlled Fusion, Volume 1: Plasma Physics*. Springer.
- Cully, C., Ergun, R. E., and Eriksson, A. I. (2007). Electrostatic structure around spacecraft in tenuous plasmas. *J. Geophys. Res.*, 112:A09211, doi:10.1029/2007JA012269.
- Engwall, E. (2006). *Cold magnetospheric plasma flows: Properties and interaction with spacecraft*. Licentiate thesis, Department of Astronomy and Space Physics, Uppsala University, Sweden.
- Eriksson, A. I., Boström, R., Gill, R., Åhlén, L., Jansson, S.-E., Wahlund, J.-E., André, M., Mälkki, A., Holtet, J. A., Lybekk, B., Pedersen, A., and Blomberg, L. G. (2007). RPC-LAP: The Rosetta Langmuir Probe Instrument. *Space Science Reviews*, 128:729–744.
- Forest, J., Hilgers, A., Thiebault, B., Eliasson, L., Berthelier, J.-J., and de Feraudy, H. (2006). An open-source spacecraft plasma interaction simulation code PicUp3D: Tests and validations. *Plasma Science, IEEE Transactions on*, 34(5):2103–2113.
- Glassmeier, K.-H., Boehnhardt, H., Koschny, D., Kührt, E., and Richter, I. (2007). The Rosetta Mission: Flying Towards the Origin of the Solar System. *Space Science Reviews*, 128:1–4.
- Hastings, D. and Garret, H. (1996). *Spacecraft–Environment Interactions*. Cambridge Atmospheric and Space Science Series. Cambridge University Press, Cambridge, U.K.; New York, U.S.A.
- McFadden, L.-A. A., Weissman, P. R., and Johnson, T. V. (2006). *Encyclopedia of the Solar System, Second Edition*. Academic Press.
- Nakamura, M. (2005). Space plasma environment at the adeos-ii anomaly. In Goka, T., editor, *Proceedings of the 9th International Spacecraft Charging Technology Conference (SCTC-9)*, JAXA-SP-05-001E. Japan Aerospace Exploration Agency.
- NASA (2006). Stardust - nasa's comet sample return mission - mission overview. <http://stardust.jpl.nasa.gov/mission/index.html>.
- NASA (2009a). Deep impact legacy site. <http://deepimpact.jpl.nasa.gov/>.

## REFERENCES

---

- NASA (2009b). Jpl small-body database browser. <http://ssd.jpl.nasa.gov/sbdb.cgi?sstr=67P/Churyumov-Gerasimenko>.
- Roussel, J.-F. and Berthelier, J.-J. (2004). A study of the electrical charging of the Rosetta orbiter: 1. Numerical model. *Journal of Geophysical Research (Space Physics)*, 109:1104–+.
- Roussel, J.-F., Rogier, F., Dufour, G., Mateo-Velez, J.-C., Forest, J., Hilgers, A., Rodgers, D., Girard, L., and Payan, D. (2008). SPIS open-source code: Methods, capabilities, achievements, and prospects. *Plasma Science, IEEE Transactions on*, 36(5):2360–2368.
- Roussel, J.-F., Rogier, F., Volpert, D., Forest, J., Rousseau, G., and Hilgers, A. (2005). Spacecraft plasma interaction software (SPIS): Numerical solvers - methods and architecture. In *Proceedings of 9th Spacecraft Charging Technology Conference, Tsukuba, Japan*.

# A

## LISTING OF ALL SIMULATIONS

<b>090316</b>		<b>090330</b>	
Model:	Cuboid	Model:	Spherical
Simulation time:	$5 * 10^{-4}$ s	Simulation time:	$5 * 10^{-4}$ s
Electron temperature:	-	Electron temperature:	-
Ion temperature:	-	Ion temperature:	-
Photoelectron temperature:	-	Photoelectron temperature:	-
Plasma density:	-	Plasma density:	-
Ion flow speed:	-	Ion flow speed:	-
Spacecraft potential:	10 V	Spacecraft potential:	10 V
Distance to the Sun:	-	Distance to the Sun:	-
electronSpeedUp:	-	electronSpeedUp:	-
Simulation box size (x,y,z):	30x60x30 m	Simulation box size (x,y,z):	45x60x30 m
Number of cells: <sup>1</sup>	130,000	Number of cells:	260,000
Number of electrons: <sup>1,2</sup>	-	Number of electrons: <sup>2</sup>	-
Number of ions: <sup>1,2</sup>	-	Number of ions: <sup>2</sup>	-
Number of photoelectrons: <sup>1,2</sup>	-	Number of photoelectrons: <sup>2</sup>	-
<i>Cuboid Rosetta in vacuum.</i>		<i>Spherical Rosetta in vacuum at 10 V.</i>	

<sup>1</sup>For the cuboid Rosetta simulations, where one named simulation (for example 090316) consists of several individual simulations, the number of cells and number of particles are an average of the numbers in the individual simulations.

<sup>2</sup>This is actually the number of macroparticles, representing the given particle species, in the last time step of the simulation where the number of particles should be stabilized.

APPENDIX A. LISTING OF ALL SIMULATIONS

---

**090407 0V**

Model:	Spherical
Simulation time:	$5 * 10^{-4}$ s
Electron temperature:	12 eV
Ion temperature:	12 eV
Photoelectron temperature:	-
Plasma density:	$5 \text{ cm}^{-3}$
Ion flow speed:	400 000 km/s
Spacecraft potential:	0 V
Distance to the Sun:	-
electronSpeedUp:	40
Simulation box size (x,y,z):	30x60x30 m
Number of cells:	245,000
Number of electrons: <sup>2</sup>	1,120,000
Number of ions: <sup>2</sup>	1,185,000
Number of photoelectrons: <sup>2</sup>	-

*First plasma simulation, done in order to compare various spacecraft potentials.*

---

**090407 5V**

Model:	Spherical
Simulation time:	$5 * 10^{-4}$ s
Electron temperature:	12 eV
Ion temperature:	12 eV
Photoelectron temperature:	-
Plasma density:	$5 \text{ cm}^{-3}$
Ion flow speed:	400 000 km/s
Spacecraft potential:	5 V
Distance to the Sun:	-
electronSpeedUp:	40
Simulation box size (x,y,z):	30x60x30 m
Number of cells:	245,000
Number of electrons: <sup>2</sup>	1,135,000
Number of ions: <sup>2</sup>	1,185,000
Number of photoelectrons: <sup>2</sup>	-

*First plasma simulation, done in order to compare various spacecraft potentials.*

---

**090416 0V**

Model:	Spherical
Simulation time:	$5 * 10^{-4}$ s
Electron temperature:	12 eV
Ion temperature:	5 eV
Photoelectron temperature:	-
Plasma density:	$5 \text{ cm}^{-3}$
Ion flow speed:	400 000 km/s
Spacecraft potential:	0 V
Distance to the Sun:	-
electronSpeedUp:	26
Simulation box size (x,y,z):	30x60x30 m
Number of cells:	245,000
Number of electrons: <sup>2</sup>	1,160,000
Number of ions: <sup>2</sup>	1,180,000
Number of photoelectrons: <sup>2</sup>	-

*Simulation to examine the effect of ion temperature, compared to 090407 0V.*

---

**090416 5V**

Model:	Spherical
Simulation time:	$5 * 10^{-4}$ s
Electron temperature:	12 eV
Ion temperature:	5 eV
Photoelectron temperature:	-
Plasma density:	$5 \text{ cm}^{-3}$
Ion flow speed:	400 000 km/s
Spacecraft potential:	5 V
Distance to the Sun:	-
electronSpeedUp:	26
Simulation box size (x,y,z):	30x60x30 m
Number of cells:	245,000
Number of electrons: <sup>2</sup>	1,180,000
Number of ions: <sup>2</sup>	1,180,000
Number of photoelectrons: <sup>2</sup>	-

*Simulation to examine the effect of ion temperature, compared to 090407 5V.*

---

---

**090420**

Model:	Spherical
Simulation time:	$5 * 10^{-4}$ s
Electron temperature:	-
Ion temperature:	-
Photoelectron temperature:	-
Plasma density:	-
Ion flow speed:	-
Spacecraft potential:	5 V
Distance to the Sun:	-
electronSpeedUp:	-
Simulation box size (x,y,z):	30x60x30 m
Number of cells:	245,000
Number of electrons: <sup>2</sup>	-
Number of ions: <sup>2</sup>	-
Number of photoelectrons: <sup>2</sup>	-

*Spherical Rosetta in vacuum at 5 V.*

---

**090430**

Model:	Cuboid
Simulation time:	$5 * 10^{-4}$ s
Electron temperature:	12 eV
Ion temperature:	5 eV
Photoelectron temperature:	-
Plasma density:	$5 \text{ cm}^{-3}$
Ion flow speed:	400 000 km/s
Spacecraft potential:	5 V
Distance to the Sun:	-
electronSpeedUp:	26
Simulation box size (x,y,z):	45x60x30 m
Number of cells: <sup>1</sup>	150,000
Number of electrons: <sup>1,2</sup>	700,000
Number of ions: <sup>1,2</sup>	700,000
Number of photoelectrons: <sup>1,2</sup>	-

*The main simulation of cuboid Rosetta in plasma without photoelectrons*

---

**090508**

Model:	Cuboid
Simulation time:	$5 * 10^{-4}$ s
Electron temperature:	6 eV
Ion temperature:	5 eV
Photoelectron temperature:	-
Plasma density:	$5 \text{ cm}^{-3}$
Ion flow speed:	400 000 km/s
Spacecraft potential:	5 V
Distance to the Sun:	-
electronSpeedUp:	26
Simulation box size (x,y,z):	45x60x30 m
Number of cells: <sup>1</sup>	150,000
Number of electrons: <sup>1,2</sup>	690,000
Number of ions: <sup>1,2</sup>	700,000
Number of photoelectrons: <sup>1,2</sup>	-

*Simulation to examine the effect of electron temperature, compared to 090430.*

---

**090513**

Model:	Cuboid
Simulation time:	$5 * 10^{-4}$ s
Electron temperature:	12 eV
Ion temperature:	5 eV
Photoelectron temperature:	2 eV
Plasma density:	$5 \text{ cm}^{-3}$
Ion flow speed:	400 000 km/s
Spacecraft potential:	5 V
Distance to the Sun:	1 AU
electronSpeedUp:	40
Simulation box size (x,y,z):	60x60x30 m
Number of cells: <sup>1</sup>	165,000
Number of electrons: <sup>1,2</sup>	760,000
Number of ions: <sup>1,2</sup>	820,000
Number of photoelectrons: <sup>1,2</sup>	150,000

*Simulation to examine the effect of spacecraft potential. Compared to 090514. Bad eSpeedUp.*

---

APPENDIX A. LISTING OF ALL SIMULATIONS

---

**090514**

Model:	Cuboid
Simulation time:	$5 * 10^{-4}$ s
Electron temperature:	12 eV
Ion temperature:	5 eV
Photoelectron temperature:	2 eV
Plasma density:	$5 \text{ cm}^{-3}$
Ion flow speed:	400 000 km/s
Spacecraft potential:	10 V
Distance to the Sun:	1 AU
electronSpeedUp:	40
Simulation box size (x,y,z):	60x60x30 m
Number of cells: <sup>1</sup>	165,000
Number of electrons: <sup>1,2</sup>	770,000
Number of ions: <sup>1,2</sup>	810,000
Number of photoelectrons: <sup>1,2</sup>	90,000

*Reference simulation in plasma with photoelectrons. Bad eSpeedUp.*

---

**090518**

Model:	Cuboid
Simulation time:	$5 * 10^{-4}$ s
Electron temperature:	12 eV
Ion temperature:	5 eV
Photoelectron temperature:	2 eV
Plasma density:	$5 \text{ cm}^{-3}$
Ion flow speed:	400 000 km/s
Spacecraft potential:	10 V
Distance to the Sun:	1 AU
electronSpeedUp:	40
Simulation box size (x,y,z):	60x60x30 m
Number of cells: <sup>1</sup>	165,000
Number of electrons: <sup>1,2</sup>	770,000
Number of ions: <sup>1,2</sup>	820,000
Number of photoelectrons: <sup>1,2</sup>	30,000

*Simulation to examine the contribution to the probe potentials from the photoelectrons emitted from the booms. Compared to 090514. Bad eSpeedUp.*

---

**090531**

Model:	Cuboid
Simulation time:	$5 * 10^{-4}$ s
Electron temperature:	12 eV
Ion temperature:	5 eV
Photoelectron temperature:	2 eV
Plasma density:	$5 \text{ cm}^{-3}$
Ion flow speed:	400 000 km/s
Spacecraft potential:	10 V
Distance to the Sun:	2 AU
electronSpeedUp:	40
Simulation box size (x,y,z):	60x60x30 m
Number of cells: <sup>1</sup>	165,000
Number of electrons: <sup>1,2</sup>	780,000
Number of ions: <sup>1,2</sup>	810,000
Number of photoelectrons: <sup>1,2</sup>	120,000

*Simulation to examine the behavior at larger distance from the Sun compared to 090514. Bad eSpeedUp.*

---

**090601 1eV**

Model:	Cuboid
Simulation time:	$5 * 10^{-4}$ s
Electron temperature:	12 eV
Ion temperature:	5 eV
Photoelectron temperature:	1 eV
Plasma density:	$5 \text{ cm}^{-3}$
Ion flow speed:	400 000 km/s
Spacecraft potential:	10 V
Distance to the Sun:	1 AU
electronSpeedUp:	40
Simulation box size (x,y,z):	60x60x30 m
Number of cells: <sup>1</sup>	165,000
Number of electrons: <sup>1,2</sup>	770,000
Number of ions: <sup>1,2</sup>	820,000
Number of photoelectrons: <sup>1,2</sup>	40,000

*Simulation to examine the effect of lower photoelectron temperature compared to 090514. Bad eSpeedUp.*

---

---

**090601 4eV**

Model:	Cuboid
Simulation time:	$5 * 10^{-4}$ s
Electron temperature:	12 eV
Ion temperature:	5 eV
Photoelectron temperature:	4 eV
Plasma density:	$5 \text{ cm}^{-3}$
Ion flow speed:	400 000 km/s
Spacecraft potential:	10 V
Distance to the Sun:	1 AU
electronSpeedUp:	40
Simulation box size (x,y,z):	60x60x30 m
Number of cells: <sup>1</sup>	165,000
Number of electrons: <sup>1,2</sup>	770,000
Number of ions: <sup>1,2</sup>	820,000
Number of photoelectrons: <sup>1,2</sup>	220,000

*Simulation to examine the effect of higher photoelectron temperature compared to 090514. Bad eSpeedUp.*

---

**090611**

Model:	Cuboid
Simulation time:	$5 * 10^{-4}$ s
Electron temperature:	12 eV
Ion temperature:	5 eV
Photoelectron temperature:	2 eV
Plasma density:	$5 \text{ cm}^{-3}$
Ion flow speed:	400 000 km/s
Spacecraft potential:	10 V
Distance to the Sun:	1 AU
electronSpeedUp:	1
Simulation box size (x,y,z):	60x60x30 m
Number of cells: <sup>1</sup>	165,000
Number of electrons: <sup>1,2</sup>	800,000
Number of ions: <sup>1,2</sup>	810,000
Number of photoelectrons: <sup>1,2</sup>	160,000

*Reference simulation in plasma with photoelectrons.*

---

**090625**

Model:	Cuboid
Simulation time:	$5 * 10^{-4}$ s
Electron temperature:	12 eV
Ion temperature:	5 eV
Photoelectron temperature:	2 eV
Plasma density:	$5 \text{ cm}^{-3}$
Ion flow speed:	400 000 km/s
Spacecraft potential:	10 V
Distance to the Sun:	2 AU
electronSpeedUp:	1
Simulation box size (x,y,z):	60x60x30 m
Number of cells: <sup>1</sup>	165,000
Number of electrons: <sup>1,2</sup>	810,000
Number of ions: <sup>1,2</sup>	810,000
Number of photoelectrons: <sup>1,2</sup>	340,000

*Simulation to examine the behavior at larger distance from the Sun compared to 090611.*

---

**090710**

Model:	Cuboid
Simulation time:	$5 * 10^{-4}$ s
Electron temperature:	12 eV
Ion temperature:	5 eV
Photoelectron temperature:	2 eV
Plasma density:	$5 \text{ cm}^{-3}$
Ion flow speed:	400 000 km/s
Spacecraft potential:	5 V
Distance to the Sun:	1 AU
electronSpeedUp:	1
Simulation box size (x,y,z):	60x60x30 m
Number of cells: <sup>1</sup>	165,000
Number of electrons: <sup>1,2</sup>	790,000
Number of ions: <sup>1,2</sup>	820,000
Number of photoelectrons: <sup>1,2</sup>	200,000

*Simulation to examine the effect of spacecraft potential. Compared to 090611.*

---

APPENDIX A. LISTING OF ALL SIMULATIONS

---

**090711**

Model:	Cuboid
Simulation time:	$5 * 10^{-4}$ s
Electron temperature:	12 eV
Ion temperature:	5 eV
Photoelectron temperature:	1 eV
Plasma density:	$5 \text{ cm}^{-3}$
Ion flow speed:	400 000 km/s
Spacecraft potential:	10 V
Distance to the Sun:	1 AU
electronSpeedUp:	1
Simulation box size (x,y,z):	60x60x30 m
Number of cells: <sup>1</sup>	165,000
Number of electrons: <sup>1,2</sup>	820,000
Number of ions: <sup>1,2</sup>	820,000
Number of photoelectrons: <sup>1,2</sup>	50,000

*Simulation to examine the effect of lower photoelectron temperature compared to 090611.*

---

**090716**

Model:	Cuboid
Simulation time:	$5 * 10^{-4}$ s
Electron temperature:	12 eV
Ion temperature:	5 eV
Photoelectron temperature:	4 eV
Plasma density:	$5 \text{ cm}^{-3}$
Ion flow speed:	400 000 km/s
Spacecraft potential:	10 V
Distance to the Sun:	1 AU
electronSpeedUp:	1
Simulation box size (x,y,z):	60x60x30 m
Number of cells: <sup>1</sup>	165,000
Number of electrons: <sup>1,2</sup>	790,000
Number of ions: <sup>1,2</sup>	820,000
Number of photoelectrons: <sup>1,2</sup>	310,000

*Simulation to examine the effect of higher photoelectron temperature compared to 090611.*

---

**090719**

Model:	Cuboid
Simulation time:	$5 * 10^{-4}$ s
Electron temperature:	12 eV
Ion temperature:	5 eV
Photoelectron temperature:	2 eV
Plasma density:	$5 \text{ cm}^{-3}$
Ion flow speed:	400 000 km/s
Spacecraft potential:	10 V
Distance to the Sun:	3 AU
electronSpeedUp:	1
Simulation box size (x,y,z):	60x60x30 m
Number of cells: <sup>1</sup>	165,000
Number of electrons: <sup>1,2</sup>	820,000
Number of ions: <sup>1,2</sup>	820,000
Number of photoelectrons: <sup>1,2</sup>	420,000

*Simulation to examine the behavior at larger distance from the Sun compared to 090611.*

---

# B

## HOW TO MAKE A SIMULATION OF THE ROSETTA SPACECRAFT

If I am asked to describe the SPIS software for anyone, I would say it is a lot like an old car. When it runs, it runs well, but you have to be aware of what SPIS likes and what SPIS dislikes in order to get it going. With this in mind, this appendix will be my personal reflections on how to make SPIS run, and I will explain some of the problems and solutions I have experienced during my work with SPIS. It is intended for someone who has never used SPIS before, as a guide to a first attempt on making simulations. It is written from my point of view with the settings that I for some reasons used. Sometimes the reasons have been unclear, if so, I have used anything that happens to work.

The versions of SPIS used in the simulations are 3.7RC05 and 3.7RC09, with the modification that GMSH 2.3.0 is used instead of the one that comes with SPIS 3.7 (which is 2.0.8).

### B.1 The World inside SPIS

SPIS has an easy to understand graphical interface with a toolbar ordered in the way the buttons should be used - from left to right. Below the toolbar is the workspace and at the very bottom you find the log space where all the confusing errors show up, and they sure will show up. You might have to resize the windows inside SPIS to be able to see the log.

In order to start a simulation set-up, the first thing needed is a model to simulate. When talking about a model as far as SPIS is concerned, a model includes a simple model of the spacecraft itself together with the simulation box. The making of a model can often be the hard part, as there are a lot of compromises to be done, and how to make these compromises is not always clear - more about this in the next section. The model is made in a program called GMSH which is 3D finite element grid generator and has its own built-in CAD engine. GMSH is distributed under the terms of GNU General Public License (GPL) and can be downloaded separate from SPIS, but is also distributed with SPIS as a third part program.

When the model is done it is loaded into SPIS. The next step is to tell SPIS what parts of the model has what kind of property; for example that surface 1 is a part of the spacecraft and surface 2 is a part of the boundary surface of the simulation box. In

SPIS there are a lot of pre-defined properties for various materials and various boundary conditions that are used, and these properties are most of the time sufficient.

The next step is to tell SPIS to use GMSH to create a 3D grid (mesh) of the model and thereafter assign the chosen properties for the various parts of the model. If the model is created in advance, you have probably tuned the mesh to behave as desired. In this case, the meshing in SPIS is just a matter of waiting a minute or two. What is left to do now is to define the properties for the simulation, for example simulation time, plasma properties and so on. This is made in the step called Global Settings. When the Global Settings are done, everything that has been set up is converted to the format SPIS uses by pressing the next button. Also this process is just a matter of waiting half a minute or so, and then it is time to press the big red launch button, or *Solver* as it is called in SPIS.

The simulation time depends on many things, and varies from a minute to infinity. When the model and settings are tuned in, a reasonable time scale would be something from a couple of hours to a couple of days at the most. The model and settings that are made in this simulation took me from three to 10 hours to run, depending on how heavily the computer was loaded with other simulations.

When the simulation run is done, the data wanted is extracted and converted to a viewable format. Analyzing the data can be made with the built-in program Cassandra or some other software, for example Paraview which is the one I prefer.

## B.2 Creating a Model

I first start by explaining some keywords that will be critical for the understanding of my description.

- **Characteristic length:** For each point defined in the model, a characteristic length is also defined. When GMSH creates the mesh, it is the characteristic lengths that sets the limitations of the mesh, in other words how coarse the mesh is allowed to be around that point. For example, a characteristic length of 1<sup>1</sup> means that the mesh entities (tetrahedrons) in the region of the point have sides that are all smaller or equal to 1.
- **Simulation box:** When a spacecraft is created, it has to be put inside a simulation box where SPIS will make the calculations. The simulation box represents the space around the spacecraft and has to be sufficiently large so that the boundary conditions for the simulation box are not reflected in the simulation results. This is usually the case when the spacecraft is at least a couple of Debye lengths away from every boundary of the simulation box.
- **Nested (or construction) volume:** In some cases, a big simulation box is needed, but one might not be interested in the result itself close to the boundaries of the simulation box. In these cases, an adaptive mesh can be constructed by defining different characteristic lengths for the boundaries and for the spacecraft. There is however a problem with different sizes of the characteristic lengths, they can not differ a lot without helping GMSH by creating an intermediate step of characteristic

---

<sup>1</sup>The characteristic lengths are measured in meters, as SPIS is mostly dealing with SI-units except for the case of temperatures in eV

length. This is done by creating a nested volume, which is like ‘a box in the box’, with the spacecraft inside. In the case of Rosetta, the characteristic length for the outer boundary is set to 3 and for the spacecraft it is set to 0.3. By creating a nested volume, sufficiently large so that Rosetta with solar panels fit into it, with characteristic length 1, the transition in mesh size will be smoother. An extreme example when this is not the case is shown in Figure B.1.

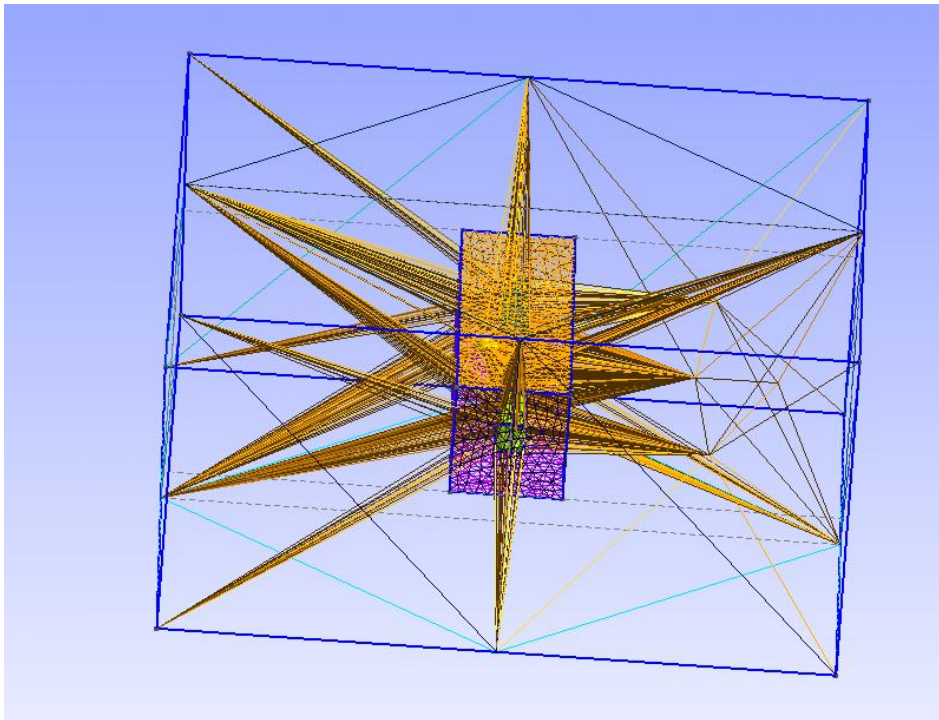


**Figure B.1:** *An extreme example of what may happen if the characteristic lengths are varied too much in one step*

When creating and modifying the model, I have found it more convenient to use a stand-alone version of GMSH rather than working inside SPIS. The work in GMSH is bottom-up, which means that first the points are created, points are then connected with lines, lines connected to surfaces, and finally surfaces are connected to volumes. It is possible to add points, lines etc. either by using the graphical interface or editing the .geo file where the model is saved. When the model is done, it is time for tuning of the mesh. This is made by changing the characteristic length of the points in the model. Each point has four elements; the x,y- and z-coordinates, and also the characteristic length (by default set to  $1e+022$ ).

### B.2.1 Numbering in the .geo file

Each geometrical entity gets an individual number in the .geo file. When creating for example a line, the lines refer to the appropriate points. By using the graphical interface,

the numbering and ordering in the .geo file will become quite messy after a while. A good way to avoid this is to use some kind of numbering system and modify the .geo file to fit into the system. I have usually used numbers between 1 and 99 for the points of the spacecraft body, numbers 100-199 for the points of the solar panels and so on. The lines are then numbered 1000-1099 for the spacecraft body and 1100-1199 for the lines of the solar panels. Further on, so called line loops are numbered on 2000-level, surfaces on 3000-level and so on up to the volumes. To make this work it is needed to work with a combination of the graphical interface and inside the .geo file. For example, after connecting points to form a line in the graphical interface, I simply go in to the .geo file and give the line the right number, before making the surfaces. It is a bit painful work when creating the model for the first time, but it will pay off when running into the geometry errors in SPIS, which you are very likely to do.

### B.2.2 Creating points and lines

In the Rosetta model that has been used the most in my work, the model consists of a cuboidic shaped S/C body, the solar panels and the two booms where the Langmuir probes are attached. The simulation box consists of one large box and a smaller, nested, box.

For Rosetta, first the points of the cubic shaped S/C body are created. The origin is put in the center of the S/C body and the corner coordinates are seen in Table C.1. The points are connected with straight lines in the graphical interface and the line numbers are changed according to the explanation above. Next step is to add the solar panels, which is done in a straightforward way with the coordinates in Table C.2. Note that in the model, the solar panels are not attached to the S/C body. This may look awkward, but is not a problem as they are defined to belong to the same body in SPIS later on (and thus get the same potential), and the rod-like supports actually connecting them are of little concern to us.

The booms in the model I have used have a quadratic cross section. The reason to use this instead of cylindrical booms, which is the real case, is that experiences of other SPIS users show that GMSH handles similarly shaped volumes better when making the mesh. As the S/C body and the solar panels are not cylindrical in any way, and neither is the computational box, the booms were created with the quadratic cross section to keep the rectangular shapes. To add the booms, some more work than just adding points is needed, which is described in the next section.

### B.2.3 Rotation and translation

In the Rosetta model, the booms are not aligned along any of the coordinate axes and they need to be translated and rotated onto their positions. The booms are however created along one of the axes at first, and are then moved onto the right position. The coordinates for boom 1 are found in Table C.3 and the coordinates for boom 2 are found in Table C.4. Before rotating and translating the booms, they are defined as starting at the origin in order to make the translation easier.

After some time spent looking at the blueprints of Rosetta, it is clear that boom 1 needs to be rotated  $\pi/4$  radians around the positive x-axis and then translated onto its starting position. For boom 2 it is a little bit more complicated. The boom is created along the

negative x-axis and by using the coordinates from personal communication with Chris Cully, it can be calculated that it needs to be rotated 0.6303914638 radians around the negative y-axis and thereafter 0.100201891 radians around the negative z-axis. When this is done it can be translated to its actual position. The actual starting positions, in other words the positions to which the booms should be translated, are found in Table C.5.

Together with the booms, I have also introduced construction volumes around the booms and also around the probe centers. The construction volumes are created in a similar way as the booms, but have a cross section with about 3 cm larger side and extend about 30 cm from the boom tip. The construction volume for the probe center is used to avoid large fluctuations of the potential at the probe center (which is actually a position in the plasma in this model). It is a cube with a side of 4 cm, which is created and simply translated to the probe centers, the coordinates are found in Table C.6.

The rotations and translations of the booms are made within the graphical interface of GMSH. All the lines of the boom are selected to be rotated by holding down the Ctrl-key. For the rotation, the coordinates of an axis point need to be defined. In the case of the booms these coordinates are all zero as the boom starts at the origin. For the rotation of boom 1, the number one should be put in the box for 'x component of axis direction' and then the angle that the lines should be rotated. This is done in the same way for the different rotations. For the translation, simply put in the coordinates that you want to move your entity to.

If everything has worked out, the lines created should now have some similarities with the real Rosetta spacecraft. It is then time to put Rosetta out in space, which is done in GMSH by creating the simulation box, representing the space. For the Rosetta simulations I have used a box with the dimensions 60x60x30 meters. This can be modified and improved, but I got it working with this box and then I kept on going. The coordinates for the simulation box are found in C.7, and the coordinates for the nested volume are found in C.8.

#### B.2.4 Creating surfaces, volumes and physicals

It is time to move on and start creating surfaces, which will be simpler if you adhered to the advice above and used a logical numbering system for the points and lines rather than rely on the defaults from the graphical interface. The creation of surfaces is simply done in the graphical interface by selecting the lines bounding a surface. Afterwards, it is a good idea to number the surfaces according to the numbering system chosen, as they will build up the volumes, which is the next step and done easily in the graphical interface. When working with construction volumes, they have to be added in the volume definition. This means that, for example, the simulation box should be defined as a volume with the construction volume as a hole. Then the construction volume should be defined as another volume with the spacecraft as a hole, or in the Rosetta case the boom construction volumes, solar panels and S/C body as holes, and so on.

In order to help SPIS interpret the different surfaces and volumes as objects with various physical properties, there is something called 'physicals'. The physicals are entities which can be given different properties later on in SPIS, for example an external boundary or the spacecraft body. In the Rosetta models there are three different physicals, which is also the smallest number of physicals allowed by SPIS. The first one is the outer boundary of the simulation box, the second one is the surface of the spacecraft and the third

one is the whole volume around the spacecraft (the simulation box). The surfaces are added by just selecting them in the graphical interface. The volumes, however, must be added manually. This is done by editing the .geo file manually. After the lines with the Physical Surfaces, add a line with Physical Volume. Within the braces should be all the volumes that are not the spacecraft, which means the outer boundary volume, the construction volume and so on. Please note here the difference between defining a volume and a physical volume; when adding more surfaces inside the braces for a volume, the volumes that the surfaces make up are subtracted. When adding more volumes into the definition of a physical volume on the other hand, the volumes are added.

The model should now be ready and it is time to fire up SPIS. If this is your first run and you expect everything to work at once, be prepared to run into a wall of frustration. First, there might be some settings in SPIS you want to change in order to get the model working.

### B.3 Customizing SPIS

For the simulations I have done, SPIS 3.7 RC5 and RC9 have been used. When downloading and installing these versions, GMSH 2.0.8 is included as a third part software. This might be a problem if a later version of GMSH is used when creating the model (which is probably the case if you followed the instructions), but this problem has an easy solution. Just download the latest version of GMSH and tell SPIS to use this one. In the case of SPIS 3.7, it is done by copying the GMSH folder into `Spis3_7RC09/ThirdPart/Gmsh/Linux-I386` (if using Linux, of course). When this is done, open the file `Spis3_7RC09/SpisUI/Bin/config.py` and scroll down to something like line 127. Somewhere in this region you will see the line that is calling GMSH from inside SPIS, simply change the path from `gmsh-2.0.8` to the version you just copied into the folder above, and you have the latest version of GMSH also from inside SPIS.

To make sure the mesh created is the best attainable, there is probably a change in the GMSH default setting that needs to be changed. This is done by opening GMSH from the folder you just copied it into. Go to Tools and then Options. Click on 'Mesh' in the left part of the window and click the tab 'Advanced'. Check the option 'Optimize quality of tetrahedra', if this is not already done. To make sure this is saved for next time, click on File and then 'Save Default Options'.

If the model to be used has a detailed mesh and it is needed to throw around a lot of particles in SPIS, a big amount of RAM memory is desirable. If you are also lucky enough to have that big amount of RAM memory, you can change how much memory SPIS should address when starting up. The default value is usually something like 1.6 GB. To change this, open the file `Spis3_7RC09/ThirdPart/Jython/jython-2.1/jython`. In the line starting with `"${JYTHON_HOME}...`, you will see something like `-Xmx1611m`. This is the amount of memory addressed by SPIS. If you are running on a 32-bit machine without any special settings, you are probably limited to about 3.6 GB of memory, so try by putting something like 3600 instead of the 1611. If you try to address too much, SPIS will not start, then just put the value as high as possible.

### B.4 Configuring Simulation Settings and Starting the Simulation

#### B.4.1 Loading the geometry

I will now go through how you set up SPIS to run a simulation with the newly built model and properties similar to the ones I have used in some of my simulations. The first thing to do after launching the SPIS window is to load the model into SPIS. This is done by clicking the 'Call the CAD tools'-button, the third one from the left. A window pops up, in this window click on 'Add file' to find and select the .geo file already created. Now it is important to mark the loaded file and also click 'Set as main' to tell SPIS that this is really the file to use. When this is done, the Geometry/CAD manager can be closed. Now click the next button, 'Load the defined geometry into the framework', which will do exactly what it says. By looking at the Jython log in the bottom of the SPIS window (you might need to resize the windows to see the log), it is possible to see when every step is finished. Loading the geometry into the framework only takes a couple of seconds.

#### B.4.2 Physical properties

Now click the next (green) button, 'Load the default catalogues of material, electrical and numerical properties'. There is a number of default properties for the materials, boundaries and so on, these are loaded into the framework in this step. The default properties are in most cases enough. The next step is to assign the now loaded properties to the different parts of the model. This is done by giving each defined physical (see section B.2.4) one material property, one electrical property and one plasma property. Click the colorful 'Call the GEOM-property groups editor' button and another window pops up. In the left part of the window, you see some numbers and if we are living in a perfect world you should recognize the numbers of the physicals defined in the model, together with some more numbers. *It is of critical importance to order these numbers in the right way.* You arrange them simply by marking the numbers and clicking 'Move Up' or 'Move down'.

- All the numbers that are not physicals are default groups, added by SPIS, and is nothing to worry about more than to put them at very the bottom of the list, after all the physicals.
- The first physical in the list should be the one defining the boundaries of the simulation box.
- The second physical in the list should be the one corresponding to the spacecraft surfaces.
- The third physical in the list should be the actual volume (plasma volume) of the simulation box.

Now that the order is set, it is time to give the physicals their properties. The surface group defining the boundary should have no material property and no electrical property, which is done by selecting 'None' in the boxes, respectively. The plasma should be set to 'Boundary, default', which gives the outer boundary a Fourier boundary condition (the only option available today). The spacecraft surfaces should have the material set to 'ITO, default' (as the solar panels which make up the largest area are covered by Indium Tin

Oxide, ITO), the electrical set to ‘Spacecraft ground (ElecNode-0)’ and plasma set to ‘Spacecraft, default’. For the volume in the simulation box, both material and electrical should be set to ‘None’, whereas the plasma should be set to ‘Plasma Model in Volume, Default’. The different physicals now have properties, so click OK.

### B.4.3 Creating mesh and assigning groups

It is now time for SPIS and GMSH to create the mesh of the model, followed by converting the defined groups for the physicals into mesh groups and thereafter assign the groups to the model. There are three buttons for this, but SPIS will do it all automatically, so by clicking only the third one it will go through the whole process, which can take up to a couple of minutes, depending on the computer and the model created.

### B.4.4 Global properties

The model is now loaded into the SPIS framework, and the last part before starting the simulation is to set the simulation parameters. A description of all the parameters can be found in the SPIS documentation, in the file `Spis3_7RC09/Doc/DocSpisNum/HowTo/ControllingNUMfromUI.html`, or by going through the help section from the SPIS window. Here I will only go through the ones that are changed from their default values in the Rosetta simulation.

By clicking the ‘Call the Global Parameters editor’ button, the next in line, a window with all the settings, ordered in different tabs, pops up. There is one important thing to notice when working in this window. After a value has been changed it is important to press Return/Enter to actually lock the value. If this is not done, the entered value might not be saved. The parameters for the Rosetta simulation, together with a short description, are shown in Table B.1. When all these values have been changed and stored, press the ‘save and quit’ button.

### B.4.5 The last, critical, step; starting the simulation

The next step is to tell SPIS to convert the parameters to numerical values to make calculations on. This is done by pressing the button ‘Convert data from UI to NUM data structure’. If there are some problems with the model or the groups, the errors will probably show up in this step. This is usually the time of heavy frustration as SPIS will not tell you what is wrong, only that *something* is wrong, usually with the group settings.

If there is a problem with the group settings, one first attempt on solving it is to look at the groups in a 3D-model. This is done by clicking at ‘Groups’ and then ‘Show groups (Mesh)’. This requires a proper installation of VTK on the computer. It will take some while to load all the groups. By showing the various groups, which is done by putting a mark in their checkboxes, it is easy to see if, for example, one part of the spacecraft is missing in one of the groups. This is just a first, simple, attempt on trying to solve the problem, sometimes it works, sometimes you have to start looking in the definitions in the .geo file for the error. There is no other simple way (that I know of), just trial and error, and of course a huge amount of patience.

When the error is gone, or maybe it never appeared, SPIS is ready to start working. The simulation is started by clicking the ‘Launch the numerical kernel and performs the

simulation' button. SPIS starts building the simulation model, and after a while the actual simulation is started. The simulation process can be followed by looking at the Standard Log, where the time steps will be monitored, instead of Jython Log which is opened at startup.

### B.5 Exporting and Saving the Data

After a while, the simulation should be ready and SPIS will tell you that with a pop-up window. Before you can look at the results, the data has to be exported into a suitable format and then opened in a third part program, like Cassandra or ParaView. In the case of the Rosetta simulation, it is usually the potential or maybe the density of some particles which is of interest. To export this data, click on the second really colorful button, 'Call the DataFields manager for data analysis, extraction and conversion'. In the window, choose the results you want to look at, for example the final potential. To export this, select 'Cell' in the field 'View on' and then click 'Export to VTK'. The selection of 'Cell' means that the data is data in volume, in the case of data for a surface, for example the spacecraft surface, the selection 'Face' should be used. SPIS will now export the potential in the simulation box to a VTK format that can be opened in the software mentioned above. The export of data will take a while, varying from order of seconds to a sometimes tens of minutes. Make sure the Jython log is visible, as this log will tell you when the export is ready.

Other data of interest in the Rosetta simulations that I have done are usually ion density, electron density, photoelectron density and emitted current from spacecraft surface due to photoelectrons (this one is found under the tab for the spacecraft data). When all the data wanted is exported, the project should be saved, and the newly exported vtk-files will be saved automatically (in a subfolder called `vtk` to the project folder). The project could be opened at a later time. If so, make sure you select all the checkboxes available when open the project to get all the results loaded into the framework.

### B.6 Looking at the VTK files - Working with ParaView

I have used ParaView as a VTK-viewer, simply because it seems to have more functions and an easier interface than Cassandra. Paraview has to be downloaded and installed separately from SPIS. When this is done, open ParaView. The default window of ParaView is divided into three smaller windows; 'Pipeline Browser', 'Object Inspector' and a window where the graphical data will show up. In ParaView, you can apply different filters to the VTK files loaded. Some frequently used filters in the case of Rosetta simulations are:

- **Slice:** Creates a cutting plane in the 3D model so it is easy to see, for example, the potential in one plane of the model. Inputs are the coordinates of the plane and the direction of the normal of the plane.
- **Probe location:** Gives the data for a specific point in the volume, for example the potential at the probe centers of the Rosetta model. Input is the coordinates of the point.

- **Plot over line:** Shows a graph of the data along a straight line, for example how the potential varies outwards from the booms. Inputs are the coordinates of start and end points. In ParaView 3.4.0, the one I have used, there is no support for other than straight lines. This is on the ‘wish-list’ for upcoming versions though, and might be implemented already in the 3.6.0.

The filters are usually quite self-explaining and there is lots of information available on the web about ParaView. If a filter is to be applied, mark the file that the filter should work on, select the filter in the menu, choose the inputs and click apply. By clicking on the small eye next to the file or the filter, you can change what is to be viewed in the graphical window. If you use the Slice filter for the potential, you usually want to show the scale for the colors. This is done by clicking on the colorful button above the calculator. The button to the right of that one is used for changing the scale.

When using the Probe location, the value of the data field in the probe position is shown by clicking on the tab ‘Information’ in the Object Inspector, where it shows up with the name ‘scalars’. It can also be shown by adding a spreadsheet view to ParaView, which is done by clicking on one of the ‘splitting’ buttons in the top right corner of the graphical window and selecting Spreadsheet View. Also here, the eye is determining what is going to be shown in the different (splitted) windows.

## B.7 Final Words about the Rosetta Simulations

With the description above, together with patience and a smile, it should hopefully be possible to create simulations similar to the ones I have done during my work. There is always room for improvements, but you have to start somewhere and this is a start in getting to know SPIS. For the purpose of my simulations, the short description of ParaView should be enough as I seldom used any other functions in this quite capable software.

To create the plots I have with probe potentials vs. solar aspect angle, one simulation is needed for each angle in the Rosetta model with booms. The easiest way to do this as I know of today, is to simply have one master .geo file, then add a rotating command for the S/C body and booms and create different .geo files for the different simulation runs. I have found no other, shorter, way through this work. Of course, the probe locations changes when rotating the spacecraft and booms. The way I used for finding the different probe locations is to create a .geo file with two lines, one for each boom. The points of the lines consist of the starting point of the boom and the probe center. The first step is to translate and rotate the ‘booms’ onto the original positions, and then rotate them accordingly to what is done in the spacecraft model. If you save the file from inside GMSH (with a new filename in order not to overwrite the old file), GMSH will save the file with the coordinates written instead of all rotations. In this way you have found the coordinates for the probe centers for different angles. This too is quite boring work, but at least it works.

Another problem when running the Rosetta model with different angles is that SPIS will not accept some angles. The reason for this is unclear (it will complain about that the mesh is not consistent, so it may be a GMSH problem). It is easiest solved by choosing another angle one degree from the first attempt, and hope for the best.

## B.7. FINAL WORDS ABOUT THE ROSETTA SIMULATIONS

---

If there are any questions about my model or the way of working with GMSH, SPIS and ParaView, I will most likely be available for questions thru e-mail ([alex.ph.sjogren@gmail.com](mailto:alex.ph.sjogren@gmail.com)), and I will gladly do what I can to help.

APPENDIX B. HOW TO MAKE A SIMULATION OF THE ROSETTA SPACECRAFT

Setting	Value	Description
<i>Simulation Control</i> duration	5.0e-4	The duration of the simulation. In this case it is chosen so that it is a couple of times larger than the ion speed divided by the box length.
<i>Plasma</i> electronDensity electronSpeedUp electronTemperature ionDensity ionTemperature ionVx	5e6 1 12 5e6 5 -4e5	The density used for modelling the solar wind This is the default value, and should most likely be used. See Appendix D for more information. The electron temperature used for modelling the solar wind The density used for modelling the solar wind The ion temperature used for modelling the solar wind The ion speed used for modelling the solar wind. In the model used the ions only have a speed in the negative x-direction.
<i>Surface Interactions</i> photoEmission secondarySpeedUp sunX sunZ	3 1 1 0	The value 3 corresponds to that all spacecraft surfaces that are sunlit will have photo emission and the photo electrons are modelled as ‘particle in cell’ (PIC) electrons. Please note that SPIS does not take into account if a surface is in shadow, it only accounts for the direction of the normal for each surface. Defined in the same way as electronSpeedUp, but this parameter concerns the photoelectrons. The x-direction of the Sun (should have opposite sign compared to ionVx). The value is normalized to the Sun flux at 1 AU. If the Sun is in the x-direction, this parameter scales as $sunX = \frac{1}{r^2[AU]}$ . The Sun in this model is in the x-direction.
<i>Spacecraft</i> electricCircuitIntegrate initPot	0 10	When set to 0, the potential of the S/C is locked with Dirichlet boundary condition. When set to 1, the potential is floating. The (initial) potential used for the S/C. If the potential is locked, this will be the potential during the simulation.

**Table B.1:** *Global Parameters*

# C

## COORDINATES FOR THE ROSETTA MODEL

The coordinates for Rosetta that are used are taken from personal communication with Chris Cully at the IRF. The difference is that the panels in the model used here are thicker in order to avoid problems with the mesh and that the booms have a quadratic cross-section area. The coordinates for the booms are calculated with the aim of having the same cross-section area as the cylindrical booms specified by Chris Cully.

X	Y	Z
-1.125	-1.000	-1.321
-1.125	-1.000	1.334
-1.125	1.000	-1.321
-1.125	1.000	1.334
1.125	-1.000	-1.321
1.125	-1.000	1.334
1.125	1.000	-1.321
1.125	1.000	1.334

**Table C.1:** *Spacecraft body coordinates.*

X	Y	Z
0.075	1.95	1.125
-0.075	1.95	1.125
0.075	1.95	-1.125
-0.075	1.95	-1.125
0.075	16.35	1.125
-0.075	16.35	1.125
0.075	16.35	-1.125
-0.075	16.35	-1.125

**Table C.2:** *Solar panel +Y coordinates (thickness of panel is 15 cm). Change all y-coordinates to negative for -Y panel.*

APPENDIX C. COORDINATES FOR THE ROSETTA MODEL

---

<b>X</b>	<b>Y</b>	<b>Z</b>
0.033	0	0.033
0.033	0	-0.033
-0.033	0	0.033
-0.033	0	-0.033
0.022	2	0.022
0.022	2	-0.022
-0.022	2	0.022
-0.022	2	-0.022

**Table C.3:** *Boom 1 Coordinates.*

<b>X</b>	<b>Y</b>	<b>Z</b>
0	0.033	0.033
0	0.033	-0.033
0	-0.033	0.033
0	-0.033	-0.033
1.386	0.022	0.022
1.386	0.022	-0.022
1.386	-0.022	0.022
1.386	-0.022	-0.022

**Table C.4:** *Boom 2 Coordinates*

	<b>X</b>	<b>Y</b>	<b>Z</b>
Boom 1	-1.185	0.850	0.979
Boom 2	-1.185	0.650	-1.021

**Table C.5:** *Booms' starting coordinates*

	<b>X</b>	<b>Y</b>	<b>Z</b>
Probe 1	-1.185	2.430	2.559
Probe 2	-2.480	0.780	-1.971

**Table C.6:** *Probe centers' coordinates*

<b>X</b>	<b>Y</b>	<b>Z</b>
30	30	15
30	30	-15
-30	30	15
-30	30	-15
30	-30	15
30	-30	-15
-30	-30	15
-30	-30	-15

**Table C.7:** *Simulation Box Coordinates*

---

<b>X</b>	<b>Y</b>	<b>Z</b>
5	18	5
5	18	-5
-5	18	5
-5	18	-5
5	-18	5
5	-18	-5
-5	-18	5
-5	-18	-5

**Table C.8:** *Construction volume coordinates*

Spacecraft body	0.3
Booms	0.04
Inner part of solar panels (close to spacecraft body)	0.3
Outer part of solar panels	0.75
Outer boundary	3
Construction volume for the whole spacecraft	1
Construction volumes for booms	0.1
Construction volumes for probe centers	0.01

**Table C.9:** *Characteristic lengths*



# D

## THE ELECTRON SPEEDUP PARAMETER

When introducing denser plasmas and more photoelectrons, the time to run simulations with SPIS increases, sometimes to times which are not possible to handle. To make simulations run faster, the parameter *electronSpeedUp* (*eSU*) has been introduced in the Global Properties in SPIS User Interface. The parameter can be used for fast populations of particles, which could be the case for electrons or fast ions (for ions the parameter is, of course, named *ionSpeedUp*). The default value of the parameter is set to 1, which means no speedup is used. When the value is changed, the fast particles are only integrated over a smaller time than the other, slower, particles. This decreases the simulation time. The definition of *eSU* from the SPIS documentation is as follows:

*Numerical times speed-up factor for electrons (relevant for PIC only). Electrons are only moved of a fraction  $1/\text{electronSpeedUp}$  of actual physical times (valid in quasi-steady conditions for electrons).*<sup>1</sup>

At beginning, the value of *eSU* used in this project was set to 40 in order to make the simulation times shorter. The value of 40 is an approximation of  $\sqrt{\frac{m_{ion}}{m_{electron}}}$ . However, this value did not take the ion flow speed, which in the solar wind is a factor 10 higher than the ion thermal speed, into account. A more proper value for speeding up the plasma electrons in the solar wind simulations should thus be 4. This was found at a late time of the project, and in order to make new, correct, simulations a comparison between various *electronSpeedUp* values was done. Please note that all the simulations in this appendix have photoelectrons. For the case when there are no photoelectrons and the 'reference' parameters are used for the plasma, changing the *eSU* to 1 did not have any effect. The reason is the low temperature of the photoelectrons (2 eV) compared to the ions and plasmaelectrons.

In Figure D.1 the two reference simulations are shown, one with *eSU* = 1 and one with *eSU* = 40. The signature of the curves look similar, but there is a large overestimation of the potential in the case of higher value of *eSU*. The difference is on the order of 0.4 V, or about 7%. As every single simulation is represented by two dots (one for probe 1 and one for probe 2), there are lots of simulations pointing this error out.

In Figure D.2, the same comparison is made with various values of *eSU*, but for the case with lower solar UV flux. For various reasons, the number of simulations done

---

<sup>1</sup>Taken from *How to control NUM from UI* in the SPIS documentation that comes with the package

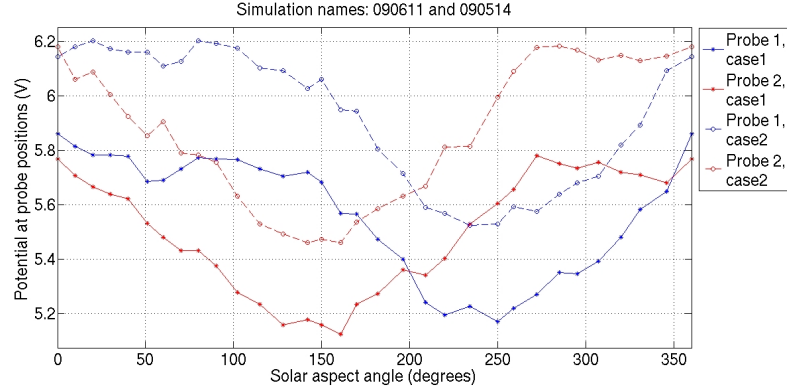


**Figure D.1:** Various *electronSpeedUp* for reference simulations; potential at probe positions as a function of solar aspect angle for two cases: 1)  $eSU = 1$ , 2)  $eSU = 40$ . Parameters:  $T_e = 12$  eV,  $T_i = 5$  eV,  $T_{ph} = 2$  eV,  $n = 5$  cm<sup>-3</sup>,  $v_i = 400$  km/s,  $V_{S/C} = 10$  V,  $r = 1$  AU. Simulation names: 090611 and 090514.

with  $eSU = 40$  is smaller than the number of simulations done with  $eSU = 1$ . The plot does however show a significant difference when the  $eSU$  is set to 40 instead of 1. The difference is on the order of 0.2 V or 3-4%, but is an underestimation instead of the overestimation shown in the previous case.

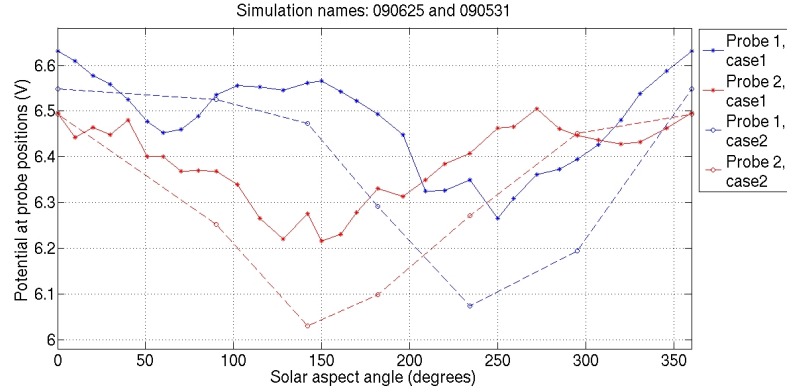


**Figure D.2:** Various *electronSpeedUp* for large solar distance; potential at probe positions as a function of solar aspect angle for two cases: 1)  $eSU = 1$ , 2)  $eSU = 40$ . Parameters:  $T_e = 12$  eV,  $T_i = 5$  eV,  $T_{ph} = 2$  eV,  $n = 5$  cm<sup>-3</sup>,  $v_i = 400$  km/s,  $V_{S/C} = 10$  V,  $r = 2$  AU. Simulation names: 090625 and 090531.

The various electron temperatures for varying  $eSU$  is shown in Figure D.3 and Figure D.4. For both cases, an over estimation of the potential is done when the  $eSU$  is set to 40. The difference for the 1 eV case is not very large, on the order of 2%. In the case of 4 eV photoelectron temperature, the difference is large, on the order of 10%.

For the case of low spacecraft potential, set to 5 V, the difference between various  $eSU$  is shown in Figure D.5. Again, an over estimation is made when the  $eSU$  is set to a

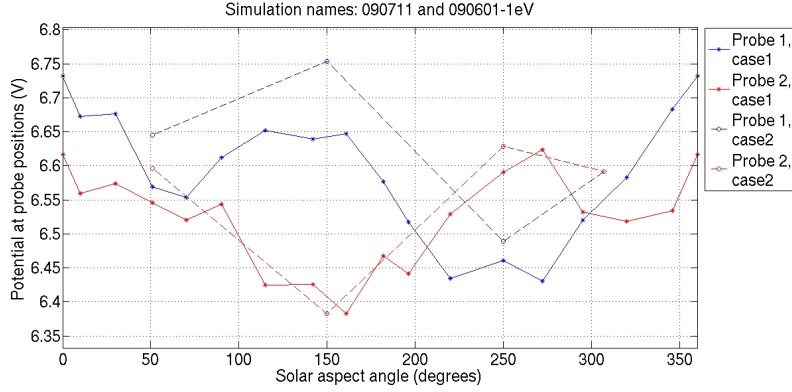


**Figure D.3:** Various *electronSpeedUp* for low photoelectron temperature; potential at probe positions as a function of solar aspect angle for two cases: 1)  $eSU = 1$ , 2)  $eSU = 40$ . Parameters:  $T_e = 12$  eV,  $T_i = 5$  eV,  $T_{ph} = 1$  eV,  $n = 5$  cm<sup>-3</sup>,  $v_i = 400$  km/s,  $V_{SJC} = 10$  V,  $r = 1$  AU. Simulation names: 090711 and 090601 1eV.

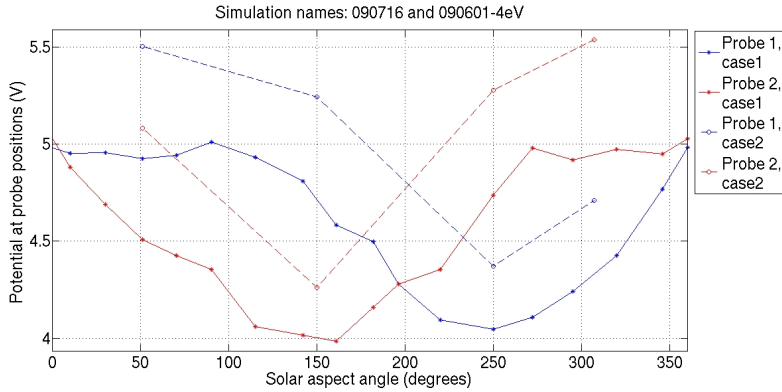


**Figure D.4:** Various *electronSpeedUp* for high photoelectron temperature; potential at probe positions as a function of solar aspect angle for two cases: 1)  $eSU = 1$ , 2)  $eSU = 40$ . Parameters:  $T_e = 12$  eV,  $T_i = 5$  eV,  $T_{ph} = 4$  eV,  $n = 5$  cm<sup>-3</sup>,  $v_i = 400$  km/s,  $V_{SJC} = 10$  V,  $r = 1$  AU. Simulation names: 090716 and 090601 4eV.

higher value. The difference is on the order of 20% at the most.

Simulations were also done with varying  $eSU$  for two angles, and also changing the simulation time. It was examined if the same result would appear if, when increasing the  $eSU$ , the simulation time was also increased four times. The result of the simulations is shown in Table D.1. It can be seen that the hypothesis of increasing the time when also increasing the  $eSU$  was not right, or at least did not give the same result as the case of  $eSU = 1$ . It is however hard to see any clear pattern in the results of the simulation, but for all cases when  $eSU$  is set to 40, the potential is overestimated as shown also in previous plots. It should also be noted that when a specific simulation is run twice, at two different times but with all parameters set to the same values, it gives the same result both times.

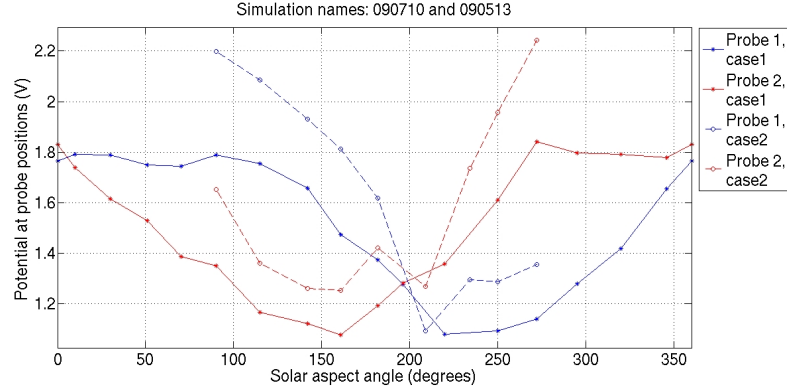


**Figure D.5:** Various electronSpeedUp for low spacecraft potential; potential at probe positions as a function of solar aspect angle for two cases: 1)  $eSU = 1$ , 2)  $eSU = 40$ . Parameters:  $T_e = 12$  eV,  $T_i = 5$  eV,  $T_{ph} = 2$  eV,  $n = 5$  cm<sup>-3</sup>,  $v_i = 400$  km/s,  $V_{S/C} = 5$  V,  $r = 1$  AU. Simulation names: 090710 and 090513.

It is shown that the  $eSU$  parameter does have effect on the result, and one should be clear about the definition and what value is reasonable before using it. It might also be worth comparing various  $eSU$  to examine the effect of the parameter. It might not save you time in the end, if you have to re-run all the simulations just because the  $eSU$  was set to a value which is not really valid.

$eSU$	Simulation time (s)	PROBE 1		PROBE 2	
		Potential at probe position (V)	Difference from $eSU = 1$ (V)	Potential at probe position (V)	Difference from $eSU = 1$ (V)
<b>Solar aspect angle is 0°</b>					
1	$5 \cdot 10^{-4}$	5.86117	0.000	5.76917	0.000
4	$5 \cdot 10^{-4}$	5.90794	0.047	5.82402	0.055
4	$2 \cdot 10^{-3}$	5.85251	-0.009	5.79001	0.021
40	$5 \cdot 10^{-4}$	5.14438	0.283	6.18064	0.411
<b>Solar aspect angle is 182°</b>					
1	$5 \cdot 10^{-4}$	5.47330	0.000	5.27388	0.000
4	$5 \cdot 10^{-4}$	5.50677	0.033	5.25602	-0.018
4	$2 \cdot 10^{-3}$	5.51001	0.037	5.26262	-0.011
40	$5 \cdot 10^{-4}$	5.80449	0.331	5.58647	0.313

**Table D.1:** Probe potentials for various electronSpeedUp

# E

## SIMULATION WITH BOOMS IN SHADOW

There are some limitations when using SPIS, one of them has to do with shadowing. In the case of Rosetta, the problem shows up for the solar aspect angles where the booms are in shadow. This also means that the problem only shows up for the cuboid Rosetta model and not the spherical model used in this project, as there are no booms in the spherical model.

The problem is that shadowing effects of one body on another are not included in SPIS. When the booms are behind the spacecraft with respect to the Sun, the booms are partially or fully shadowed by the spacecraft and no photoelectrons should be emitted from the boom surfaces in eclipse. In SPIS, what determines the photoelectron emission is only the direction of the normal of the surfaces, so the booms will be emitting photoelectrons although they are not sunlit.

To examine the effect of this limitation, simulations were made also with the photoemission ‘turned off’ for the two booms for all angles. The spacecraft body and the solar panels were set to emit photoelectrons. The result of the simulations is shown in Figure E.1.

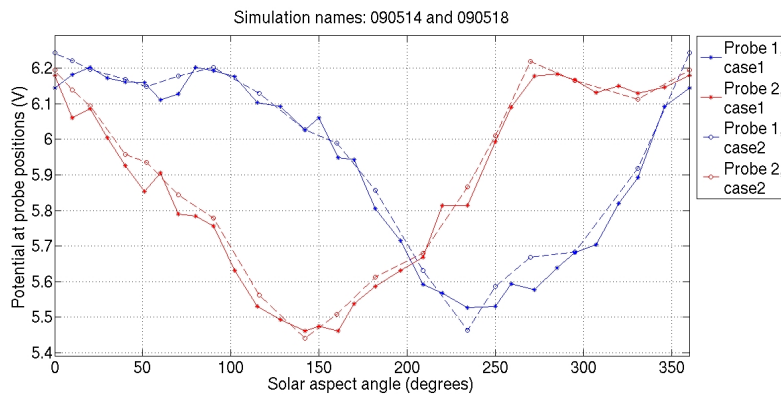


**Figure E.1:** Effect of photoemission from the booms; Potential at probe positions as a function of solar aspect angle for two cases: 1) Booms emitting photoelectrons when facing the Sun, also in shadow, 2) Booms not emitting photoelectrons at all. Parameters:  $T_e = 12$  eV,  $T_i = 5$  eV,  $T_{ph} = 2$  eV,  $n = 5$  cm<sup>-3</sup>,  $v_i = 400$  km/s,  $V_{S/C} = 10$  V,  $r = 1$  AU,  $eSU = 40$ . Simulation names: 090514 and 090518.

As can be seen from the plot, the effect of the photoelectrons from the booms is small compared to other effects. In theory, the simulation with photoelectrons turned off should give a more realistic result when the booms are in eclips, which happens around  $50^\circ$  for probe 1 and  $330^\circ$  for probe 2, while photoemitting booms is a better description for most of the rest of the angular range. However, the difference is small compared to simulation noise, and in practice we do not have to care about this effect.